TAMPEREEN TEKNILLINEN YLIOPISTO
TAMPERE UNIVERSITY OF TECHNOLOGY

Tiiu Niemelä

Self-Reinforced Bioceramic and Polylactide Based Composites

Julkaisu 926 • Publication 926

Tampere 2010

Tiiu Niemelä

Self-Reinforced Bioceramic and Polylactide Based Composites

Thesis for the degree of Doctor of Science in Technology to be presented with due permission for public examination and criticism in Rakennustalo Building, Auditorium RG202, at Tampere University of Technology, on the 5th of November 2010, at 12 noon.

Abstract

Some bioceramics are known to have osteoconductive or osteoinductive potential and excellent bone bonding properties. However, they do not have the required mechanical properties, especially bending properties, to replace bone tissue due to their brittle behavior. Polymeric biomaterials have in many cases more acceptable mechanical behavior, but most of the polymers do not have the properties to facilitate bone tissue healing. Composites of osteoconductive component and polymeric biomaterial could be ideal for bone tissue implant material due to the option to tailor their mechanical properties and osteoconductivity to meet the specific requirements of each application.

The main objective of this thesis was to study self-reinforced osteoconductive bioabsorbable composites composed of either bioactive glass 13-93 or β-tricalcium phosphate as a filler material and different copolymers of polylactide and polyglycolide as a matrix material. The composites studied were compounded using a twin-screw extruder. The samples containing 0 – 50 weight-% of filler material were further self-reinforced by die-drawing to achieve better mechanical properties and porous structure. By self-reinforcing, for example, the shear strength of the plain matrix polymer poly-L/D-lactide 96/4 could be increased by 150 % at best (from 43 MPa to 120 MPa). Self-reinforcing also made initially brittle samples ductile. Compounding and self-reinforcing together turned out to be a suitable method for achieving a homogeneous filler distribution. Different composite compositions were characterized by determining the changes in mechanical properties, thermal properties, molecular weight, mass loss and water absorption in phosphate buffered saline (PBS) at 37 °C for up to 104 weeks. The bioactivity of certain samples and the changes in pH of the buffer solution were also defined.

The results showed that the addition of the osteoconductive filler material impaired the initial mechanical properties of the composites. Osteoconductive filler addition was also observed to modify the degradation kinetics and material morphology of the matrix material. The overall degradation rate of the matrix polymer was observed to be delayed when filler material was added. This was thought to be due to the neutralizing capability of the osteoconductive filler materials.

All composites studied exhibited certain degradation behavior depending on the filler and matrix material used and their proportions as well as on microstructural, macrostructural and environmental factors. Thus it is difficult to predict the exact degradation profile for a certain composite composition. The optimal combination of the matrix polymer and the filler material will be largely dependent on the application planned. When the optimal composition of the composite is found, self-reinforced osteoconductive bioabsorbable composites can be considered as a potential implant material for small bone fracture fixations.

Acknowledgements

Table of contents

List of original publications

The thesis is based on the following publications. They will be later referred to by their Roman numerals:

I. Niemelä T, Kellomäki M and Törmälä P. 2004. *In vitro* degradation of osteoconductive poly-L/DL-lactide / β-TCP composites. In: Key Engineering Materials Vols. 254 – 256. pp. 509 – 512.

II. Niemelä T, Niiranen H, Kellomäki M and Törmälä P. 2005. Self-reinforced composites of bioabsorbable polymer and bioactive glass with different bioactive glass contents. Part I: Initial mechanical properties and bioactivity of the composites. Acta Biomaterialia 1. pp. 235 – 242.

III. Niemelä T. 2005. Effect of β-tricalcium phosphate addition on the *in vitro* biodegradation of self-reinforced poly-L,D-lactide. Polymer Degradation and Stability 89. pp. 492 – 500.

IV. Niemelä T and Kellomäki M. 2007. Three composites of bioactive glass and PLA-copolymers: mass loss and water absorption *in vitro*. In: Key Engineering Materials Vols. 330 – 332. pp. 431 – 434.

V. Niemelä T, Niiranen H and Kellomäki M. 2008. Self-reinforced composites of bioabsorbable polymer and bioactive glass with different bioactive glass contents. Part II: In vitro degradation. Acta Biomaterialia 4. pp. 156 – 164.

VI. Niemelä T, Aydogan DB, Hannula M, Hyttinen J and Kellomäki M. 2010. Determination of bioceramic filler distribution and porosity of self-reinforced bioabsorbable composites using micro-computed tomography. Submitted to Composites Part A: Applied Science and Manufacturing.

Author's contribution

The author's contributions to the publications on which this thesis is based are the following:

I.   The author was responsible for the all work for this paper, including the experimental design of the study, sample processing as well as the analysis of the data. The author was the principal author of the publication.

II.   The author took part in the experimental design of the study and sample processing together with the second author. The author was responsible for the analysis of the data and writing of the manuscript.

III.   The author was responsible for the all work for this paper, including the experimental design of the study, sample processing as well as the analysis of the data. The author was the sole author of the publication.

IV.   The author was responsible for the all work for this paper, including the experimental design of the study, sample processing as well as the analysis of the data. The author was the principal author of the publication.

V.   The author took part in the experimental design of the study and sample processing together with the second author. The author was responsible for the analysis of the data and writing of the manuscript.

VI.   The author was responsible for the sample processing and evaluating the μ-CT analysis data. The author did the editing and the major part of the writing of the manuscript.

Abbreviations

2D	Two-dimensional
3D	Three-dimensional
am-TCP	Amorphous TCP
ap-TCP	Apatitic TCP
BaG	Bioactive glass
BCP	Biphasic calcium phosphates
Bioglass®	Trade name for original bioactive glass composition
CPLA	Copolymerized poly-L-lactide
DR	Draw ratio
DSC	Differential scanning calorimetry
EDX	Energy dispersive X-ray
FA	Fluoroapatite
GA	Glycolic acid, glycolide
GPC	Gel permeation chromatography
HA	Hydroxyapatite
HAPEX™	Trade name for hydroxyapatite / high density polyethylene composite
HCA	Hydroxyl-carbonate apatite
HDPE	High density polyethylene
LA	Lactic acid, lactide
M_n	Number average molecular weight
M_w	Weight average molecular weight
MWD	Molecular weight distribution
OH^-	Hydroxyl ion
PBS	Phosphate buffered saline
PGA	Polyglycolic acid or polyglycolide
PHBV	Polyhydroxybutyrate-polyhydroxyvalerate
PLA	Polylactic acid or polylactide
PLGA	Poly-L-lactide-co-glycolide
PLGC	Poly-L-lactide-co-glycolide-co-ε-caprolactone
PLLA	Poly-L-lactide
PSU	Polysulfone
SEC	Size exclusive chromatography
SEM	Scanning electron microscopy
SR	Self-reinforced
SR-PGA	Self-reinforced polyglycolide
SR-PLA	Self-reinforced polylactide
TCP	Tricalcium phosphate
T_g	Glass transition temperature
TGA	Thermogravimetric analysis

TIPS	Thermally induced phase separation
T_m	Melting temperature
vol-%	Volume percent
WA	Water absorption
WL	Weight loss
wt-%	Weight percent
α-TCP	α-tricalcium phosphate
β-TCP	β-tricalcium phosphate
ΔH	Melting enthalpy
μ-CT	Micro-computed tomography
$-CH_3$	Methyl group
-H	Hydrogen group

Definitions

Definitions are mainly from the Williams Dictionary of Biomaterials (Williams 1999).

Aliphatic polyester	Polymer which contains the ester functional group in the main chain and which does not contain an aromatic ring.
Amorphous	Lack of distinct crystallinity.
Angiogenesis	A physiological process involving the growth of new blood vessels from pre-existing vessels.
Anisotropic	Term describing any material whose physical properties depend upon direction.
Autocatalysis	Catalysis in which a product of the reaction hastens the catalysis.
Autograft	Graft taken from a source in the individual who receives it (the donor and the recipient are the same).
Bioabsorbable	Capable of being degraded or dissolved and subsequently metabolized within an organism.
Bioactive glass	1. Any glass or glass ceramic that displays characteristics of bioactivity. 2. Amorphous solid that is not intrinsically adhesive and that is capable of forming a cohesive bond with both hard and soft tissue when exposed to appropriate *in vivo* or *in vitro* environments by developing a surface layer of hydroxycarbonate apatite by release of ionic species from the bulk material. 3. Any glass or glass ceramic that is used to achieve a bond to mineralized tissue associated with the transfer or ion species and the formation of an apatite layer at their surface.

Bioactive material	1. Material which has been designed to induce specific biological activity.
	2. Biomaterial that is designed to elicit or modulate biological activity.
Bioactivity	Phenomenon by which a biomaterial elicits or modulates biological activity.
Bioceramic	Any ceramic, glass or glass ceramic that is used as a biomaterial.
Biocompatibility	1. The ability of a material to perform with an appropriate host response in a specific application.
	2. The quality of not having toxic or injurious effects on biological systems.
	3. Comparison of the tissue response produced through the close association of the implanted candidate material to its implant site within the host animal to that tissue response recognized and established as suitable with control materials.
Biodegradation	1. Gradual breakdown of a material mediated by specific biological activity.
	2. Breakdown of a material mediated by a biological system.
	3. Alteration undergone by the biomaterial or medical device involving loss of their integrity or performance when exposed to a physiological or simulated environment.
	4. Series of processes by which living systems render chemicals less noxious to the environment.

Biomaterial	1. Non-viable material used in a medical device, intended to interact with biological systems.
	2. Material intended to interface with biological systems to evaluate, treat, augment or replace any tissue, organ or function of the body.
	3. Synthetic, natural or modified natural material intended to be in contact and interact with the biological system.
	4. Any substance (other than drug), synthetic or natural, that can be used as a system or part of a system that treats, augments, or replaces any tissue, organ, or function of the body.
	5. Solid materials which occur in and are made by living organisms, such as chitin, fibrin or bone.
Biostable	Material which resists chemical or structural degradation within a biological environment.
Composite material	Structural material made of two or more distinctly different materials, where each component contributes positively to the final properties.
Copolymer	Polymer consisting of molecules characterized by the repetition of two or more different types of monomeric units.
Crystalline	Having a regular internal arrangement of atoms, ions, or molecules.
Devitrification	Crystallization of an amorphous substance.
Differentiation	Expression of cell- or tissue-specific genes which results in the functional repertoire of a distinct cells types.
Draw ratio	A measure of the degree of stretching during the orientation of a fiber or filament, expressed as the ratio of the cross-sectional area of the undrawn material to that of the drawn material.
Homogeneous	1. Of uniform quality, composition, or structure throughout.
	2. Mixture or solution comprised of two or more substances that are uniformly dispersed in each other.
Homopolymer	A polymer formed from a single monomer.

Hydrolysis

1. Chemical reaction of a compound with water.

2. Process by which a polymer undergoes degradation resulting from exposure to water, with or without effects due to other environmental factors.

3. The cleavage of a compound by the addition of water, the hydroxyl group being incorporated in one fragment and the hydrogen atom in the other.

Hydrophilic

Having an affinity for water.

Hydrophobic

Not readily absorbing or interacting with water.

Hydroxyapatite

1. Hydrated calcium phosphate occurring widely in natural tissues such as enamel, bone, etc.

2. Hydrated calcium phosphate, prepared by any one of several routes and existing in several different forms, that is used as a ceramic biomaterials.

Implant

1. (noun) Medical device made from one or more biomaterial that is intentionally placed within the body, either totally or partially buried beneath an epithelial surface.

2. (noun) Medical device that is placed into a surgically or naturally formed cavity of the human body if it is intended to remain there of a period of 30 days or more.

3. (verb) To insert any object into a surgically or naturally formed site in the body, with the intention of leaving it there after the procedure is complete.

in vitro

1. Literally, "in glass" or "test tube"; used to refer to processes that are carried outside the living body, usually in the laboratory, as distinguished from *in vivo*.

2. Pertaining to a situation which involves the experimental reproduction of biological processes in the more easily defined environment such as a culture vessel.

in vivo

1. Within the living body.

2. Pertaining to a biological process occurring within the living organism or cell.

Inert	Not readily changed by chemical means.
Interface	Sharp contact boundary between two substances, materials, or phases, either or both of which may be solid, liquid or gaseous.
Isomers	Molecules that contains the same number and kind of atoms, but which differ in structure, thus displaying wide differences in properties.
Matrix	1. More or less continuous matter in which something is embebbed. 2. Intercellular substance of a tissue or the tissue from which a structure develops. 3. Component of a composite material in which the fibers or filler materials are embedded.
Monomer	Substance comprised of small molecules with high chemical reactivity, each being capable of linking up with others to produce polymer chains.
Morphology	Study of the shapes of micro-structural units in material.
Oligomer	Polymer formed by the combination of relatively few monomers.
Osteoblast	Bone-forming cell.
Osteoconduction	A growth of bone along the implant surface from the implant / bone interface.
Osteoinduction	The generation of the new bone on the implant, but away from the implant / bone interface, to the place where bone normally does not exist.
Phagocytosis	Engulfing of micro-organisms or other cells and foreign particles by phagocytes.
Proliferation	Growth or extension by the multiplication of cells.
Racemic	Optically inactive, being composed of equal amounts of left- and right-handed enantiomers.
Resorbable	Capable of being resorbed into the body.

Self-reinforcing	A temperature controlled mechanical deformation process (e.g. die drawing), where molecular chains are deformed mechanically to create oriented structures such as fiber strands to produce aligned molecular chains.
Semicrystalline	Material that is only partially crystalline.
Stereoisomerism	Isomerism in which the isomers have the same structure (same linkages between atoms) but different spatial arrangements of the atoms.
Stress shielding	Reduction in bone density (osteopenia) as the result of removal of normal stress from the bone by an implant.
Tissue engineering	1. The persuasion of the boy to heal itself, through the delivery to the appropriate sites of molecular signals, cells and supporting structures.

2. Application of scientific principles to the design, construction, modification, growth and maintenance of living tissues.

3. The application of the principles and methods of engineering and life sciences towards the fundamental understanding of structure / function relationship in normal and pathological mammalian tissues and the development of biological substitutes to restore, maintain or improve functions.

4. An emerging discipline that applies engineering principles to create devices for the study, restoration, modification and assembly of functional tissues from native or synthetic sources. |

1. INTRODUCTION

Poly-α-hydroxyacids are one of the most widely used bioabsorbable polymers in medical implants. Because of their degradable nature and the degradation rate, which can be tailored by copolymerization, they have been used in temporary applications, such as sutures and bone fixation devices. Bioabsorbable implants hold the healing tissue in place and offer an appropriate strength during the first stages of healing. After that the load may be gradually transferred to the tissue, so that the degradation rate of the implant and healing rate of the tissue are similar. When the tissue is healed, no second surgery is needed to remove the implant, because the degradation products of the implant can be excreted by the natural metabolic process of the body. However, some problems have been encountered regarding the release of acidic degradation products. Another limitation of poly-α-hydroxyacids is the lack of bioactive functions, which means that they do not allow bone bonding on their surfaces, which would be beneficial especially in bone tissue applications.

Some bioceramics, such as bioactive glass and tricalcium phosphate, have osteoconductive potential and excellent bone bonding properties and are thus preferable for bone repair. However, at the same time they are essentially ceramics, which usually means brittle behavior, and thus they do not fulfill the required mechanical properties to replace bone tissue as such as do most polymeric biomaterials. Thus, if biodegradation and bioactivity need to be combined in the same material, then the design of composite materials is a desirable solution. A combination of the osteoconductive bioceramic and bioabsorbable polymer creates an osteoconductive and bioabsorbable composite material with tailored physical and mechanical properties. In addition to enhanced bioactivity, the mechanical properties and structural integrity of the composite are often also enhanced. One great advantage of adding osteoconductive bioceramic to the bioabsorbable polymer is the option to alter the degradation behavior of the matrix polymer.

This thesis presents studies on the osteoconductive bioabsorbable composites composed of either bioactive glass (BaG) or β-tricalcium phosphate (β-TCP) and different copolymers of polylactide (PLA) and polyglycolide (PGA). Mechanical properties and structure of the composites were modified using self-reinforcing, in this thesis meaning solid state die-drawing. In the first five publications several different combinations of osteoconductive filler material and bioabsorbable polymer matrixes were studied *in vitro*. The aim was to ascertain how the different filler material and its content affect the mechanical properties, bioactivity and especially degradation behavior of the composite. The sixth manuscript presents a different approach to the composites studied. Micro-computed tomography (μ-CT) image analysis was used to examine the microstructure

of the composites, mainly the distribution of the osteoconductive filler material in the polymer matrix.

The literature review provides an overview of the basics of bioabsorbable polymers, mainly poly-α-hydroxyacids, such as polylactide, polyglycolide and their copolymers, and also their degradation behavior. Bioceramics in general are introduced briefly and bioactive glasses and tricalcium phosphate in more detail. The basics of the composites are also presented. At the end of the literature review there is an overview of the osteoconductive bioabsorbable composites and their degradation behavior, which are already reported in the literature.

2. LITERATURE REVIEW

2.1. Bioabsorbable polymers

Bioabsorbable polymers are one of the most important biomaterials. They have so far been extensively used in biomedical applications. The current trend shows that in the future bioabsorbable polymers may gradually replace biostable biomaterials. There are several reasons why bioabsorbable polymers are preferred to biostable biomaterials. The major reason is that there is no need for revision surgery due to the degradation of the implant. Secondly, stress shielding and weakening of the fixed tissue are prevented, because the implant degrades gradually and the stresses are also transferred gradually to the healing tissue. (Törmälä *et al.* 1998, Middleton and Tipton 2000, Zhang and James 2006, Nair and Laurencin 2007) The reason is also the emergence of novel biomedical technologies, such as tissue engineering and controlled drug release, which require bioabsorbable materials. (Nair and Laurencin 2007)

Bioabsorbable polymers can be classified in several ways, for example by dividing them into the groups of natural and synthetic polymers. Both can be used in biomedical applications, but synthetic polymers have several advantages over natural polymers as implant materials (Middleton and Tipton 2000). Natural polymers are derived from renewable resources, which means, for example, plants, animals and micro-organisms, and thus most of them have excellent biocompatibility and are naturally bioabsorbable. (Zhang and James 2006, Nair and Laurencin 2007, Gomes *et al.* 2008) In addition to being made of renewable resources bioabsorbable polymers can be manufactured synthetically from petrochemical resources. These polymers are called synthetic bioabsorbable polymers and their properties can be modified in many ways, such as by blending and copolymerization. Aliphatic polyesters, such as polylactide, polyglycolide and their copolymers, are synthetic bioabsorbable polymers which have been most extensively used, beginning in the 1960s. In those days the application was in wound closure, including biodegradable sutures. Nowadays biomedical applications of these bioabsorbable polymers include large implants, such as bone screws, small implants, such as nano-sized drug delivery devices and porous structures for tissue engineering. (Middleton and Tipton 2000, Vert 2005, Nair and Laurencin 2007)

2.1.1. Polyglycolide

Polyglycolide (PGA) is the simplest synthetic aliphatic polyester (Table 1). It can be considered to be the first bioabsorbable polymer used in biomedical application. PGA is highly crystalline polymer (45 – 55 %) and thus insoluble in most organic solvents. Although the solubility is low, PGA can be manufactured into several forms and

structures such as fibers. (Kohn and Langer 1996, Middleton and Tipton 2000, Nair and Laurencin 2007) Due to its high crystallinity, PGA also has good initial mechanical properties. One of the stiffest bioabsorbable polymeric systems used clinically is self-reinforced PGA (SR-PGA), which may have even better initial strength values than metals. (Törmälä 1992, Maurus and Kaeding 2004) The excellent initial mechanical properties do not, however, guarantee a suitable degradation rate. PGA degrades rapidly. It is known to lose its mechanical properties in as little as $1 - 2$ months and to be completely absorbed in $6 - 12$ months. (Maurus and Kaeding 2004, Borden 2006) Fast degradation rate, release of acidic breakdown products and low solubility limits the use of PGA in biomedical applications. Thus glycolic acid (GA) has been often copolymerized with other monomers, such as lactic acid (LA). (Nair and Laurencin 2007)

Table 1.
Chemical structures of polyglycolide, polylactide and their copolymers.

Chemical structure

Polyglycolide (PGA)	
Polylactide (PLA)	
Lactic acid stereocopolymers	
Lactic-glycolic copolymers	

4

2.1.2. Polylactide

Polylactide (PLA) is the most commonly used synthetic bioabsorbable polymer. Unlike PGA, PLA has chiral carbon in its structure and thus exists in three stereoisomeric forms: poly-L-lactide, poly-D-lactide and rasemic poly-DL-lactide. Poly-L-lactide is more commonly used in surgical implants than poly-D-lactide because the L-monomer is the naturally occurring isomer. (Kohn and Langer 1996, Middleton and Tipton 2000, Maurus and Kaeding 2004, Nair and Laurencin 2007) When different forms of PLA are used, polymers with significantly different properties can be synthesized. The starting isomers influenced the physical properties of the material. The homopolymers poly-L-lactide and poly-D-lactide are semicrystalline polymers, which have good strength and long degradation period (3 − 5 years). This is due to the tight packing of the polymer chains, which have all methyl groups ($-CH_3$) on one side. (Borden 2006) Poly-L-lactide has been considered an ideal material for load bearing biomedical applications due to its good mechanical properties. The methyl group in the molecular structure of the PLA makes it more hydrophobic than PGA and thus water absorption is much slower and the degradation rate is also slower. (Middleton and Tipton 2000, Maurus and Kaeding 2004, Nair and Laurencin 2007) Rasemic poly-DL-lactide has a random or alternating arrangement of $-CH_3$ and hydrogen (-H) groups, which prevents the polymer chains from packing together. This results in amorphous structure with a lower strength and shorter degradation period (9 − 12 months). (Borden 2006) These properties, lower strength and faster degradation rate, make poly-DL-lactide a very interesting material, for example for drug delivery applications. (Kohn and Langer 1996, Nair and Laurencin 2007)

Copolymers of L-lactide with D-lactide or DL-lactide have also been widely studied. The addition of the D-isomer affects the crystallinity and thereby also to the degradation rate of the material. When adding D-isomers, the proportion of the amorphous regions increases and crystallinity decreases, which lead to faster degradation. The copolymer of PLA is totally amorphous if the L/D ratio is smaller than 87.5L/12.5D (Chabot *et al.* 1983). The properties of PLA and its copolymers can be affected by many factors, such as L/D ratio, polymerization method and thus molecular weight and polydispersity, degree of chain orientation, porosity, shape and size of the implant etc. (Törmälä *et al.* 1998, Rezwan *et al.* 2006, Cotton *et al.* 2008)

The slower degradation rate of PLA compared to PGA enables the wider clinical use of PLA. Thus PLA and its copolymers have a long history in clinical use and self-reinforced, high strength poly-L-lactide (PLLA) especially has so far been used extensively in the treatment of traumas of the skeletal system as pins, screws, tacks, arrows and wires (Törmälä *et al.* 1998, Rokkanen *et al.* 2000).

2.1.3. Polylactide-co-glycolide

In order to adjust the properties of PGA to the range of possible applications, GA monomers can be copolymerized with more hydrophobic LA monomers. Copolymerization extends the range of homopolymer properties. However, there is no linear relationship between the composition and the mechanical properties and degradation behavior of the materials. (Kohn and Langer 1996, Middleton and Tipton 2000) PGA is highly crystalline, but the crystallinity is rapidly lost when GA is copolymerized with LA. It has been reported that the copolymers of L-lactide containing 25 – 75 % glycolide are amorphous (Middleton and Tipton 2000, Nair and Laurencin 2007). The morphological changes lead to a faster degradation rate and, for example, poly-L-lactide-co-glycolide 50/50 (PLGA 50/50) is hydrolytically very unstable and degrades faster than either homopolymer. (Kohn and Langer 1996, Middleton and Tipton 2000, Nair and Laurencin 2007) PLGA has been reported to have excellent biodegradability, biocompatibility and non-toxicity properties (Vert *et al.* 1992) and thus PLGA is extensively used in various biomedical applications.

2.1.4. Hydrolytic degradation of aliphatic polyesters

When implanted into the body, bioabsorbable implants maintain their properties for given length of time and then they gradually degrade and finally absorb completely and metabolize out of the body. Degradation mechanism may be enzymatic or hydrolytic. For PLA, PGA and their copolymers the main degradation mechanism is hydrolysis. This is due to the chemical structure of these polymers. These all have carbon-oxygen-carbon (C-O-C) bonds in their long polymer chain and when the polymer is exposed to water, the water molecules chemically react with the C-O-C bonds causing them to break. (Borden 2006)

The hydrolytic degradation of semi-crystalline polymers occurs in two phases. At first the water molecules penetrate into the amorphous regions of the polymer. This causes a random hydrolytic cleavage of ester bonds and reduces long polymer chains into shorter ones. Because this occurs in the amorphous regions of the polymer, the physical properties of the material remain unchanged thanks to crystalline regions which still hold the structure together. However, molecular weight started to diminish at the very beginning of the hydrolysis. At the second stage hydrolytic degradation also occurs in the crystalline regions which cause the reduction of the physical properties. At the end of the hydrolysis the fragments are metabolized by enzymes (*in vivo*) and the mass of the polymer starts to decrease rapidly. (Li 1999, Li & Vert 1999, Middleton and Tipton 2000)

The degradation of aliphatic polyesters and their copolymers in aqueous medium has been reported by Li *et al.* (Li *et al.* 1990a, Li *et al.* 1990b, Li *et al.* 1990c, Li 1999, Li and Vert 1999). The degradation was reported to start immediately after immersion in

buffer solution. The sample absorbed water, which caused the hydrolytic cleavage of the ester bonds leading to the decrease in molecular weight. The cleavage of the ester bonds yields to the formation of carboxyl end groups which further catalyze the hydrolysis of other ester bonds. This autocatalytic effect during degradation is quite common in PLA and PGA based materials (Li 1999, Li & Vert 1999, Middleton and Tipton 2000, Hill 2005, Rezwan *et al.* 2006, Avérous 2008). Li (1999) reported autocatalysis as a degradation phenomenon called heterogeneous degradation or faster internal degradation. This means that the interior of the sample degrades differently from the surface of the sample. The degradation products, soluble oligomers, near to the surface can escape from the material or they may be neutralized by the buffer solution and thus autocatalysis is avoided. However, those degradation products located inside the structure can only slowly diffuse out of the structure causing higher acidity and thus accelerated degradation inside the structure. This causes two populations of macromolecules which degrade at different rates and thus a bimodal molecular weight distribution is detected. Heterogeneous degradation is observed in both amorphous and semicrystalline polyesters and it finally leads to either a hollow or closed structure. The structure remains entire if the internal degradation by-products can recrystalline. If recrystallization is not possible the internal material finally dissolves in the aqueous medium. (Li 1999)

There are several factors, such as the chemical structure, molecular weight and distribution of the polymer, presence of residual monomers, morphology (meaning crystallinity), the shape, geometry, location, porosity and size of the sample as well as the thermal and mechanical history together with the hydrolysis conditions, such as temperature and pH, which affect the degradation kinetics of bioabsorbable polymers (Cam *et al.* 1995, Li 1999, Rezwan *et al.* 2006, Avérous 2008). Knowledge of the influence of these factors will help to modify the degradation as desired. However, degradation is a complex mechanism of combined properties and thus the exact prediction of degradation behavior is difficult.

The morphology (crystallinity or amorphousness) of the polymer has a major effect on the hydrolysis rate. The crystalline segments in the polymer are more stable than amorphous ones and thus slow down the hydrolysis rate. Also, longer polymer chains with higher molecular weights will degrade more slowly than shorter ones due to the larger number of bonds to be cleaved. Additionally, chemical structure and composition of the polymer chain play a role. Some bonds are more susceptible to hydrolysis than others and some groups in the polymer backbone are more hydrophilic or hydrophobic than others. For example, PLA has methyl groups in the backbone and thus it is more hydrophobic and thus degrades more slowly than, for example, PGA. (Li 1999, Middleton and Tipton 2000, Borden 2006, Rezwan *et al.* 2006)

The crystallinity of the polymer could change during the degradation process. Li *et al.* (1990c) reported that initially amorphous poly-L-lactide becomes slightly crystalline during degradation. Crystallization does not normally occur at a temperature of 37 °C,

but due to the cleavage of the polymer chains there is a fraction of low molecular weight species which can become crystalline more easily. The crystals formed during degradation appeared to be very resistant to further degradation. The differential scanning calorimetry (DSC) thermograms shows that the both the glass transition temperature (T_g) and the melting temperature (T_m) decrease during degradation. This is related to the decrease of the molecular weight due to the breaking of the polymer chains. (Li *et al.* 1990c, Li 1999) A bimodal molecular weight distribution (MWD) is also detected during the degradation of the polyesters. Li (1999) reported that three different kinds of bimodal size exclusive chromatography (SEC) curves could be detected. The first one results from heterogeneous degradation, which is due to the faster internal degradation of amorphous polymers. The second results from the selective degradation of amorphous domains in the semicrystalline polymers. And the third results from the crystallization of the degradation products formed during the degradation of initially amorphous but crystallizable polymers.

The composition of the polymer chain, meaning, for example, the proportions of L-isomer, D-isomer and GA, affects the degradation rate of the copolymers. Generally the addition of D-isomer or GA accelerates the degradation. (Li 1999, Middleton and Tipton 2000, Borden 2006, Rezwan *et al.* 2006) Another interesting and important factor is the incorporation of different additives in the polymer matrix. For example an acidic additive can accelerate the degradation of the composite formed whereas a basic additive can slow down the degradation rate (Li and Vert 1996, Li 1999). Also, the presence of residual monomers and oligomers in the matrix has been reported to lead to faster degradation (Hyon *et al.* 1998, Paakinaho *et al.* 2009).

When developing a novel bioabsorbable polymers or composites, most degradation experiments are usually performed *in vitro* by immersing the samples in buffer solution at body temperature (37 °C). However, *in vitro* degradation usually differs from *in vivo* degradation. In most cases degradation is faster *in vivo* than *in vitro*. (Mainil-Varlet et al. 1997, van Dijkhuizen-Radersma *et al.* 2008) The difference can be attributed to the tissue response, for example cellular enzymes and other biological factors as well as the mechanical stresses caused to the samples by the movement of the test animal. (Li and Vert 1999, van Dijkhuizen-Radersma *et al.* 2008) Due to these complex factors it is important to perform the relevant *in vivo* experiments besides *in vitro* experiments when selecting a biodegradable polymer for a specific application.

To summarize, the degradation behavior of aliphatic polyesters, like that of other bioabsorbable polymers, may be very distinct, depending on many intrinsic and extrinsic properties and factors.

2.2. Bioceramics

Bioceramics are ceramic materials that are developed for the repair, reconstruction and replacement of diseased or damaged parts of the body without causing a toxic response. (Hench and Wilson 1993, Hench 1996, Hench 1998a, Jones and Hench 2006) The aim of early bioceramics was to achieve a suitable combination of mechanical and physical properties to suit to those of replaced hard tissue. These "first generation" bioceramics were mostly inert and attached to the host tissue through morphological fixation. The "second generation" bioceramics used bioactive fixation, which improved the interfacial stability between the implant and the host tissue. However, bioactive fixation alone does not ensure an improvement in implant survivability. The materials lack the ability to self-repair and to modify their structure and properties in response to environmental factors such as mechanical load. Thus, "third generation" bioceramics are under development. Ideally, the implant should stimulate and guide cells in the body to regenerate tissues to a healthy and natural state. There is a need for biomaterial that behaves in a manner equivalent to an autograft. (Hench 1998b, Jones and Hench 2006)

All materials implanted in living tissue elicit a response from the host tissue. The response occurs in the tissue-biomaterial interface and has a direct effect on the mechanism of tissue attachment. In bioceramics, there are four general types of tissue attachments: nearly inert, porous, bioactive and resorbable. A nearly inert bioceramic does not form a bond with the tissue but forms a non-adherent fibrous capsule. It can be attached to the tissue by mechanical interlocking that is morphological fixation. The relative movement, micromotion, can occur at the tissue-implant interface, because the implant is not biologically or chemically bonded to the tissue. This may cause the fibrous capsule to become several micrometers thick and the implant may loosen very quickly. Porous surfaces have been developed to prevent the loosening of implants. The porous structure provides interfacial fixation by ingrowth of the tissue into the pores, meaning biological fixation. This kind of fixation can withstand more complex stresses. The pore size of the implant (or implant surface) is critical, because pores larger than 100 µm are needed for blood supply to the host tissue. (Hench and Wilson 1993, Cao and Hench 1996, Hench 1996, Hench 1998a) Hench defined the bioactive material as: "*a material that elicits a specific biological response at the interface of the material which results in the formation of the bond between the tissues and the material*". (Hench and Wilson 1993) This causes the bioactive material to undergo a series of physical and chemical reactions at the implant-tissue interface leading to mechanically strong interfacial bonding, called bioactive fixation. Resorbable bioceramics lead to the regeneration of the tissue instead of its replacement. They degrade gradually over time and the degradation rate must match the healing rate of the tissue. (Hench and Wilson 1993, Cao and Hench 1996, Hench 1996, Hench 1998a)

2.2.1. Bioactive glasses

Bioactive glasses were first discovered in 1969 by Larry Hench. (Hench 2006) Hench observed that bone can bond to glasses of a certain composition. Nowadays various new compositions have been found and studied. Certain compositions have been found to be capable of bonding both with soft tissue and bone tissue. The whole group of these glasses is nowadays referred as bioactive glasses. According to the manufacturing method, the bioactive glasses can be divided into melt-derived glasses and sol-gel derived glasses. (Hench and Andersson 1993)

Structure, composition and processability of bioactive glasses

The major characteristic of glasses is their amorphous structure. Silicate glasses are based on the SiO_4 tetrahedron, which is linked to oxygen ions at the corners. The amorphous structure contains both bridging oxygen bonds and non-bridging oxygen bonds. The existence of the non-bridging bonds is due to the presence of the some cations, for example Na^+, K^+ and Ca^{2+}, which disturb the network structure. (Hench and Wilson 1993, Ben-Nissan and Ylänen 2006) Ordinary soda-lime silica glass contains more than 65 weight-% of network former SiO_2, less than 14 wt-% of Na_2O and about 10 wt-% of CaO. The composition of bioactive glasses differs from that of soda-lime silica glass mainly in content of SiO_2. (Ben-Nissan and Ylänen 2006) There are three key compositional features, which differentiate bioactive glasses from conventinal glasses: (1) the amount of the SiO_2 is $45 - 60$ wt-%, (2) the Na_2O and K_2O content is high and (3) the Ca / P ratio is relatively high. (Hench 1996, Hench 1998a, Ben-Nissan and Ylänen 2006) These features make the surface of the glass highly reactive in aqueous media. Too high SiO_2 content increases the number of bridging oxygen ions, which reduces the network dissolution rate of the glasses, whereas too low SiO_2 content will lead to totally dissolved SiO_4 units. (Ben-Nissan and Ylänen 2006)

Hench and co-workers studied series of glasses containing SiO_2, Na_2O, CaO and constant 6 wt-% of P_2O_5. The compositional diagram for bone-bonding of this system is shown in Figure 1. The diagram is divided into four regions, $A - D$. Only the compositions inside the region A are bioactive. There is also a smaller region S (dashed line) inside region A, which indicates the compositions which can bond to both bone and soft tissues. The original bioactive glass, Bioglass® or 45S5, with a composition of 45 wt-% SiO_2, 24.5 wt-% Na_2O, 24.5 wt-% CaO and 6 wt-% P_2O_5 belongs to this kind of osteoinductive glasses. (Hench and Andersson 1993, Cao and Hench 1996, Hench 1998, Hench 2006)
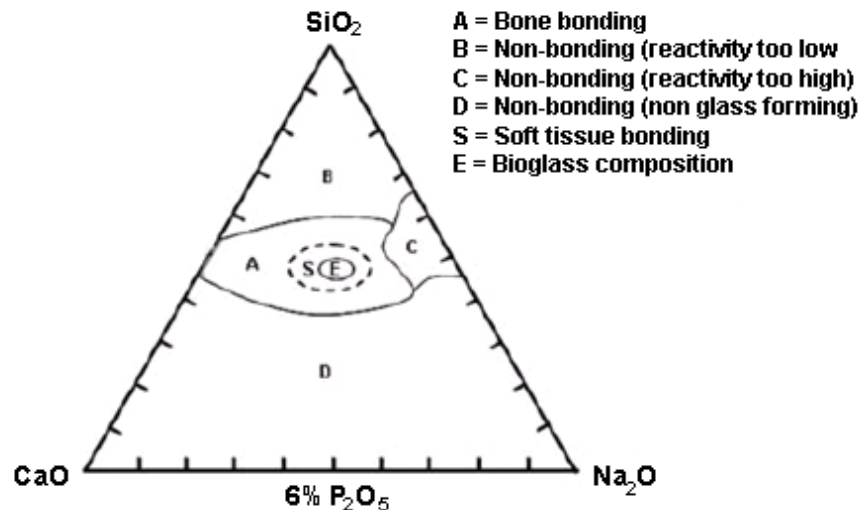
Figure 1.
Compositional diagram for bone-bonding. Region S in the middle is a region where bioactive glasses bond to both bone and soft tissues. (Modified from Hench 2006)

The bioactive response as well as the working properties, meaning the processability of the bioactive glasses, can be controlled by glass composition, for example by the addition of different compounds, such as MgO, K_2O, B_2O_3 and Al_2O_3. The exact effect of the addition of oxide in the multicomponent system is difficult to predict. Brink (1997a, 1997b) did an extensive study about the viscosity-temperature dependence and biological activity of several different glass compositions in the system Na_2O-K_2O-MgO-CaO-B_2O_3-P_2O_5-SiO_2. She reported that certain glass compositions have a wider working range compared to conventional bioactive glasses. Too low SiO_2 content leads to bioactivity, but the glass devitrifies (crystallizes), which limits is use only in the forms of crushed particles. When the SiO_2 content is increased to $53 - 56$ mol-%, devitrification can be avoided and the working range enlarged. The contents of alkali oxides and alkali earth oxides were also noticed to influence the working range of the glasses studied. The larger working range enables the expanded medical use of the bioactive glasses due to the possibility, for examples, of fiber spinning and flame spraying into microspheres. (Brink 1997a, Brink 1997b)

Recently some studies on bioactive glasses with a wide compositional range have been reported (Arstila 2008, Zhang 2008). Arstila (2008) examined the crystallization tendency of 36 different multicomponent glasses. The results indicated that the crystallization tendency was heavily dependent on the composition of the glass. For all glasses with compositions within the range of bioactivity, the crystallization tendency was found to be high. Early crystallization makes the melt processing of the glasses difficult and thus, for example, fiber spinning is not possible. Zhang (2008) studied 47 novel glass compositions and their compositional dependence on the *in vitro* behavior of the glasses and found that the *in vitro* reactivity correlated strongly with glass composition.

11

Table 2 presents some compositions of most commonly used melt-derived bioactive glasses.

Table 2.
Compositions of some melt-derived bioactive glasses (in wt-%).

Glass type	SiO_2	Na_2O	CaO	P_2O_5	K_2O	MgO	B_2O_3
Bioglass® (45S5)	45	25.5	25.5	6			
13-93	53	6	20	4	12	5	
9-93	54	12	11	2	15	5	1
1-98	53	6	22	2	11	5	1
S53P4	53	23	20	4			

Bioactivity

The concept of bioactivity is defined by Hench as follows: "*A bioactive material is one that elicits a specific biological response at the interface of the material which results in the formation of the bond between the tissues and the material*". This include a large number of different bioactive materials with different mechanism of bonding, the time dependence of bonding, the strength of bonding and the thickness of the bonding layer (Hench and Wilson 1993, Cao and Hench 1996). The level of bioactivity of the material can be ascertained using an index of bioactivity, I_B. The index of bioactivity relates to the time taken for more than 50 % of the interface to bond to bone ($t_{0.5bb}$):

$$I_B = \frac{100}{t_{0.5bb}} \tag{1}$$

where $t_{0.5bb}$ is the time for more than 50 % of the implant interface to be bonded to bone. According to the bioactivity index, bioactive materials can be classified into two classes: class A and class B. Materials having I_B value greater than eight ($I_B > 8$) can be considered class A bioactive material. (Cao and Hench 1996, Jones and Hench 2006, Jones 2007) These materials can bond with both bone and soft tissue and are thus both osteoconductive and osteoinductive. Osteoconduction is defined as a growth of bone along the implant surface from the implant / bone interface. Thus an osteoconductive material provides a biocompatible interface along which bone can migrate. Osteoinduction refers to the generation of the new bone on the implant, away from a bone interface, in the place where bone normally does not exist. (Jones 2007) Materials with I_B value between 0 and 8 ($I_B = 0 - 8$) are considered class B bioactive material. Class B materials are only osteoconductive. (Cao and Hench 1996, Jones and Hench 2006, Jones 2007)

Mechanism of bioactivity

A common characteristic of bioactive materials is their ability to react chemically in aqueous environments. This complex series of reactions leads to bone bonding. The bone bonding of the bioactive materials has been attributed to formation of hydroxyl-carbonate apatite (HCA) layer on the glass surface. The HCA is very similar to bone mineral and thus the bone can bond to it easily. (Hench and Wilson 1993)

The first reaction stages occurring on the surface of a bioactive glass do not depend on the presence of tissue. Only the aqueous environment is needed and thus the reactions also occur in distilled water and buffer solutions. The first reactions occur rapidly after the immersion in an aqueous solution. A rapid exchange of Na^+ and K^+ occurs from the glass with H^+ and H_3O^+ from the solution. The ion exchange happens easily because those cations are network modifiers and thus only weakly bonded to the glass network. The pH of the solution increases due to the replacement of H^+ ions with cations. The increase of hydroxyl (OH^-) ion concentration in the solution leads to the breakdown of the silica network (Si-O-Si bonds). Soluble silica is lost from the glass to the surrounding environment and silanol (Si-OH) groups are formed on the surface of the glass. The silanols need to go through condensation and repolymerization to form a silica rich layer on the glass surface. The Ca^{2+} and PO_4^{3-} ions released from the glass, together with those from the solution, form an amorphous calcium phosphate rich layer on top of the silica rich layer. Finally the calcium phosphate layer crystallizes into HCA, resembling the hydroxyapatite of the bone. The above stages happen quite quickly, within hours or days. The rate of the surface reactions is mainly controlled by the glass composition. (Hench and Andersson 1993, Jones and Hench 2006, Ben-Nissan and Ylänen 2006, Jones 2007)

After formation of the HCA layer, bonding of the tissue to the layer requires an additional series of reactions. These reactions are not so well defined and the factors controlling the rate of the reactions are not entirely known (Hench and Andersson 1993). The biological mechanisms of bonding that follow the HCA layer formation are suggested to involve the adsorption of growth factors in the HCA layer to activate differentiation of stem cells. This is followed by the attachment of the stem cells and their differentiation to bone growing cells, such as osteoblasts. (Jones and Hench 2006, Jones 2007) A rapid repair of bone requires both differentiation and proliferation of osteoblasts. A synchronized sequence of genes must be activated in the osteoblasts so that they undergo cell division and then synthesize an extracellular matrix capable of mineralizing to become bone. Recent studies have shown that the cellular response of osteoblasts to bioactive glasses is under genetic control. (Hench 2001, Hench and Polak 2005, Hench 2006)

2.2.2. Tricalcium phosphates

Calcium phosphates are the major components of bone mineral. Thus it is natural that calcium phosphate based bioceramics have been used clinically for more than twenty years. Depending on whether a resorbable or bioactive material is desired, different phases of calcium phosphate bioceramics can be used (Hench 1996, Hench 1998a, LeGeros 2008). Tricalcium phosphates (TCP) are one of the most commonly used resorbable calcium phosphate bioceramics in implant materials. TCP has been shown to resorb *in vivo* with new bone growth replacing the implanted TCP. Thus TCP can be considered an osteoconductive biomaterial. This is a significant advantage compared to other biomedical materials which are not resorbed and replaced by bone.

The chemical composition of TCP is $Ca_3(PO_4)_2$, which means a Ca / P ratio of 1.5 (Klein *et al.* 1993, Rey *et al.* 2008). TCP is known to exist in four different forms, amorphous TCP (am-TCP), apatitic TCP (ap-TCP), α-TCP and β-TCP, all of which have been used as biomaterials (Table 3). The two first mentioned are low-temperature, unstable phases, which are generally achieved by precipitation, whereas the two last mentioned are high-temperature crystalline phases. The use of TCP as biomaterial depends on their stability domains and thus sintered ceramics can only be obtained from α- and β-TCP. (Rey *et al.* 2008) α-TCP has aroused same interest in the biomedical field due to its quick resorption rate. On the other hand, β-TCP is a slowly degrading bioresorbable bioceramics, which has been observed to have significant biological affinity and activity. (Kalita *et al.* 2007)

When TCP is implanted into living tissue, it interacts with body fluids to form hydroxyapatite (HA) as follows: (Cao and Hench 1996, Hench 1996, Oonishi and Oomamiuda 1998)

$$4\ Ca_3(PO_4)_2\ (solid) +\ 2\ H_2O\ \rightarrow Ca_{10}(PO_4)_6(OH)_2\ (surface) +\ 2\ Ca^{2+} + 2HPO_4^{2-} \quad (2)$$
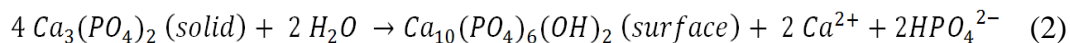
TCP is theoretically considered to be an ideal implant material due to its degradation and replacement with natural tissues over time. This leads to the regeneration of tissues and thus solves the problem of interfacial stability. However, there are some limitations in the clinical use of resorbable TCP. One is that the mechanical performance of the implant must match the healing and repair rate of tissue. Thus the degradation rate must be controlled. (Cao and Hench 1996)

Table 3.
Tricalcium phosphate as biomaterial. (Rey et al. 2008)

Type of material	Type of TCP involved	Application	Main TCP-related effects
Ceramics	α- and β-TCP	Bone substitutes	Biodegradable
		Small bone replacement	Dissolution and hydrolysis (for α-TCP)
		Tissue engineering	
Ca-P ionic cements	α-TCP, am-TCP,	Bone substitutes	Active hardening agents
	ap-TCP (end-product)	Dental applications	Biodegradable, surface reactivity
	β-TCP (brushite cements)		Provider of Ca^{2+} and PO_4^{3-} ions
Coatings	am- and ap-TCP,	Coating of metallic prostheses	Biodegradable, reactive coating
	α- and β-TCP		
Mineral-organic composites	am-TCP, α- and β-TCP	Bone replacement and bone substitutes	Mechanical properties,
		Tissue engineering	Ca and P release in relation with
		Dental restorative materials	biological activity

am-TCP = amorphous TCP
ap-TCP = apatitic TCP

15

The resorption or biodegradation of different calcium phosphate bioceramics, including tricalcium phosphate, is caused by three factors: physiochemical dissolution, which depends on the pH of the surrounding environment, physical disintegration into small particles and biological factors, such as phagocytosis. (Hench 1996, LeGeros 2008) All calcium phosphate bioceramics degrade at varying rates. The degradation rates are in the following order: (Koerten *et al.* 1992, Hench 1996, Hench 1998a, Oonishi and Oomamiuda 1998, Huang and Best 2007, LeGeros 2008, Rey et al. 2008)

$$\text{Tetracalcium phosphate} > \alpha\text{-TCP} > \beta\text{-TCP} \gg \text{HA} > \text{Fluoroapatite (FA)} \qquad (3)$$

The degradation rate of calcium phosphates depends on many factors. Increase in the surface area increases the degradation rate. Thus powders degrade faster than porous solids, which degrade faster than dense solids. The crystallinity of the calcium phosphate affects and thus the degradation rate decreases when the crystallinity, crystal perfection and crystal and grain size increases. The ionic substitutions also affect the degradation. (Hench 1996) The degradation rate can be tailored by using biphasic calcium phosphates (BCP), meaning a mixture of HA and β-TCP. The HA / β-TCP ratio can be varied and the higher the β-TCP content in BCP, the higher the dissolution rate. (Huang and Best 2007, LeGeros 2008)

The *in vivo* bone formation, degradation and resorption of TCP have been reported in numerous studies (e.g. Koerten and van der Meulen 1999, Merten *et al.* 2001, Yuan *et al.* 2001, Wiltfang et al. 2002, Kondo *et al.* 2005, Ogose *et al.* 2006). Clinical studies of β-TCP as a bone substitute have also been published (e.g. Galois *et al.* 2002, Ogose *et al.* 2006).

Yuan *et al.* (2001) studied the bone formation on α- and β-TCP in dogs. The results indicated that there were enormously different tissues responses between α- and β-TCP. β-TCP seemed to induce bone formation in the soft tissues of dogs, whereas α-TCP seemed not to. The behavior of α-TCP may be a result of its rapid dissolution, which produces large amounts of Ca^{2+} and PO_4^{3-} ions. The local concentration could become too high for the cells to survive and this may inhibit bone formation. Wiltfang *et al.* (2002), for one, used minipigs with cancellous bone defects to compare the degradation characteristics of α- and β-TCP. According to this study both materials can be classified as bone-rebuilding materials. Histological and cellular level events occurring around the β-TCP implanted in rat femoral condyles were studied by Kondo *et al.* (2005). The results showed that the highly purified β-TCP provided early bone conduction, which was followed by bioresorption of β-TCP. This led to the replacement of large parts of the β-TCP with newly formed bone. In conclusion the results suggested that β-TCP is a biocompatible and resorbable bioceramic. Koerten and van der Meulen (1999) compared the *in vitro* and *in vivo* degradation of three different calcium phosphate ceramics, β-TCP, HA and FA. The degradation was observed to occur under all conditions, but the rate of degradation depended on the type of ceramic. As reported by

others *in vitro*, β-TCP was observed to degrade faster than HA and HA faster than FA both *in vitro* and *in vivo*. (Koerten and van der Meulen 1999)

2.3. Composites

2.3.1. Basic concept of composites

There are three main points to be made when dealing with a definition of an acceptable composite material for use in structural applications:

i. It consists of two or more physically distinct and mechanically separable materials.

ii. It can be made by combining the separate materials in such a way that the dispersion of one material in the other can be done in a controlled way to achieve optimum properties.

iii. The properties of the resulting composite are superior, and possibly unique in some specific respects compared to the properties of the individual components.

The last point provides the main reason for the development of composite materials. (Hull 1981) Composite materials offer a variety of advantages over homogenous materials. The one advantage of the composites is that the mechanical, biological and physiological properties can be tailored to the requirements of the applications better than with individual homogeneous materials (Reinhart and Clements 1987, Huang and Ramakrishna 2004). Composites as biomaterials also impose requirements. The most important is the demand for biocompatibility. It is absolutely essential that each constituent component of the composite, as well as the entire composite, is biocompatible. (Lakes 2003)

Composite materials can be composed in many ways. The different phases of the composite can be selected from any material classes, including metals, ceramics and polymers. Combinations of materials of the same type are also possible. To simplify, when focusing on a two-component composite, the phases which can be distinguished are a continuous phase, a dispersed phase and an interface (Figure 2). The continuous phase is better known as matrix material. Matrix material confers the overall form of the composite. The dispersed phase may be continuous or discontinuous. Most often the dispersed phase is stiffer than the matrix material and thus it is considered to be a reinforcement component. (Daniel and Ishai 1994, De Santis *et al.* 2009) However, the composite structure can also give some additional functionality to biomedical composites, such as bioactivity, controlled drug release and desired biodegradation profile.

17
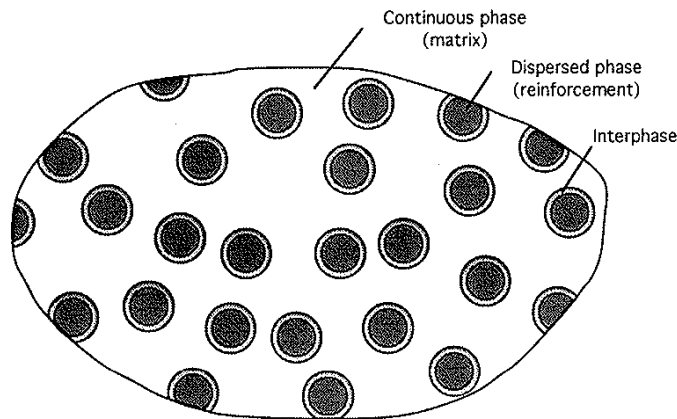
Figure 2.
Phases of composite materials. (Daniel and Ishai 1994)

The material properties of composites can be tailored by altering the composition, interfacial bonding and physical arrangement of the different phases in the composite (Huang and Ramakrishna 2004). The properties depend very much on the structure of the composite. Specifically, the most important things affecting the properties of the composites are the shape of the dispersed phase, the volume fraction occupied by the dispersed phase and the interface between the constituents (Daniel and Ishai 1994, Lakes 2003). The distribution of the dispersed phase determines the homogeneity and uniformity of the material. If the distribution is nonuniform, the material is more heterogeneous and thus there is a higher probability of failure. The anisotropy of the composite properties depends on the geometry and orientation of the disperse phase. (Daniel and Ishai 1994) The interface between the constituents also plays a major role, especially when determining the mechanical performance and environmental stability of the composites. Thus the interface is very important in the field of biomedical composites. The adhesion at the interface of the constituents can be based on either mechanical or chemical bonding or both. The mechanical bonding depends on the surface topography and morphology of the constituents, whereas the chemical bonding is ideally promoted by surface treatments or coatings. (De Santis *et al.* 2009)

Composites can be classified in various manners. The classification may be based on either the matrix phase or the dispersed phase. When classifying according to the matrix material used, the resulting classes are metal matrix composites, ceramic matrix composites and polymer matrix composites. In biomedical applications the most used are polymer matrix composites. (Huang and Ramakrishna 2004) Besides classification by matrix phase, composites can be divided according to the dispersed phase, mostly based on the shape of the dispersed phase. The main shape categories are particles (with no long dimensions), fibers (with one long dimension) and platelet or lamina (with two long dimensions). (Lakes 2003)

18

Different phases have different roles in the composite material. The roles depend on the composite type and application. In the case of low or medium performance composites, the reinforcement provides some stiffening and only local strengthening of the material. In these cases the reinforcement phase is usually in the form of short fibers or particles. The mechanical properties of such composites are based on the matrix material, which is responsible for the main load-bearing. In the case of high performance structural composites, the reinforcement is the backbone of the material. Usually the continuous fibers determine the stiffness and strength of the composites in the direction of the fibers. The function of the matrix material is to protect and support the sensitive fibers and transfer local stresses. (Daniel and Ishai 1994)

Composites are used in biomedical applications mainly due to the possibility of the tailoring their mechanical properties to meet the specific requirements of each application. This needs a clear understanding of the structure-property relationship of the composites. In many composite materials this relationship is highly complex and thus predicting the mechanical properties beforehand is almost impossible. However, for some structures, the prediction of the properties is relatively simple. (Lakes 2003) The simplest estimation of the properties of the composites is the equation called the 'rule of mixtures'

$$E_{composite} = E_f V_f + E_m V_m \qquad (4)$$

where $E_{composite}$ is the modulus of the final composite, E_f the modulus of the reinforcing phase (most often fiber), E_m the modulus of the matrix material, V_f the volume fraction of the reinforcing phase and V_m the volume fraction of the matrix material. (Lakes 2003, Hull and Clyne 1996, Callister 2000) The rule of mixtures can also be applied to some other properties of composites, such as density and strength. However, this requires that there is no porosity or void-space in the structure of the composite. (Ashby 2001) The rule of mixture simply indicates that the composite property is a weighted mean between the properties of the two components, depending only on the volume fraction of the reinforcing phase (Hull and Clyne 1996). Most often it is not that simple. There is a need for more powerful micromechanics theories, thus leading to more complicated mathematical formulae. (Daniel and Ishai 1994, Hull and Clyne 1996, Callister 2000, Ashby 2001, Kelly and Mortensen 2001, Huang and Ramakrishna 2004, Lakes 2003)

Mechanical properties of the composite can be improved, for example, by increasing the interfacial bond strength between the reinforcing phase and matrix material. That is because the failure of the composite depends mostly on the failure of the interface between the phases. If the interfacial bond strength is high enough, the composite will stand higher forces. (Hull and Clyne 1996) Generally, the wetting of the surface of the reinforcing phase with matrix material is important. The bonding of the reinforcing phase to the matrix material depends on the hydrophilicity or polarity of the reinforcement and the available polar groups of the matrix material. Thus the chemical

interactions in the interface will lead to much improved bonding, and further mechanical properties. (Wang *et al.* 2000a) One way to influence the durability and mechanical strength of the interface is to use certain coatings, usually termed coupling agents, or surface treatment. For example, silane coupling agents are widely used in cases of glass fiber reinforced polymer matrix composites. Coupling agent is intended to react both with the surface of the glass and matrix phase. (Hull and Clyne 1996) Also mechanical interlocking between the reinforcing phase and matrix material can make the interface much stronger.

2.3.2. Composites for bone repair

Human bone can be considered to be a very complex composite structure. Thus it is quite obvious that an ideal material for bone repair is a composite structure, which mimics the structure of the natural bone. One reason for the use of composite materials in bone repair is that the mechanical properties of the implant can be tailored to match those of the bone tissue. The stiffness of bone repair implants especially should be similar to that of bone and only few, or even no, individual materials have been reported to have stiffnesses close to those of cortical bone. Additionally, in most cases the initial strength of the implant should be high enough, higher than that of bone. The second reason for the use of composites is the tailoring of the biological properties. The composite structure can enable the formation of a strong biological interface between the implant and the bone tissue. The third reason relates to biodegradable composites. They degrade gradually and thus allow the gradual transfer of the load from the implant to the bone. The releasing of products which may accelerate bone healing would also be advantageous. (Tanner 2010)

Some bioceramics have osteoconductive potential and excellent bone bonding properties and are thus optimal for bone repair. However, at the same time they are ceramic in their nature, which usually means brittle behavior, and thus they do not as such fulfill the required mechanical properties to replace bone tissue. On the other hand, polymeric biomaterials have more applicable mechanical properties, but most of these polymers do not have properties to facilitate bone tissue healing. Bioactivity and bone bonding ability together would be beneficial for bone tissue implants and thus many research groups have started to study the possibility of combining the bioceramics together with polymeric materials.

The idea of the combining bioceramic and biomedical polymer is not new. The need for such load-bearing structures started with studies of bone substitutes, with physiological and mechanical properties similar to those of living bone as early as in the 1980's. Hydroxyapatite (HA) reinforced high density polyethylene (HDPE) composite (HA/HDPE) (known commercially as HAPEX^{TM}) was the first bioactive ceramic-polymer composite to be developed as a biomaterial for bone replacement on the basis

of producing suitable mechanical compatibility. HA was shown to stiffen PE, and PE to toughen the composite. Additionally, because HA resembles bone mineral, natural bone will grow onto HA. (Bonfield 1993) HA/PE composite is a biostable composite, hence it does not degrade over time, and its mechanical properties were shown to remain constant in physiological solution. In addition, HA/PE composite has been found to provide a favourable environment for human osteoblast-like cell attachment (Huang *et al.* 1997a).

The research and development of other osteoconductive composites using the same basis than HA/PE has grown due to the encouraging results with HA/PE composites. Various filler and matrix materials have been studied. HA can be replaced by more bioactive bioceramic, such as bioactive glass, to obtain a stronger bond between the implant and the bone tissue. The formation of the bone-like apatite on the Bioglass®/PE composite surface *in vitro* was observed to be faster than on the surface of HA/PE composite. This indicated higher bioactivity. However, the mechanical properties of the Bioglass®/PE composite decreased during immersion in aqueous environment, whereas the mechanical properties of the HA/PE remained unchanged. (Huang *et al.* 1997b, Wang 2003)

Changing the matrix polymer from PE to polysulfone (PSU), serves to improve the mechanical properties of the composite. Therefore, HA/PSU composite has been developed as a hard tissue replacement material. (Wang *et al.* 2001) Hydrostatic extrusion provides a different approach to improve the mechanical properties of the HA/PE composites. In this method the polymer chains are aligned to a certain orientation using back pressure. This leads to an increase in the stiffness and strength in the orientation direction. Method is suitable also for brittle materials, because only compressive stresses are used. (Ladizesky *et al.* 1997a, Wang *et al.* 2000b) Ladizesky *et al.* (1997a) have reported that using hydrostatic extrusion the highly filled HA/PE composite achieved the mechanical properties within the bounds for cortical bone and thus showed promise also for major load-bearing applications. Another technique to improve the mechanical properties of HA/PE composite involve the reinforcement of the polymer matrix with high-performance polyethylene fibers (Ladizesky *et al.* 1997b, Ladizesky *et al.* 1998).

The mechanical properties of HA/PE composites have also been improved by increasing the interfacial bond between the HA particles and PE matrix. Different surface treatments were used; silane coupling for HA and acrylic acid grafting for PE. This was reported to produce interdigitation of PE into the HA particles, which increased the mechanical properties and gave a more ductile material. (Deb *et al.* 1996, Wang *et al.* 2000a)

Self-reinforced polymers are a specific group of composites. Self-reinforced structure is formed when part of the microstructure of the polymer is transformed into the fibrous, oriented reinforcement elements. This creates an oriented, high strength structure with

reinforcing fibrous element having the same chemical composition as the matrix polymer. Thus the self-reinforced polymer can be considered to be a composite of polymer fibers or fibrils in the polymer matrix. The adhesion between the fibers and matrix polymer is excellent, because the chemical composition is the same, and thus the mechanical properties of the polymer are enhanced. Self-reinforced structure can be achieved in different ways, such as by mechanical deformation. The most effective way to create the self-reinforced structure is solid state die-drawing, in which the polymer billet is drawn through a heated die at a temperature above the glass transition temperature of the polymer. This method was successfully performed for bioabsorbable polymers already in the 1980's. Self-reinforced bioabsorbable polymers have so far been used extensively in implants in bone fixation, for example in orthopedics. (Törmälä 1992, Törmälä *et al.* 1998, Rokkanen *et al.* 2000) Self-reinforced structures can also be prepared by starting from fibers followed by very controlled compression molding. In this method, the compression temperature is chosen to melt only the surfaces of the fibers allowing the matrix polymer to form and attach the fibers together. The choice and controlling of the process parameters, such as temperature, pressure and time, is crucial. The reinforcing effect of the fibers must be retained despite processing. (Hine *et al.* 1993). Both solid state die-drawing and compression molding of the fibers have also been successfully applied to prepare bioceramic and bioactive glass containing bioabsorbable composites (Kellomäki *et al.* 1997, Niiranen and Törmälä 1999, Kellomäki 2000, Kellomäki *et al.* 2000, Bleach *et al.* 2001, Niiranen *et al.* 2001, Bleach *et al.* 2002, Niiranen *et al.* 2004, Ellä *et al.* 2005, Huttunen *et al.* 2006).

2.3.3. Osteoconductive ceramic / bioabsorbable polymer composites

It has been reported that the ideal bone graft should be biocompatible, osteoconductive, possessing mechanical properties similar to those of natural bone, and able to support angiogenesis. A bioabsorbable bone graft is especially advantageous due to its controlled degradation and thus replacement by host tissue. (Laurencin and Lu 2000) As no single material possesses all these properties of an ideal bone graft, a logical approach is to develop composite material consisting of osteoconductive ceramic and bioabsorbable polymer.

It is probable that the bioceramic addition, among other things, affects the properties and degradation behavior of the bioabsorbable polymer matrix. The following paragraphs review several studies on the effects of the different bioceramic additions on the properties and degradation behavior of the various bioabsorbable matrix polymers. The comparison of these reviewed studies is problematic due to the number of factors that can affect degradation behavior of polyesters (Table 4).

Table 4.

Some factors that can affect degradation behavior of polyesters. (Modified from Törmälä et al. 1998, Rezwan et al. 2006, Cotton et al. 2008)

Factor	Example
Microstuctural factors	
Polymer or copolymer chemical composition / monomer ratio	Increasing glycolide units increases hydrolytic degradation
Crystallinity	Increasing crystallinity retards degradation
Resiudal monomer / oligomer content (acidic end groups)	Increasing acidic end groups content increases hydrolytic degradation
Initial molecular weight / iv	Higher molecular weight increases the time to total degradation
Filler addition	Depending on the material and content of the filler, the degradation can be either slowed or acceletared
Porosity	Pores may also either slow or acceletare the degradation
Macrostructural factors	
Size and geometry of the implant	Large implants degrade slower
Environmental factors	
Surrounding environment	May either retard or acceletare the degradation
Moisture content	Affets degradation during storage and processing initiating the formation of acid end groups

Bioactive glass / bioabsorbable polymer composites

Bioactive glass can be combined with bioabsorbable polymer matrix in different forms, such as particles, fibers and coatings. Currently the most bioactive glasses are used as particulates, but there is also increasing interest in other physical forms of bioactive glasses.

Several studies have been reported on porous composites containing bioactive glass and bioabsorbable polymer (Boccaccini *et al.* 2002, Roether *et al.* 2002, Blaker *et al.* 2003, Gough *et al.* 2003, Lu *et al.* 2003, Maquet *et al.* 2003, Boccaccini and Maquet 2003, Maquet *et al.* 2004, Li *et al.* 2005). Maquet *et al.* (2003, 2004) studied highly porous composites of poly-D,L-lactide and poly(lactide-co-glycolide) and bioactive glass particles (45S5 Bioglass®). The composites were manufactured by thermally induced phase separation process (TIPS) and subsequent solvent sublimation using different bioactive glass contents (0 – 50 wt-%). The bioactive glass addition was observed to enhance the mechanical properties of the foams and decrease the pore volume. The presence of the bioactive glass was also observed to delay the *in vitro* degradation rate of the polymer in terms of molecular weight compared to the plain polymer foams. This

was thought to be due to the buffering effect of the buffer solution, which was caused by dissolution of the alkaline ions from the Bioglass®. During the *in vitro* period studied, the water absorption (WA) of the plain poly(lactide-co-glycolide) foams was significantly lower than in the composites but still slightly higher than in the plain poly-D,L-lactide foams. This confirms the greater hydrophilicity of poly(lactide-co-glycolide) as compared to poly-D,L-lactide. The weight loss (WL) of the plain matrix polymers remained nearly unchanged whereas the bioactive glass containing composites lost 9 – 15 % of their weight during the *in vitro* period studied. The weight loss depended on the bioactive glass content so that the weight loss was greater with higher bioactive glass content. The bioactive glass content also affected the bioactivity of the composites. This was inferred from the rapid formation of a hydroxyapatite layer on the surface of the composites containing bioactive glass. All samples studied were observed to retain their structural integrity and three-dimensional (3D) morphology throughout the whole *in vitro* period studied (12 – 18 weeks) which indicated that the degradation process is still in an early stage. Maquet *et al.* (2003, 2004) concluded that it was possible to modulate the degradation rate of the composite scaffolds by varying the composition of the composite. Similar results have been reported by Boccaccini and Maquet (2003).

Delayed degradation of the matrix polymer was also observed in the porous composite scaffolds of polyhydroxybutyrate-polyhydroxyvalerate (PHBV) with sol-gel derived bioactive glass (58S). Porous composites containing 0 – 20 wt-% of bioactive glass were manufactured by compression molding, thermal processing and salt particulate leaching method. The *in vitro* degradation results showed that the bioactive glass addition increased the water absorption and resulted in an increased weight loss due to the dissolution of the bioactive glass particles. The decrease in the molecular weight of the bioactive glass containing composites was slower than in plain matrix polymer. The *in vitro* bioactivity of the bioactive glass containing scaffolds was confirmed as the composites induced the formation of hydroxyapatite layer after being soaked in SBF for 3 days. The results revealed the option to modify the degradation rate of the scaffold by incorporation of bioactive glass into the polymer matrix. (Li *et al.* 2005)

Li and Chang (2005) also studied the pH compensation effect of the inorganic fillers, such as hydroxyapatite (HA), wollastonite (W) and bioactive glass 45S5, on the degradation of porous poly(lactide-co-glycolide) (PLGA) scaffolds. The results indicated that the pH of the PLGA decreased to a value of 4.3 during the 8 weeks *in vitro* period, whereas the pH of the composites containing wollastonite or bioactive glass was maintained fairly constant throughout the *in vitro* period. In addition the pH stabilization, the wollastonite and bioactive glass additions delayed the degradation of PLGA in the composites. HA, for one, was reported to accelerate the degradation.

In addition to highly porous structures, dense systems of bioactive glass and bioabsorbable polymers have also been studied. Zhou *et al.* manufactured bioactive glass poly-L-lactide composite membranes by solvent evaporation technique. (Zhou *et*

al. 2007, Zhou *et al.* 2009) The sol-gel derived bioactive glass was homogenously distributed in the composite achieving a 10 wt-% bioactive glass content. The *in vitro* degradation results showed that the addition of bioactive glass reduced the overall degradation rate in terms of mechanical properties, mass loss and molecular weight loss. Zhou *et al.* (2009) thought that the reason for such behavior was the neutralizing effect of the dissolving of the bioactive glass. The interfaces between the matrix and filler material were also thought to be important because they facilitate the diffusion of the degradation products. In the solvent evaporated composite the matrix polymer was seen to cover the bioactive glass particles on the composite surface and thus the bioactive glass cannot immediately be in contact with the surroundings when immersed in the buffer solution. Thus the hydroxyapatite layer on the surface of the bioactive glass is not formed as fast as, for example, in the porous composites reviewed above. However, despite thus the rod-like crystals were deposited on the surface after 3 days *in vitro* and after 14 days the hydroxyapatite layer was formed. (Zhou *et al.*, 2007)

Bioactive glass can also be added to composites as a coating. For example, the coating of biodegradable polymer sutures with bioactive glass has been studied (Stamboulis *et al.* 2002a, Stamboulis *et al.* 2002b, Boccaccini *et al.* 2003, Bretcanu *et al.* 2004). The hypothesis in coating biodegradable sutures is that their bioactivity, and thus bone bonding ability, can be enhanced. Another reason is the controlling of the morphological changes, such as degradation rate. Stamboulis *et al.* (2002a) have conducted preliminary experimental work on coating commercially available Polyglactin 910 (Vicryl®) sutures with bioactive glass (Bioglass®) powder. The coating, which was achieved by a simple layer-pressing procedure, was not very uniform and homogeneous. However, the results showed that the mechanical performance of the suture can be altered by coating with bioactive glass. Bioactive glass was seen to act as a protective barrier affecting both the extent and rate of the degradation of the sutures. Another coating technique, slurry-dipping, was examined (Bretcanu *et al.* 2004). The bioactive glass coating was observed to reduce the initial tensile properties of the sutures. However, the strength retention was improved, which means slower degradation rate.

As noted, many research groups have reported the neutralization of acidic degradation products of polylactide based composites caused by bioactive glass. This is based on the alkaline environment created when the bioactive glass reacts with surrounding fluids. The neutralization slows down the degradation of polyesters when used as a matrix polymer for bioactive glass.

However, contradictory results have also been reported. Rich *et al.* (2002) reported that the presence of bioactive glass S53P4 filler particles in poly(ε-caprolactone-co-DL-lactide) matrix accelerated degradation compared with a plain matrix polymer sample. The composite samples were manufactured by compounding and compression molding using different amounts (40, 60 and 70 wt-%) of bioactive glass with different particle size distributions (< 45 μm and $90 - 135$ μm). The presence of bioactive glass was

observed to affect the degradation rate of the composites *in vitro*. The water absorption into the bioactive glass containing samples was observed to be higher than absorption into the plain matrix polymer. Small particles with a larger surface / volume ratio, also enhanced water absorption compared to larger particles. This is because the diffusion mostly occurs along the interfaces between the bioactive glass and the matrix polymer. In turn the increased water absorption clearly has an influence the hydrolytic degradation. The molecular weight of the bioactive glass containing composite decreased more rapidly the greater the number of particles and the smaller the particle size distribution of the bioactive glass was. Moreover the *in vitro* bioactivity was found to be dependent on the number of particles and the particle size distribution of the bioactive glass used. The higher the bioactive glass content and the surface / volume ratio, the faster was the Ca-P formation *in vitro*. (Jaakkola *et al.* 2004, Rich *et al.* 2002)

Tricalcium phosphate / bioabsorbable polymer composites

The addition of tricalcium phosphate (TCP), both β-TCP and α-TCP, to bioabsorbable polymer matrix has been widely studied by many research groups (Ignatius *et al.* 2001, Kikuchi *et al.* 2002, Mellon *et al.* 2003, Kikuchi *et al.* 2004, Kobayashi and Sakamoto 2006, Ehrenfried *et al.* 2008, Kobayashi and Sakamoto 2009, Yang *et al.* 2009). TCP addition was reported to both slow and accelerate the degradation rate of the matrix polymer.

Kikuchi *et al.* (2002) studied the pH buffering effect and the changes in mechanical properties *in vitro* for the composites containing β-tricalcium phosphate (β-TCP) and copolymerized poly-L-lactide (CPLA). The results showed that the TCP / CPLA composites retained their mechanical strength longer than plain CPLA. This was due to the pH buffering effect observed for composites. The pH of the surrounding solution remained neutral throughout the *in vitro* period. Kikuchi *et al.* (2004) also combined β-tricalcium phosphate (β-TCP) with flexible and thermoplastic copolymer poly(L-lactide-co-glycolide-co-ε-caprolactone) (PLGC). A pH maintenance effect during the *in vitro* experiments was observed and in addition a chemical interaction between the surface of the TCP and the ester C = O bonds of the polymer was seen. The chemical interaction enhanced the mechanical strength of the composites and thus the composites were reported to have even better mechanical strength than plain matrix polymer. The molecular weight of the composites also decreased more slowly than that of plain matrix polymer. The total decomposition of the plain matrix polymer occurred after 8 weeks *in vitro,* whereas the composites only decomposed after 24 weeks *in vitro*.

Kobayashi and Sakamoto (2006, 2009) studied injection molded β-tricalcium phosphate (β-TCP) / poly-L-lactide (PLLA) composites with different β-TCP contents (5 – 14 wt-%). It was observed that the bending strength of the composites decreased with increasing β-TCP content, whereas bending modulus increased with increasing

β-TCP content. However, the bending properties of the composites were within that of cortical bone. The 8-week *in vitro* experiment in pH 7.4 revealed that the mechanical properties remained practically unchanged throughout the period studied. (Kobayashi and Sakamoto 2006) The effect of the different pH (7.4 and 6.4) of the buffer solution on the retention of the mechanical properties of the composites containing β-TCP and poly-L-lactide (PLLA) was also ascertained (Kobayashi and Sakamoto 2009). The retention of the mechanical properties depended on β-TCP content. If the content was low, the mechanical properties were mainly retained longer, hence the composites with larger β-TCP content degraded fastest. In the lower pH, the degradation of all composites was accelerated.

Claes *et al.* (1996) have developed a new pin made of poly-L/DL-lactide for reduction of small bone fractures. The pin had an initial bending strength of 155 – 163 MPa, which was enough for the fixation of small bones. The degradation rate of the pin was also reported to be slow enough for the healing of the bone tissue. To further improve the biocompatibility of these pins, 10 and 30 wt-% of β-TCP was added to the polymer matrix (Ignatius *et al.* 2001). The biocompatibility was successfully improved but it happened at the expense of the mechanical properties and degradation rate. β-TCP addition reduced the initial mechanical properties and it was also observed that the mechanical properties of these composites decreased faster *in vitro* than plain matrix polymer. The composite containing 30 wt-% of β-TCP behaved differently from composite containing 10 wt-% of β-TCP. The changes in the shape, especially in the diameter of the samples, were most significant in composite containing 30 wt-% of β-TCP. It swelled remarkably during hydrolysis. This was thought to be due to the large uptake of water. The water uptake, and thus the decrease in adhesion between the filler material and matrix polymer, is also thought to be a reason for the faster loss of mechanical properties. As a conclusion, Ignatius *et al.* discovered that requirements for the fixation of small bone fractures with improved biocompatibility were fulfilled by composite containing 10 wt-% of β-TCP, but not by composite containing 30 wt-% of β-TCP.

Although α-TCP resorbs very quickly, it has also been studied in composites with bioabsorbable polymers. Ehrenfried *et al.* (2008) examined the effect of the addition of different fractions (0 – 40 wt-%) of α-TCP powder to poly(lactide-co-glycolide) (PLGA) by the hot-pressing method. The mechanical properties of the PLGA were found to be enhanced when α-TCP was added. In addition, the degradation rate of these samples was significantly slower and the pH of the solution was successfully buffered. However micro-computed tomography (μ-CT) images revealed that all samples degraded faster inside the structure, as is typical for PLGA polymers (Li *et al.* 1990b, Li 1999), although the buffering within the sample might be expected to reduce the internal autocatalysis. (Ehrenfried *et al.* 2008)

A comparative study of α-TCP and β-TCP addition to the poly(lactic-co-glycolic acid (PLGA) was conducted by Mellon *et al.* (2003). The samples containing 20, 40 and 60 wt-% of α-TCP and 40 wt-% of β-TCP were manufactured by hot pressing and the surface of the samples were polished to expose TCP particles on the surface. The degradation of the samples was followed by measuring the pH of the solution and mass loss of the samples during the *in vitro* experiment. The rate of degradation was: PLGA >> 20 wt-% α-TCP > 40 wt-% β-TCP > 40 w-% α-TCP > 60 wt-% α-TCP. Both α-TCP and β-TCP were seen to delay autocatalytic degradation of PLGA by up to 6 times by stabilizing the pH. α-TCP dissolved more rapidly than β-TCP and thus stabilized the pH and degradation of PLGA more effectively.

The size of the TCP particles has been also reported to effect the degradation rate of the matrix polymer (Yang *et al.* 2009). 20 and 40 wt-% of α-TCP nanoparticles and microparticles was added to the poly(D,L-lactide-co-glycolide) (PLGA) matrix by a modified solvent-evaporation method. The results indicated that the nanocomposites degraded more slowly and more homogenously than the microcomposites and plain PLGA.

Other osteoconductive bioceramics / bioabsorbable polymer composites

In addition to bioactive glasses and TCP, also some other osteoconductive bioceramics, such as hydroxyapatite (Verheyen *et al.* 1993, Van der Meer *et al.* 1996, Guo *et al.* 1998, Bleach et al. 2001, Kasuga *et al.* 2001, Li and Chang 2005, Gay *et al.* 2009, Aboudzadeh *et al.* 2010, Chuenjitkuntaworn *et al.* 2010), biphasic calcium phosphate (Iooss *et al.* 2001, Bleach *et al.* 2002), calcium carbonate (Ara *et al.* 2002, Cotton *et al.* 2008) and coral (Li and Vert 1996) have been used in composites with bioabsorbable polymers. Hydroxyapatite is probably the most commonly used filler material due to its long history and similarity to bone mineral. Hydroxyapatite has also been reported to act either as a hydrolysis barrier, thus delaying the degradation of bioabsorbable polymers (Verheyen *et al.* 1993, Van der Meer *et al.* 1996, Guo *et al.* 1998) or as an activator which accelerated the degradation rate (Li and Chang 2005).

Cotton *et al.* (2008) modified the degradation rate of poly(DL-lactide-co-glycolide) by the addition of calcium carbonate (16, 36 and 51 wt-%). The addition of calcium carbonate decreased the degradation rate of injection molded plain matrix polymer. High filler content negatively affected the mechanical properties of the composite and because a higher than 36 wt-% concentration of calcium carbonate was not found to delay degradation further, the 36 wt-% calcium carbonate content was selected for optimal filler content for use in orthopedic fixation devices due to its good initial strength, sufficient pull-out strength during degradation and final degradation rate in terms of mass loss. Ara *et al.* (2002) compared the effect of different calcium compounds with different acidity and basicity on the degradation behavior of poly(DL-

lactic acid-co-glycolic acid). The results showed that the most basic calcium carbonate was the most effective in delaying the degradation, whereas the most acidic calcium dihydrogenphosphate was least effective.

Natural coral was incorporated into high molecular weight poly(DL-lactic acid) in a weight ratio 40/60. Data on water absorption, weight loss, release of L-lactic acid, molecular weight and morphological changes showed that the presence of coral considerably modified the degradation characteristics of poly(DL-lactic acid). In particular, the faster internal degradation observed in the plain matrix polymer was not observed in the composite. The results were based on the buffering effect of the coral and to the presence of coral / polymer interfaces which facilitated ionic exchanges between the external solution and the interior of the composites. The carboxyl end groups were thus neutralized and the autocatalytic effect eliminated. (Li and Vert 1996)

3. MATERIALS AND METHODS

3.1. Materials and manufacturing

Three different bioabsorbable matrix materials and two different osteoconductive filler materials were used in this thesis. The Roman numeral after the material links the material and publication in which it was used.

Matrix polymers:

- Poly-L/DL-lactide with an initial LL/DL dimer ratio 70/30, Boehringer Ingelheim, Ingelheim am Rhein, Germany, inherent viscosity (reported by the manufacturer) 6.3 dl g^{-1} (I, II, V, VI) and 6.0 dl g^{-1} (IV)

- Poly-L/D-lactide with an initial LL/DD dimer ratio 96/4, Purac Biochem B.V., Gorinchem, The Netherlands, intrinsic viscosity (reported by the manufacturer) 6.7 dl g^{-1} (III, IV) and 7.6 dl g^{-1} (III)

- Poly-L-lactide-co-glycolide with an L/G ratio 80/20, Purac Biochem B.V., Gorinchem, The Netherlands, inherent viscosity (reported by the manufacturer) 5.2 dl g^{-1} (IV)

Filler materials:

- Spherical bioactive glass 13-93 particles (BaG) with composition 6 weight-% Na_2O, 12 wt-% K_2O, 5 wt-% MgO, 20 wt-% CaO, 4 wt-% P_2O_5 and 53 wt-% SiO_2 (Brink 1997b), Vivoxid Ltd., Turku, Finland. The particle size distribution (reported by the manufacturer) of the spheres used was $50 - 125$ μm. Brink *et al.* (1996, 1997a, 1997b) have described the manufacturing of the glass and the glass spheres. (II, IV, V, VI)

- β- tricalcium phosphate (β-TCP), CAM Implants B.V., Leiden, the Netherlands. β-TCP was used as sintered powder with particle size distribution $50 - 125$ μm, Ca/P ratio 1.5 and density $85 - 90$ % of dense β-TCP (reported by the manufacturer). (I, III, VI)

The matrix polymers were used as such or compounded with one or other of filler materials. The filler contents studied varied from 20 wt-% to 50 wt-%. Table 5 represents the 11 combinations used in this thesis.

Table 5.

The 11 combinations of the matrix and filler materials. The Roman numeral identifies the publication in which the combination was used.

Matrix material	Viscosity [dl g^{-1}] inherent	intrinsic	Filler material	Filler content [wt-%]	
Poly-L/DL-lactide 70/30	6.0 / 6.3		-	-	I, II, V
Poly-L/DL-lactide 70/30	6.0 / 6.3		BaG	20	II, IV, V, VI
Poly-L/DL-lactide 70/30	6.3		BaG	30	II, V
Poly-L/DL-lactide 70/30	6.3		BaG	40	II, V
Poly-L/DL-lactide 70/30	6.3		BaG	50	II, V
Poly-L/DL-lactide 70/30	6.3		β-TCP	20	I, VI
Poly-L/D-lactide 96/4		6.7	-	-	III
Poly-L/D-lactide 96/4		6.7	BaG	20	IV
Poly-L/D-lactide 96/4		7.6	β-TCP	20	III
Poly-L-lactide-co-glycolide 80/20	5.2		-	-	
Poly-L-lactide-co-glycolide 80/20	5.2		BaG	20	IV

The polymer granules and filler particles were mixed in desired proportions and further dried in a vacuum oven before use. The mixture was melt extruded to cylindrical rods using a twin-screw extruder (Mini ZE 20*11.5 D, Neste Oy, Koelaitepalvelut, Porvoo, Finland). The nozzle used was 7 mm in diameter and the final diameter of the non-reinforced cylindrical rods was approximately 5 – 6 mm. The extrusion temperatures depended on the matrix polymer used: 180 – 200 °C (poly-L/DL-lactide 70/30), 190 – 215 °C (poly-L/D-lactide 96/4) and 180 – 210 °C (poly-L-lactide-co-glycolide 80/20).

A small part of the non-reinforced non-sterilized rods was cut to the desired lengths and laid aside to await further characterization. The rest of the non-reinforced rods were further self-reinforced (SR) using solid state die-drawing (Törmälä 1992, Niiranen and Törmälä 1999, Kellomäki *et al.* 2003) to improve the mechanical properties of the rods and to create a porous structure to the composites containing filler material (Törmälä *et al.* 2002). In the die-drawing process the rods were drawn through a heated die. The temperature of the die depended on the matrix polymer used, being approximately 65 °C for poly-L/DL-lactide 70/30, 120 °C for poly-L/D-lactide 96/4 and 95 °C for poly-L-lactide-co-glycolide 80/20. The intended draw ratio was 3.5 – 4.0.

In general the basic principle of the self-reinforcing is to create an oriented, high strength polymeric structure with reinforcing fibrous element having the same chemical composition as matrix polymer. Self-reinforced structure can be achieved in different ways, such as using die-drawing (Törmälä 1992). In this thesis term self-reinforced (SR) is used for all samples which were die-drawn.

Half of the self-reinforced composites containing poly-L/D-lactide 96/4 and β-TCP was machined further to remove the polymer skin layer from the surface. 0.1 mm was lathed from the surface of the SR-rods. This procedure was thought to simulate, for example, the manufacturing of screws.

The self-reinforced rods were cut to desired lengths, washed with ethanol, dried in a vacuum, packed and finally sterilized with gamma irradiation (minimum 25 kGy) in lowered temperature.

The abbreviations, filler contents, draw ratios and final diameters of the studied non-reinforced and self-reinforced samples are listed in Table 6.

Table 6.
Abbreviations used, desired filler contents, draw ratios and final diameters of the combinations studied. The letters SR in abbreviations mean self-reinforcing. The Roman numeral identifies the publication in which the sample was studied.

Sample abbreviation	Matrix material	Filler material	Filler content [wt-%]	Draw ratio, DR	Diameter [mm]	
PLA70	Poly-L/DL-lactide 70/30	-	-	-	5.1 - 5.2	II
PLA70BaG20	Poly-L/DL-lactide 70/30	BaG	20	-	5.3 - 5.5	II, VI
PLA70BaG30	Poly-L/DL-lactide 70/30	BaG	30	-	5.1 - 5.5	II
PLA70BaG40	Poly-L/DL-lactide 70/30	BaG	40	-	4.7 - 5.1	II
PLA70BaG50	Poly-L/DL-lactide 70/30	BaG	50	-	5.5 - 5.8	II
PLA70TCP20	Poly-L/DL-lactide 70/30	β-TCP	20	-	5.4 - 5.8	
PLA96	Poly-L/D-lactide 96/4	-	-	-	5.5 - 5.6	
PLA96BaG20	Poly-L/D-lactide 96/4	BaG	20	-	5.3 - 5.6	
PLA96TCP20	Poly-L/D-lactide 96/4	β-TCP	20	-	5.4 - 5.6	
PLGA	Poly-L-lactide-co-glycolide 80/20	-	-	-	5.2 - 5.5	
PLGABaG20	Poly-L-lactide-co-glycolide 80/20	BaG	20	-	5.3 - 5.6	
SRPLA70	Poly-L/DL-lactide 70/30	-	-	3.5 - 4.0	2.7 - 2.9	I, II, V
SRPLA70BaG20	Poly-L/DL-lactide 70/30	BaG	20	3.5 - 4.0	2.8 - 3.1	II, IV, V, VI
SRPLA70BaG30	Poly-L/DL-lactide 70/30	BaG	30	3.5 - 4.0	3.0 - 3.1	II, V
SRPLA70BaG40	Poly-L/DL-lactide 70/30	BaG	40	3.5 - 4.0	2.7 - 3.1	II, V
SRPLA70BaG50	Poly-L/DL-lactide 70/30	BaG	50	2.0	4.1 - 4.3	II, V
SRPLA70TCP20	Poly-L/DL-lactide 70/30	β-TCP	20	3.5 - 4.0	2.9 - 3.0	I, VI
SRPLA96	Poly-L/D-lactide 96/4	-	-	3.5 - 4.0	2.6 - 2.7	III
SRPLA96BaG20	Poly-L/D-lactide 96/4	BaG	20	3.5 - 4.0	2.7 - 2.9	IV
SRPLA96TCP20	Poly-L/D-lactide 96/4	β-TCP	20	3.5 - 4.0	2.9 - 3.0	III
SRPLA96TCP20(m)[a]	Poly-L/D-lactide 96/4	β-TCP	20	3.5 - 4.0	2.7 - 2.8	III
SRPLGA	Poly-L-lactide-co-glycolide 80/20	-	-	3.5 - 4.0	2.7 - 2.9	
SRPLGABaG20	Poly-L-lactide co-glycolide 80/20	BaG	20	3.5 - 4.0	2.8 - 3.0	IV

[a] machined surface

3.2.   Determination of filler content

The filler content achieved in the self-reinforced samples was determined according to Standard ISO 1172 (1975). The samples were weighed and then calcinated at the defined temperature (500 °C), when the combustible matrix polymer was burned off. The residual non-combustible filler material was weighed and the filler content was calculated from the weights of the residual filler and original sample. At least three parallel samples were used (contents given as averages).

The filler contents in volume-% (vol-%) were calculated using measured filler contents (wt-%) and densities of the filler and matrix materials. The densities were determined according to calculations in Standard SFS-EN 1097-7 (2008).

In addition the filler contents were determined using thermogravimetric analysis, TGA, (TA Instruments Q500, TA Instruments, New Castle, Delaware, USA), which determines the change in the weight of the sample in relation to the change in temperature. The sample was heated constantly in air atmosphere using a heating rate of 20 °C/min until the temperature reached 700 °C. The filler content was calculated from the weights of the residual material and initial sample. Two parallel samples of each were analyzed.

3.3.   *In vitro* hydrolysis

The effects of the different matrix materials and filler materials on the hydrolytic behavior of gamma sterilized, self-reinforced samples were studied *in vitro*. The buffer solution used was phosphate buffered saline, PBS (ionic concentrations Na^+ 156.2 mM, HPO_4^{2-} 24.9 mM, $H_2PO_4^-$ 5.5 mM and Cl^- 100.9 mM), pH 7.4 at 37 °C. $V_{solution} / V_{sample}$ > 20 was objective. All self-reinforced samples were immersed in PBS in test tubes. The buffer solution was changed every two weeks. The pH of the buffer solution was monitored (at least three parallel samples) using a Mettler Toledo MP225 pH-meter (Mettler-Toledo GmbH, Schwerzebbach, Switzerland) and if the pH changed significantly ($\pm$ 0.2) the buffer solution was changed more often. The intended follow-up times in hydrolysis were 104 weeks (two years). The only exception was SRPLA70TCP20(m) which was studied for only 52 weeks, due to the limited number of samples.

3.4. Characterization of the samples

Table 7 summarizes the characterization methods used in this thesis.

Table 7.
Summary of characterization methods performed on the samples. TGA = thermogravimetric analysis, SEM = scanning electron microscopy, EDX = energy dispersive X-ray, μ-CT = micro-computed tomography, GPC = gel permeation chromatography, DSC = differential scanning calorimeter.

Sample abbreviation	Burning test	TGA	Bending test	Shear test	Compression test	Torsion test	Visual characterization	SEM	EDX	μ-CT	Remaining mass	Water absorption	GPC	DSC
PLA70			O	O	O	O		O					O	O
PLA70BaG20	O	O	O	O	O	O		O	O				O	O
PLA70BaG30	O		O	O				O					O	O
PLA70BaG40	O		O	O				O					O	O
PLA70BaG50	O		O	O				O					O	O
PLA70TCP20	O		O	O	O	O		O					O	O
PLA96			O	O	O	O		O					O	O
PLA96BaG20	O		O	O	O	O		O					O	O
PLA96TCP20	O		O	O	O	O		O					O	O
PLGA	O		O	O	O	O		O						O
PLGABaG20	O		O	O	O	O		O						O
SRPLA70			X	X	O	O	X	O	X		X	X	X	X
SRPLA70BaG20		O	X	X	O	O	X	O	X	O	X	X	X	X
SRPLA70BaG30		O	X	X	O	O	X	O	X		X	X	X	X
SRPLA70BaG40		O	X	X	O	O	X	O	X		X	X	X	X
SRPLA70BaG50		O	X	X	O	O	X	O	X		X	X	X	X
SRPLA70TCP20		O	X	X	O	O	X	O		O	X	X	X	X
SRPLA96			X	X	O	O	X	O			X	X	X	X
SRPLA96BaG20		O	X	X	O	O	X	O			X	X	X	X
SRPLA96TCP20		O	X	X	O	O	X	O			X	X	X	X
SRPLA96TCP20(m)		O	X	X			X	O			X	X	X	X
SRPLGA			X	X	O		X	O			X	X		X
SRPLGABaG20		O	X	X	O	O	X	O			X	X		X

X = Tests were performed during the whole *in vitro* hydrolysis.
O = Tests were performed only before *in vitro* hydrolysis to find out the initial properties.
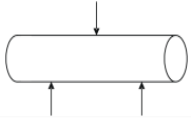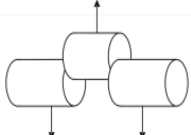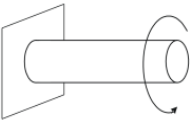
3.4.1. Mechanical testing

The mechanical tests (including bending test, shear test, compression test and torsion test) were performed on almost all non-sterilized non-reinforced samples and all gamma sterilized self-reinforced samples before *in vitro* hydrolysis. The purposes of these tests were to ascertain the effect of self-reinforcing on the mechanical properties and also to identify the initial mechanical properties of the self-reinforced samples studied. The dry samples were mechanically tested at room temperature by three-point bending and shearing using Instron 4411 mechanical testing apparatus (Instron Ltd., High Wycombe, England) and by torsion and compression using a Lloyd LR30K materials testing machine (Lloyd Instruments Ltd., Hampshire, UK). Each test was conducted on at least four parallel samples of each sample set and the reported results are given as averages.

The gamma sterilized self-reinforced samples were also tested mechanically during *in vitro* hydrolysis. Bending strength, bending modulus and shear strength retentions were studied. The samples were tested at room temperature under wet conditions immediately after removal from the buffer solution and deionized water rinsing, which removed the residual salts. At least four parallel samples were tested. The only exception was SRPLA96TCP20(m), of which only three parallel samples were tested due to the limited number of samples.

Bending strength and modulus were determined according to Standard SFS-EN ISO 178 (1997), the calculations of which were modified to the cylindrical samples. Shear testing was performed according to Standard BS 2782 method 340B (1978) and compressive properties in the direction of orientation were determined according to standard ISO 604 (1993). Both standards were also modified for the cylindrical samples. The torsion test was performed using testing arrangements described earlier by Pohjonen *et al.* (1997). The testing parameters used for each test are listed in Table 8.

Table 8.
Testing parameters for mechanical testing.

	Bending	
	Crosshead speed	5 mm / min
	Bending span[a]	46 - 90 mm
	Shear	
	Crosshead speed (tension)	10 mm / min
	Compression	
	Crosshead speed	1 mm / min
	Sample length	7 mm
	Torsion	
	Twisting speed	0.18 rpm
	Torsion span	20 mm
	Radius of the rotating wheel	40 mm

[a] Bending span depends on the diameter of the samples: $(16 \pm 1)*$diameter.

3.4.2. Visual characterization and dimensional changes

Visual characterization was done on all samples studied during the *in vitro* hydrolysis. The samples were characterized visually by the researcher's own eyes and by taking digital photographs of the samples. The aim was to observe any visual changes. The dimensions (diameter and length) of the samples were also measured before and during the *in vitro* hydrolysis. The samples were removed from the buffer solution at certain follow-up times and rinsed with deionized water and ethanol. After that the samples were dried in a vacuum at room temperature. The dimensions were measured carefully from the dry samples.

3.4.3. Scanning electron microscopy and energy dispersive x-ray spectroscopy

A scanning electron microscope (SEM, JEOL T100, Tokyo, Japan) was used for more detailed structural studies of certain samples. The effect of the self-reinforcing process on the sample structure was studied. The surface and cryo-cut longitudinal section of the samples were prepared using liquid nitrogen to avoid deformation of the internal structure during sample preparation, carbon adhesive and gold coating. Several different magnifications were used. To ensure the bioactivity of the samples, an elemental analysis of the precipitation formed at the surface of the samples during the *in vitro* hydrolysis was performed using energy dispersive X-ray, EDX (EDAX DX-4, Philips

XL 30, Eindhoven, The Netherlands) with ZAFFAZ program, using 15 kV acceleration voltage (Publication II).

3.4.4. Micro-computed tomography (μ-CT)

A micro-computed tomography (μ-CT) image analysis (SkyScan 1072 Desktop X-ray Microtomography device, SkyScan, Aartselaar, Belgium) was used for even more specific micro-structural studies for certain samples. The porosity formed during the self-reinforcing of the samples was confirmed and the size, shape and spatial distributions of the bioceramic filler materials were studied.

The imaging resolution varied between the objects due to differences in the diameters of the samples. For SRPLA70BaG20 and SRPLA70TCP20 pixel spacing of 3.90 μm and for PLA70BaG20 pixel spacing of 5.86 μm were used. All images were acquired with 52 kV of source voltage and 191 μA of source current without any filters. The reconstructions of tomography data were done using SkyScan's native program, Nrecon. Reconstructed μ-CT images were subjected to a series of preliminary processing prior to micro-structure analysis. Images were processed using MATLAB$^{®}$ (The MathWorks Inc., MA, USA) and the image processing steps (pre-processing, segmentation, connected region labeling and post-processing) were applied in order.

The parameters calculated using μ-CT image analysis were categorized as volume properties, volume distribution and particle distribution. Volume properties included both the determination of the sample diameter and length and volume ratios of the filler material, matrix material and total porosity. Small particles (less than 10 μm) were excluded, since they were negligibly small. The changes in the volume distribution of the filler material, matrix material and porosity were calculated both from center to surface in polar direction and from bottom to top in longitudinal direction. The purpose of the polar axis analysis was to observe the changes in the volume distributions when going away from the center of the sample towards to the surface of the sample and the purpose of the analysis along the longitudinal axis was to detect the changes in the volume distributions along the ray that passes through the origin of the polar plane. For these analyses, cylindrical samples were digitally cropped in the shape of cylinders keeping the heights same as in the samples and increasing the radius and in the polar planes keeping the radius the same as in the samples and increasing the distance from the bottom of the samples. Figure 3 shows examples of the regions cropped for polar axis and longitudinal axis analyses. The volume distributions were calculated in the close vicinity of all these regions. The particle distribution analysis included both size and shape analyses of the filler particles. The distribution of the filler particles along the polar and longitudinal axes were calculated using the same cropping procedure as explained previously for volume distribution analysis.
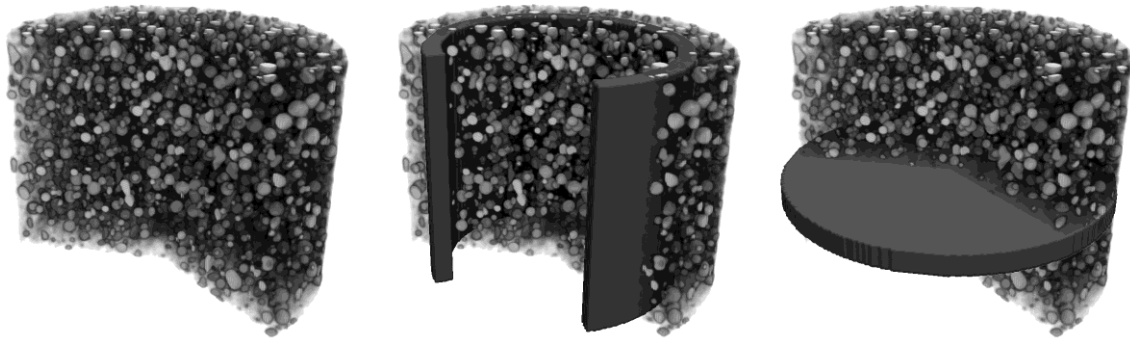
Figure 3.
Schematic illustrations of the regions analyzed for volume and particle distributions. a) 3D volume rendering, (b) region cropped for polar-axis analysis and (c) region cropped for longitudinal axis analysis. (Publication VI)

3.4.5. Weight change and water absorption

The dry samples were weighed before *in vitro* hydrolysis to ascertain the initial dry mass of the samples. The weight change and water absorption were determined from the same sample and three parallel samples were used. During *in vitro* hydrolysis, the samples were removed from the buffer solution and lightly dried with tissue paper to remove the extra water from the surface of the samples. After that the samples were weighed wet to define the water absorption (WA). After weighing, the samples were rinsed with deionized water and ethanol to remove residual salts and then dried for five days in a vacuum at room temperature. After drying, the samples were weighed again (dry mass).

The weight change, remaining mass and WA were calculated as follows (ISO 62: 2008)

$$weight\ change = \frac{m_d - m_0}{m_0} \cdot 100\%$$

(5)

$$remaining\ mass = \frac{m_d}{m_0} \cdot 100\%$$

(6)

$$water\ absorption\ (WA) = \frac{(m_w - m_d)}{m_d} \cdot 100\%$$

(7)

where m_0 = initial dry mass of the sample, m_w = wet mass of the sample during *in vitro* hydrolysis and m_d = dry mass of the sample after removing from the buffer solution. The weight measurements were done using a Mettler Toledo AG245 (Mettler-Toledo AG, Greifensee, Switzerland).

3.4.6. Molecular weight measurements

The weight average molecular weight (M_w) and number average molecular weight (M_n) of the poly-L/DL-lactide 70/30 and poly-L/D-lactice 96/4 based samples were studied using conventional gel permeation chromatography (GPC) with narrow polystyrene standards (universal calibration) using chloroform as solvent and eluent. The poly-L-lactide-co-glycolide 80/20 based samples were not studied due to their insolubility in chloroform. The equipment consisted of a differential refractometer detector (Waters 410 RI) and HPLC-pump (Waters 515) (Waters Operating Corporation, Milford, USA). The GPC columns were PLgel 5 μm Guard and two PLgel 5 μm mixed-C (Polymer Laboratories, Amherst, USA). The concentration of injected sample was 0.1 mass-%, injection volume and eluent flow rate 150 μl and 1 ml min^{-1} respectively. The Mark-Houwink parameters used were $\alpha = 0.73$, $K = 5.45*10^{-4}$ for PLA70 and $\alpha = 0.73$, $K = 1.12*10^{-4}$ for PS standard. Data are means of two repeat injections.

The samples for GPC analysis were removed from the buffer solution, rinsed with deionized water and ethanol to remove residual salts and then dried for 5 days in a vacuum at room temperature. The dried samples were dissolved in the chloroform and the filler material was filtered off using a filter paper before injection.

3.4.7. Thermal analysis

The thermal properties were determined from the vacuum dried samples using either of two differential scanning calorimeters (DSC): Perkin Elmer DSC7 (Perkin Elmer, Norwalk, USA) or a TA Instruments Q1000 (TA Instruments, New Castle, Delaware, USA). The samples were first heated using a heating rate of 20 °C min^{-1} up to 200 – 220 °C (heating A) and then cooled rapidly (200 °C min^{-1}) to 0 °C. After cooling the heating was repeated (heating B). Experiments were performed in nitrogen atmosphere and indium standard was used for calibration.

The heating A was used to determine melting temperature (T_m) and melting enthalpy (ΔH). Because ΔH is directly proportional to crystallinity, ΔH was used to estimate the changes in crystallinity during *in vitro* hydrolysis. Glass transition temperatures (T_g) were measured from heating B where half C_p extrapolated gives T_g. Reported data are means of two parallel scans.

4.   RESULTS

4.1.   Initial structure

After a few failed compounding attempts, all samples studied were successfully compounded. The structures of the non-reinforced rods are presented in Figure 4. The filler particles throughout the structure are well seen. On the surface of the rods the filler particles are under the thin polymer skin, which cause the surface to appear rough. At the inside of the rod, too, the filler particles are totally surrounded by polymer matrix. The very similar structure was observed with all combinations studied.

Figure 4.
a) Surface and b) cross section of the non-reinforced samples containing poly-L/D-lactide 96/4 and 20 wt-% of BaG (PLA96BaG20)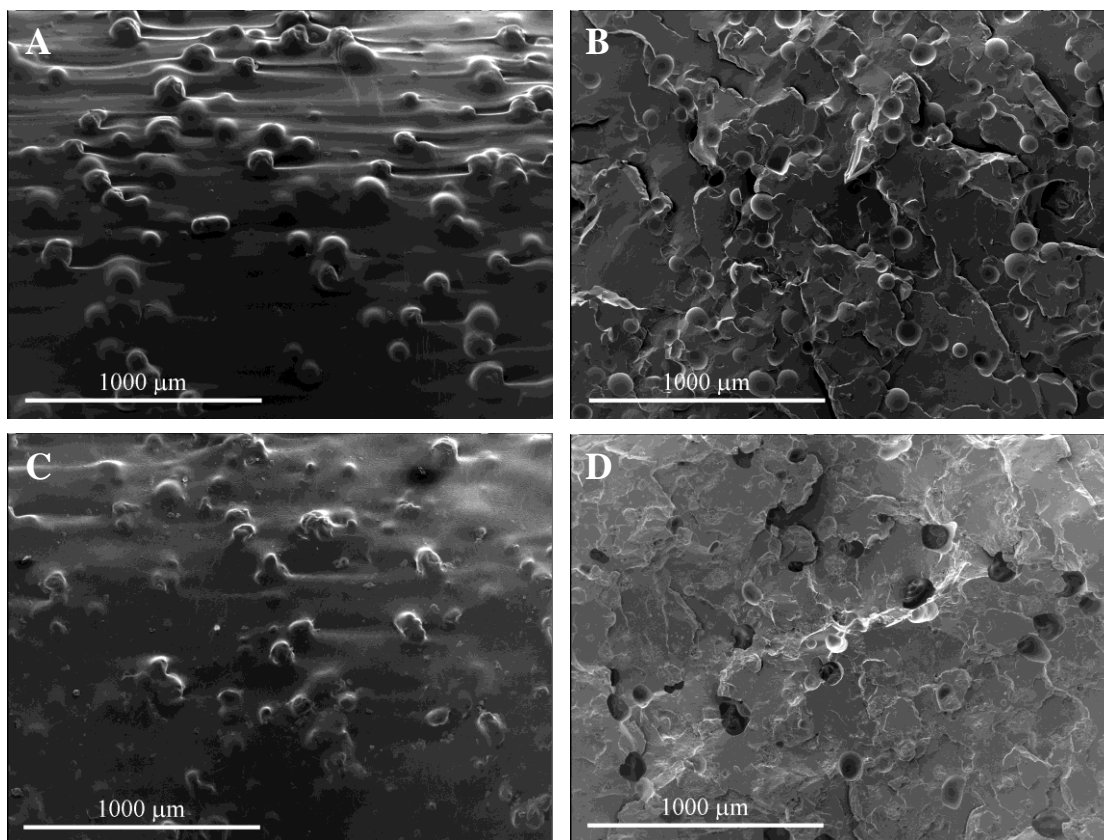. c) Surface and d) cross section of the non-reinforced samples containing poly-L/D-lactide 96/4 and 20 wt-% of β-TCP (PLA96TCP20).

The original aim of the self-reinforcing was to enhance the mechanical properties and reduce the brittleness of the materials. There are many factors such as drawing temperature, draw ratio (DR) and polymer used which affect the benefits of self-

reinforcing (Kellomäki *et al.* 2003, Törmälä 1992). In this thesis the aim in self-reinforcing was to achieve a DR of 3.5–4.0. This was easily achieved with only one exception, the sample with the largest (50 wt-%) BaG content, SRPLA70BaG50. The DRs achieved in studied samples were presented in Table 6.

The self-reinforcing modified the structure of the materials. During solid state die drawing both interior and exterior porosity were initiated by filler particles. The skin, which covered filler particles on the surface of the non-reinforced rod, were ruptured and spindle shaped pores were formed around the filler particles (Figure 5). The interior porosity and the clearly seen fibrous structure can be observed in Figure 6. From the figures it was also seen that there were no chemical reactions between the matrix polymer and filler particles. Practically there was no adhesion at all.

Figure 5.
External porosity on the surface of the self-reinforced γ-sterilized samples containing a) poly-L/D-lactide 96/4 and 20 wt-% of BaG (SRPLA96BaG20) and b) poly-L/DL-lactide 70/30 and 20 wt-% of BaG (SRPLA70BaG20).

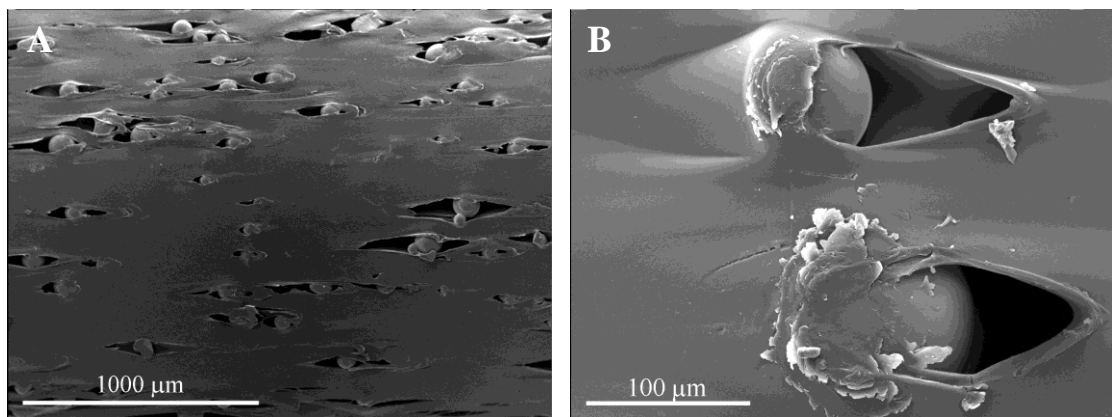*Figure 6.*
Longitudinal fracture surface of self-reinforced γ-sterilized samples containing a) poly-L/D-lactide 96/4 and 20 wt-% of BaG (SRPLA96BaG20) and b) poly-L/DL-lactide 70/30 and 20 wt-% of BaG (SRPLA70BaG20).
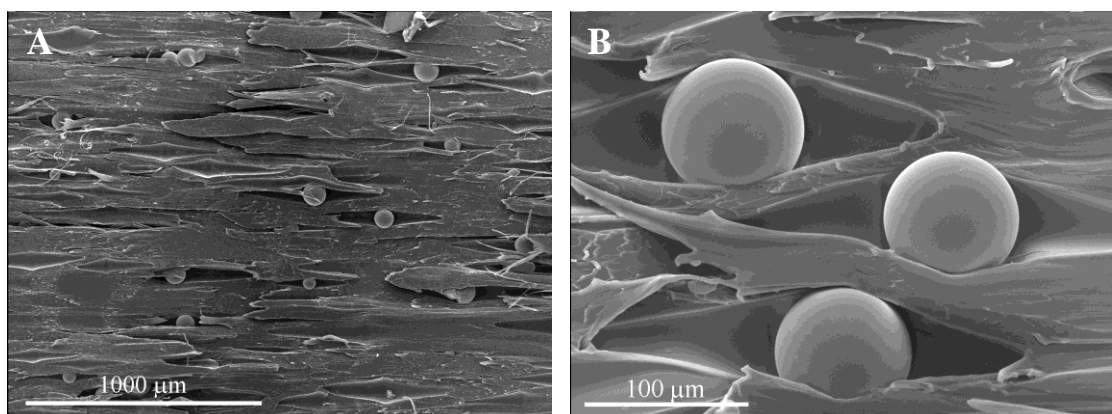
The amount of porosity formed depended on the filler material and its content. Plain matrix polymer seemed not to have any clear pores, but when the filler material was added, the pores were formed. Figure 7 illustrates how the filler content affected the exterior porosity of the samples containing poly-L/DL-lactide 70/30 and BaG. The highest porosity was observed in the sample containing 40 wt-% of BaG. If the BaG content was lower the exterior porosity was also lower. With higher BaG content the self-reinforcing became complicated, the required DR for the formation of the pores was not achieved and thus the pores were not formed.
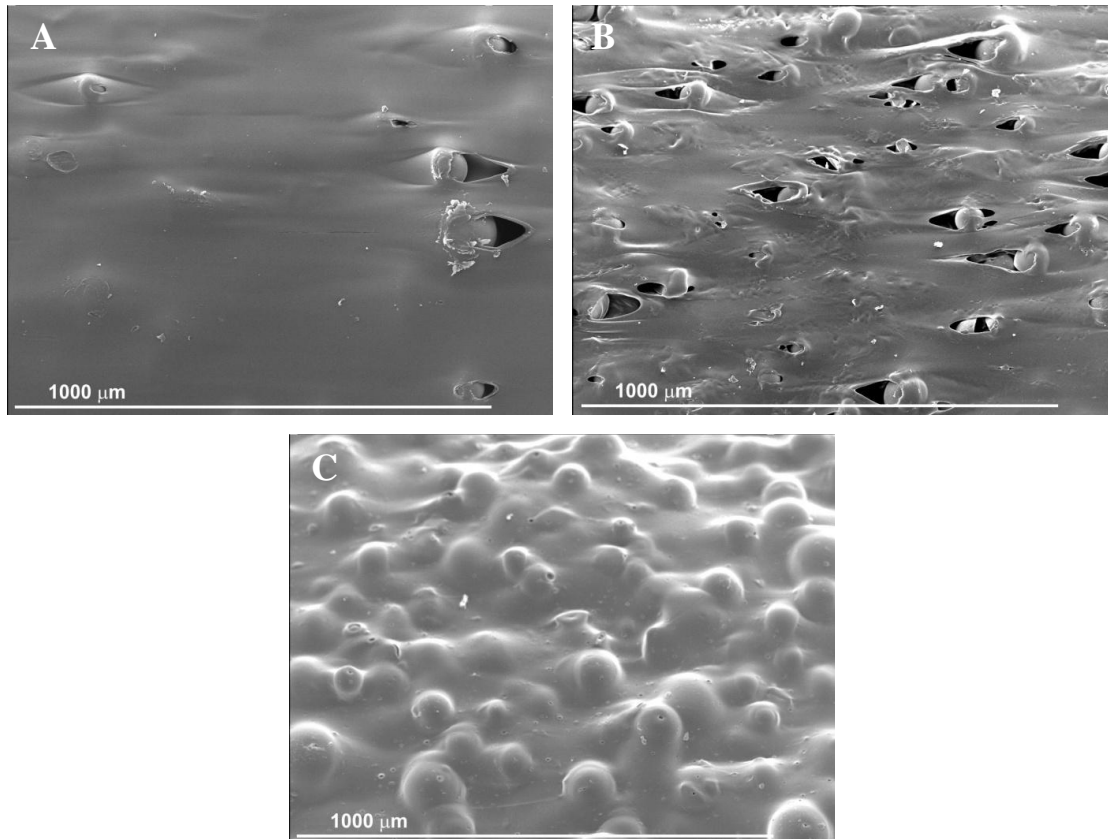
Figure 7.
Surfaces after self-reinforcing of the samples containing poly-L/DL-lactide 70/30 and BaG. The BaG content varied, being a) 20 wt-%, b) 40 wt-% and c) 50 wt-%. The effect of the BaG content on the external porosity is obvious. (Publication II)

Further machining of the surface of the sample to expose the filler phase was not necessary because the pores around the filler particles allowed them to be in direct contact with the surrounding fluids. However some of the samples containing poly-L/D-lactide 96/4 and β-TCP were machined further to remove the polymer skin layer from the surface. This additional machining seemed to expose more exterior pores and generate a rougher surface as can be seen in Figure 8.
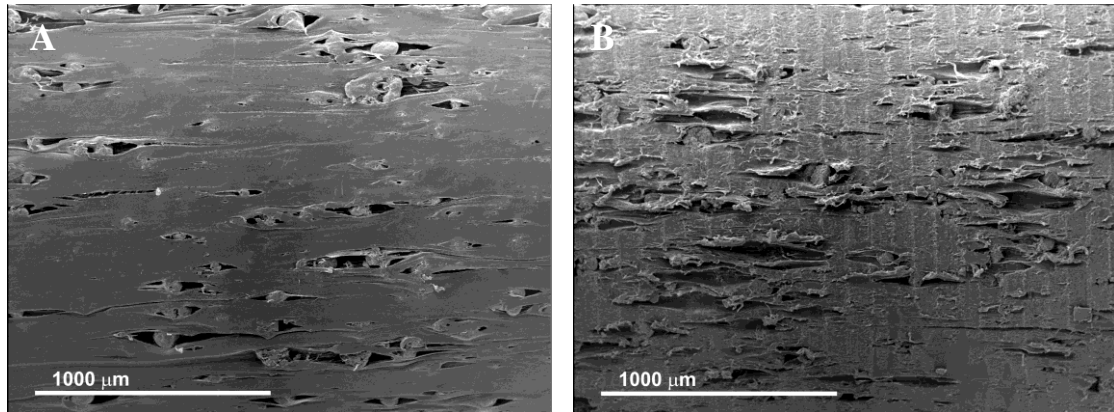
Figure 8.
Surfaces after self-reinforcing of the samples containing poly-L/D-lactide 96/4 and β-TCP:
a) Before additional machining and b) after additional machining. (Publication III)

The common porosity measurements of the samples were not applicable due to the lack of interconnectivity of the pores inside the samples. Thus μ-CT image analysis was used for the quantitative determination of the total porosity of the samples. It has been assumed, on the basis of the SEM images, that the non-reinforced samples do not have remarkable porosity. However, the μ-CT image analysis indicated that there were pores not only in the self-reinforced structure but also in the structure of the non-reinforced sample. The porosity of the non-reinforced poly-L/DL-lactide 70/30, which contains 20 wt-% of BaG (PLA70BaG20) was as much as 15 vol-%. During self-reinforcing the total porosity of the sample increased, being approximately 27 vol-% (SRPLA70BaG20). The achieved total porosity of the corresponding sample with 20 wt-% of β-TCP (SRPLA70TCP20) was clearly lower, only 19 vol-%.

μ-CT image analysis was performed on three different samples: non-reinforced poly-L/DL-lactide 70/30 containing 20 wt-% of BaG and two self-reinforced poly-L/DL-lactide 70/30 containing 20 wt-% of BaG and β-TCP. The changes in the distributions of filler material, matrix material and porosity were calculated along the polar and longitudinal axes. Figure 9 represents the volume distributions of the BaG containing samples along the polar axis. The purpose of the polar axis analysis was to observe the changes in the volume distributions when going away from the center of the sample towards to the surface of the sample.
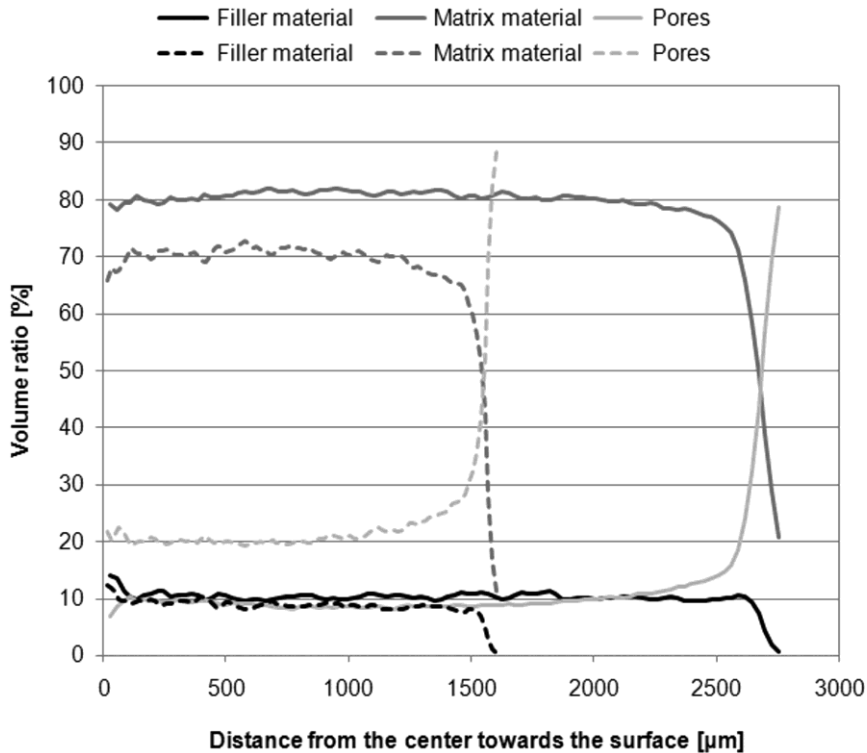
Figure 9.
Polar axis analysis of the volume distribution of the different components in the non-reinforced (solid line) and self-reinforced (broken line) samples of poly-L/DL-lactide 70/30 which contain 20 wt-% of BaG. (Publication VI)

The proportions of the different components remained almost unchanged through the whole radius. Very close to the surface the proportion of the filler particles and matrix material decreased sharply. At the same time, the porosity increased sharply. Similar behavior was also observed in self-reinforced β-TCP containing poly-L/DL-lactide 70/30 samples. The increasing of the porosity during the self-reinforcing can be also observed in Figure 9. Along the longitudinal axis the distributions of the different components were steady throughout in all samples. In this direction the porosity of the samples was observed to be slightly greater than along the polar axis. The average distances between the particles were also found slightly greater along the longitudinal axis than the polar axis.

The manufacturers of the BaG spheres and β-TCP particles reported that the particle size distribution of the used filler materials was 50 – 125 μm. μ-CT image analysis was used to examine the changes in particles size distribution during the different manufacturing processes. The particle size distributions of the three samples studied are shown in Figure 10. The distributions seemed to be slightly wider than at the beginning of processing. The greatest disintegration of the particles was noticed in the sample containing β-TCP.
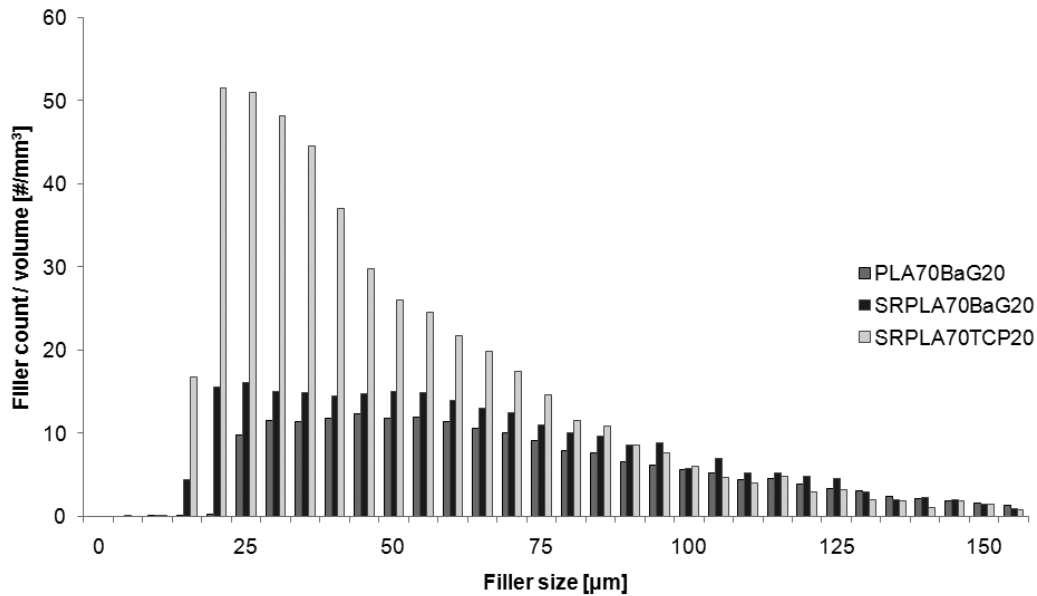
Figure 10.
Particle size distributions of the three samples studied using μ-CT.

The shape index describes how close the shape of the particle is to spherical. A perfect sphere has a shape index of 1. None of the filler particles of the three samples studied was analyzed to be completely spherical according to μ-CT image analysis. The BaG had a lower shape index than β-TCP and was thus closer to spherical.

The μ-CT image analysis enabled the 3D analysis of the filler particle distribution in the self-reinforced osteoconductive composites. The analysis along the polar axis describes how the filler particles are located between the center and surface of the sample and the analysis along the longitudinal axis describes the location between the bottom and top of the sample. Figure 11 illustrates the particle distribution along the polar axis of the two self-reinforced poly-L/DL-lactide 70/30 based composites with different filler materials (20 wt-% of BaG or β-TCP). The data points show the results calculated in the immediate vicinity of the corresponding distance from the center. The same event of the decreasing amount of filler particles very close to the surface of the samples was detected as reported in Figure 9. Inside the sample only few irregularities were noticed in the particle distribution of the BaG containing sample. The β-TCP containing sample had slightly more deviation, especially near to the center of the sample. It seemed that there were even fewer particles located near to the center. The particle distributions along the longitudinal axis were more uniform for all three samples studied using μ-CT image analysis.
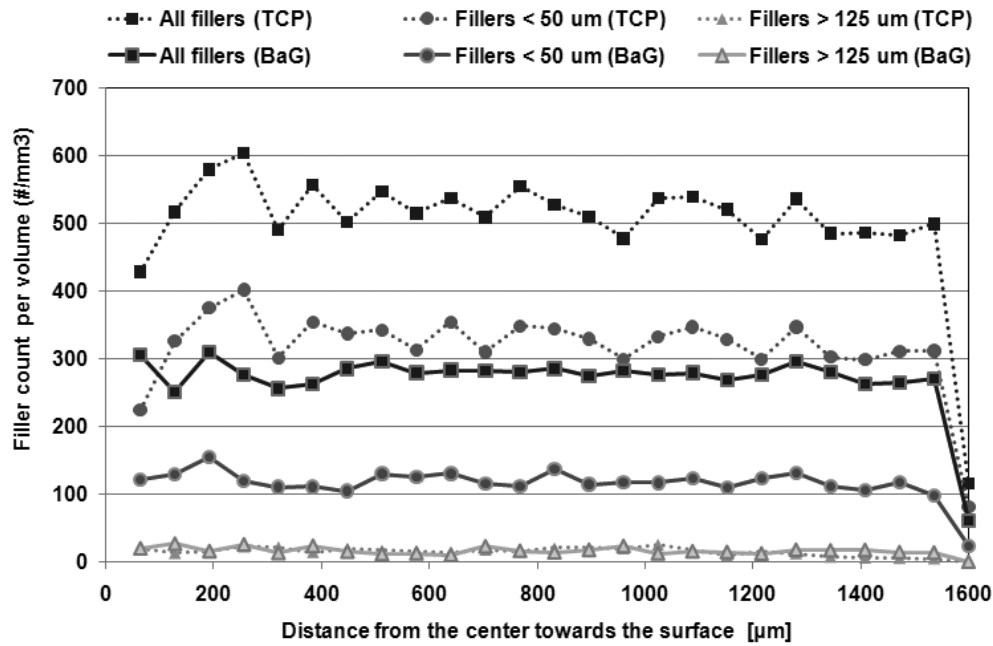
Figure 11.
Polar axis particle distribution of the two self-reinforced poly-L/DL-lactide 70/30 based composites with different filler materials (20 wt-% of BaG or β-TCP).

4.2.   Filler content

Both filler materials were suitable for the "burning test" because they are not combustible. As a comparison, the filler content was also determined using TGA. μ-CT image analysis, which was done to only the few selected samples, also provides comparable results of filler contents. The determination of the filler content using the abovementioned methods succeeded well. The results can be seen in Table 9. All results were converted to both wt-% and vol-% to facilitate the comparison of the results. The densities of the materials needed in this conversion were determined using standard SFS-EN 1097-7 (2008): $\rho_{poly-L/DL-lactide\ 70/30} = 1.26$ g/ml, $\rho_{poly-L/D-lactide\ 96/4} = 1.23$ g/ml, $\rho_{poly-L-lactide-co-glycolide\ 80/20} = 1.29$ g/ml, $\rho_{BaG} = 2.62$ g/ml and $\rho_{\beta-TCP} = 2.69$ g/ml.

Table 9.

Filler contents of the self-reinforced samples studied determined using three different methods: burning test, TGA and μ-CT. Burning test and TGA gave the result in wt-% and μ-CT in vol-%. All results were converted to both wt-% and vol-%.

Sample abbreviation	Desired filler content [wt-%]	"burning test" [wt-%]	[vol-%]*	Determined filler content TGA [wt-%]	[vol-%]*	μ-CT [wt-%]**	[vol-%]
SRPLA70	0	0	0	0	0	n.m.	n.m.
SRPLA70BaG20	20	19.0	10.1	19.4	10.4	15.5	8.1
SRPLA70BaG30	30	27.7	15.6	31.4	18.0	n.m.	n.m.
SRPLA70BaG40	40	37.2	22.2	43.2	26.8	n.m.	n.m.
SRPLA70BaG50	50	47.7	30.5	41.7	25.6	n.m.	n.m.
SRPLA70TCP20	20	18.9	9.8	18.8	9.8	16.5	8.7
SRPLA96	0	0	0	0	0	n.m.	n.m.
SRPLA96BaG20	20	17.6	9.1	21.8	11.6	n.m.	n.m.
SRPLA96TCP20	20	19.2	9.8	22.1	11.5	n.m.	n.m.
SRPLA96TCP20(m)[a]	20	19.2	9.8	22.1	11.5	n.m.	n.m.
SRPLGA	0	0	0	0	0	n.m.	n.m.
SRPLGABaG20	20	19.9	10.9	19.7 *	10.8	n.m.	n.m.

[a] machined surface

* only one sample

** calculated using measured filler contents and densities of the filler and matrix materials.

n.m. Not measured

4.3. Initial mechanical properties

The initial mechanical testing, including bending test, shear test, compression test and torsion test, were performed on non-reinforced, non-sterilized samples (Table10). It was observed that the addition of the filler material to the matrix material caused the non-reinforced samples to become weaker and more brittle. The influence of the self-reinforcing on the initial mechanical properties can also be observed in Table 10. The effect of the self-reinforcing varied depending, for example, on the matrix material, filler material, filler content used and properties measured as well as the draw ratio achieved. The most important effect of the self-reinforcing is that initially brittle samples become ductile.

Table 10.

Initial mechanical properties of the non-reinforced, non-sterilized composites and self-reinforced, γ-sterilized samples. Results are the means of at least four parallel samples. Standard deviations are in parentheses after means.

Sample abbreviation	Bending strength [MPa]	Strain at max bending load [%]	Bending modulus [GPa]	Shear strength [MPa]	Compression strength [MPa]	Torsion strength [MPa]
Non-reinforced, non-sterilized						
PLA70	127.3 (5.9)	5.0 (0.2)	2.9 (0.2)	44.6 (5.7)	84.2 (1.1)	51.5 (5.2)
PLA70BaG20	108.3 (3.3)	3.7 (0.2)	3.3 (0.1)	38.8 (0.7)	84.5 (0.7)	47.2 (3.8)
PLA70BaG30	92.1 (7.7)	3.6 (0.7)	2.9 (0.6)	36.5 (1.8)	n.m.	n.m.
PLA70BaG40	78.3 (4.6)	2.6 (0.7)	3.2 (0.4)	34.5 (2.2)	n.m.	n.m.
PLA70BaG50	79.0 (6.5)	1.8 (0.1)	4.0 (0.3)	35.5 (1.4)	n.m.	n.m.
PLA70TCP20	88.4 (5.3)	4.0 (0.1)	2.8 (0,2)	36.0 (0.4)	73.9 (1.8)	37.5 (2.1)
PLA96	116.8 (11.8)	5.4 (0.2)	2.5 (0.3)	43.1 (0.9)	101.1 (5.5)	53.3 (2.5)
PLA96BaG20	103.2 (3.9)	3.9 (0.3)	3.0 (0.1)	39.8 (2.4)	86.4 (3.8)	40.8 (8.0)
PLA96TCP20	91.7 (6.3)	4.1 (2.9)	2.9 (0.2)	35.9 (1.1)	73.6 (1.1)	41.5 (0,8)
PLGA	124.6 (3.9)	5.2 (0.1)	3.7 (0.1)	46.7 (1.2)	112.2 (3.8)	44.6 (2.6)
PLGABaG20	100.2 (2.8)	4.1 (0.2)	3.8 (0.3)	37.0 (1.0)	84.4 (6.6)	41.6 (4.1)
Self-reinforced, γ-sterilized						
SRPLA70	154.8 (13.4)	4.6 (0.5)	3.6 (0.3)	105.5 (3.3)	77.6 (4.3)	45.6 (2.2)
SRPLA70BaG20	112.3 (14.0)	5.8 (0.3)	2.7 (0.3)	81.0 (6.2)	52.8 (1.6)	25.9 (1.8)
SRPLA70BaG30	89.3 (6.0)	5.4 (0.7)	2.2 (0.2)	68.6 (3.5)	39.7 (1.6)	23.3 (1.3)
SRPLA70BaG40	70.1 (4.4)	6.1 (0.8)	2.0 (0.3)	54.5 (4.1)	33.3 (1.7)	15.7 (0.5)
SRPLA70BaG50	57.6 (11.2)	4.5 (0.4)	1.8 (0.4)	39.3 (7.2)	34.5 (1.4)	15.6 (1.4)
SRPLA70TCP20	115.6 (8.6)	5.9 (0.4)	2.8 (0.1)	79.5 (6.6)	45.4 (2.7)	28.7 (1.7)
SRPLA96	184.8 (2.2)	4.7 (0.2)	4.7 (0.1)	120.6 (1.6)	89.0 (5.1)	61.0 (6.2)
SRPLA96BaG20	127.5 (10.5)	6.7 (0.5)	3.1 (0.2)	81.9 (7.1)	49.7 (5.4)	38.1 (4.1)
SRPLA96TCP20	130.5 (8)	5.7 (0.4)	3.3 (0.1)	80.2 (4.8)	54.7 (4.3)	33.2 (4.9)
SRPLA96TCP20(m)[a]	129.8 (1.1)	6.4 (0.8)	3.3 (0.04)	78.5 (1.8)	n.m.	n.m.
SRPLGA	163.4 (1.2)	4.2 (0.1)	4.0 (0.03)	93.6 (3.4)	101.3 (10.7)	n.m
SRPLGABaG20	111.8 (3.2)	5.4 (0.3)	2.7 (0.1)	65.3 (1.6)	69.3 (1.2)	35.4 (0.9)

[a] machined surface

n.m. not measured

The effect of the filler content on the initial mechanical properties of the self-reinforced and γ-sterilized samples was studied in Publication II. The tests were performed using poly-L/DL-lactide 70/30 as a matrix polymer and BaG as a filler material. The results can also be used as a guideline to the other self-reinforced matrix polymer / filler material combinations. The best initial properties were observed in the plain matrix

polymer with no added BaG, as expected. The addition of the BaG diminished the properties except the strain at maximum bending load increased up to a certain point. This means that the samples became ductile. The property most affected by the presence of BaG was torsion (Figure 12). The torsion strength decreased almost to half of the initial value when 20 wt-% of BaG was added. The behavior of the other properties can also be observed in Figure 12.
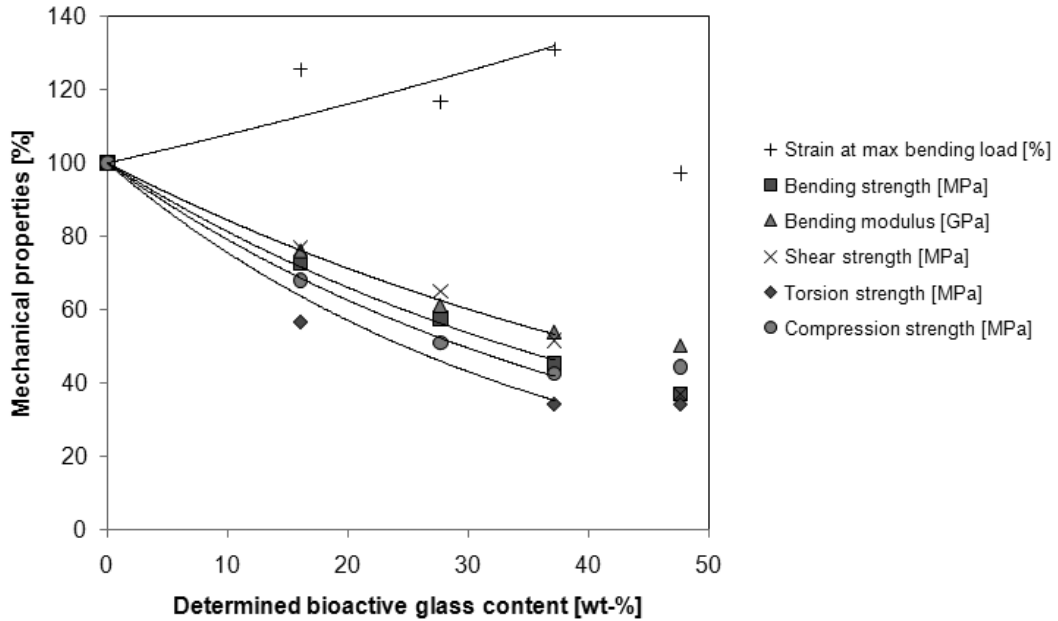

Figure 12.
Effect of the addition of BaG on the initial mechanical properties of the self-reinforced and γ-sterilized samples (DR 3.5 – 4) containing poly-L/DL-lactide 70/30 as a matrix polymer and BaG as a filler material. The properties of the plain matrix material (SRPLA70) have been marked as 100%. The BaG content determined is used as an x-axis. SRPLA70BaG50 have been excluded from the trend line due to the different draw ratio (DR 2.0).

4.4.   Hydrolysis behavior

The γ-sterilized, self-reinforced samples were successfully studied *in vitro* in PBS for up to 104 weeks. The pH of the buffer solution was monitored during the whole hydrolysis and its changes depended on the matrix polymer and filler material used. At the beginning of the hydrolysis the pH of the buffer solution remained constant (7.4 ± 0.5) and it was changed every two weeks. At certain points of the hydrolysis the pH started to decrease slightly and the buffer solution was changed weekly instead of every two weeks. In the plain self-reinforced γ-sterilized poly-L/DL-lactide 70/30 (SRPLA70) and poly-L/D-lactide 96/4 (SRPLA96) matrix materials the pH of the buffer solution remained constant for up to approximately 52 weeks *in vitro*, whereas with self-reinforced γ-sterilized poly-L-lactide-co-glycolide 80/20 matrix materials (SRPLGA) it

lasted only 12 weeks. The BaG or β-TCP addition mainly extended the pH retention. The pH of the buffer solution of the poly-L/DL-lactide 70/30 and poly-L/D-lactide 96/4 based filler containing samples started to decrease until approximately 60 – 70 weeks *in vitro*. The filler addition does not, however, have so remarkable effect on to the poly-L-lactide-co-glycolide 80/20 based sample. They retained the pH constant only a few weeks longer than plain matrix polymer.

4.4.1. Mechanical properties *in vitro*

The strength retention of the self-reinforced γ-sterilized samples during *in vitro* hydrolysis was studied in PBS. The maximum follow-up time was 104 weeks (2 years), but the most of the samples could not be tested so far because the samples became very brittle and disintegrated when testing was attempted. The matrix polymer played an important role in the degradation behavior. Figure 13 represents the differences in the bending strength retention of the plain self-reinforced γ-sterilized matrix polymers; poly-L/DL-lactide 70/30 (SRPLA70), poly-L/D-lactide 96/4 (SRPLA96) and poly-L-lactide-co-glycolide 80/20 (SRPLGA). It was observed that SRPLA96 had the highest initial bending strength. It also retained its bending strength virtually unchanged for about 36 weeks, which was much longer than the others. The shear properties behaved very similarly.
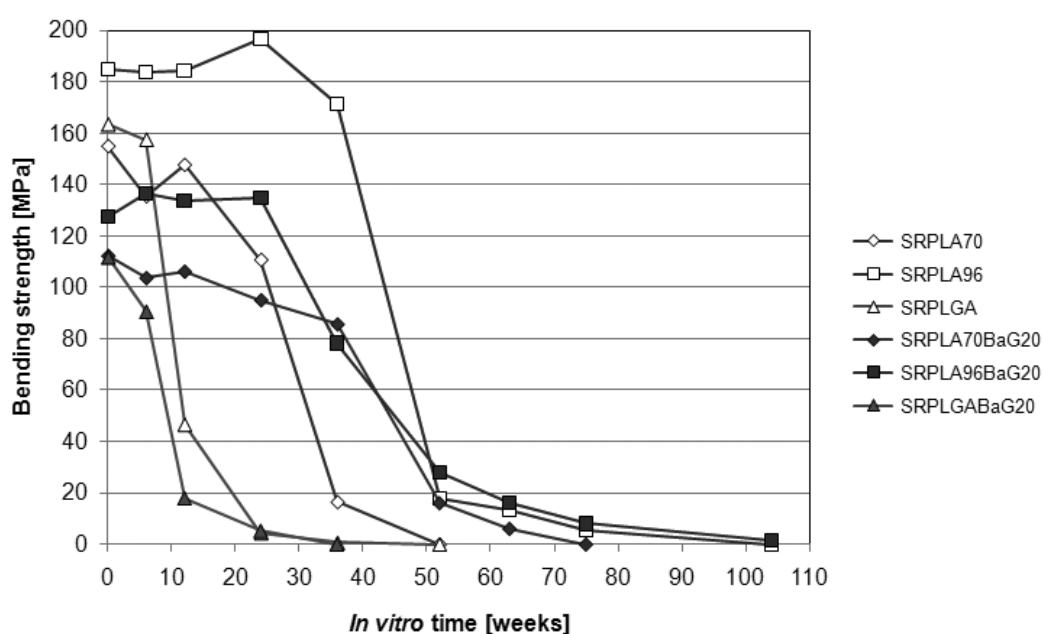

Figure 13.
Decrease of the bending strength of the self-reinforced γ-sterilized matrix polymers and samples containing 20 wt-% of BaG during hydrolysis (PBS). Each point represents the mean of at least three independent measurements.

The addition of BaG to the matrix polymer changed the strength retention behavior (Figure 13). The initial strength values were approximately 20 – 30 % lower than those with no filler material. The β-TCP addition followed the same model. The difference between these two filler materials can be better seen in Figure 14. The initial values seemed to be almost equal, but the strength retention differed. β-TCP containing samples retained their initial bending strength longer than the BaG containing samples and even longer than plain matrix polymer. After 52 weeks' hydrolysis, the β-TCP containing sample (SRPLA96TCP20) had the highest bending strength value (approximately 80 MPa, which is about 60 % of the initial value). The same finding was also seen with the other matrix polymer, poly-L/DL-lactide 70/30 and its composites. The machining of the sample surface did not influence the initial mechanical properties of the sample, but during the hydrolysis the values seemed to be slightly lower than those without machining.

Figure 14.
Decrease of the bending strength of the self-reinforced γ-sterilized poly-L/D-lactide 96/4 based samples during hydrolysis (PBS). Each point represents the mean of at least three independent measurements.

The amount of the filler material also affected the maintenance of the mechanical properties of the samples. This effect was studied in Publication II using poly-L/DL-lactide 70/30 as a matrix material and BaG as a filler material. BaG filler content varied between 20 wt-% and 50 wt-%. The initial values of the samples studied were presented in Table 10 and these can also be seen in Figure 12. Figure 15 represents the bending strength retention during hydrolysis in PBS. The decreasing trend seems to be uniform. The BaG addition affected the initial mechanical properties of the samples most as

51

already seen in Figure 12. The strength retention also differed. The higher the BaG content, the faster the sample lost its mechanical properties. The shear strength behaved very similarly.
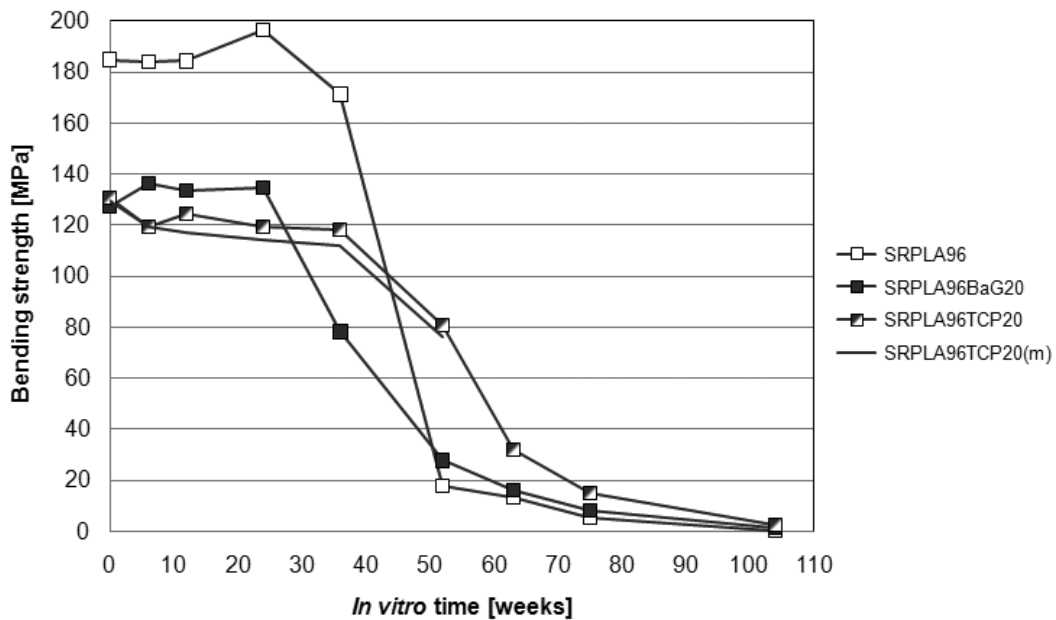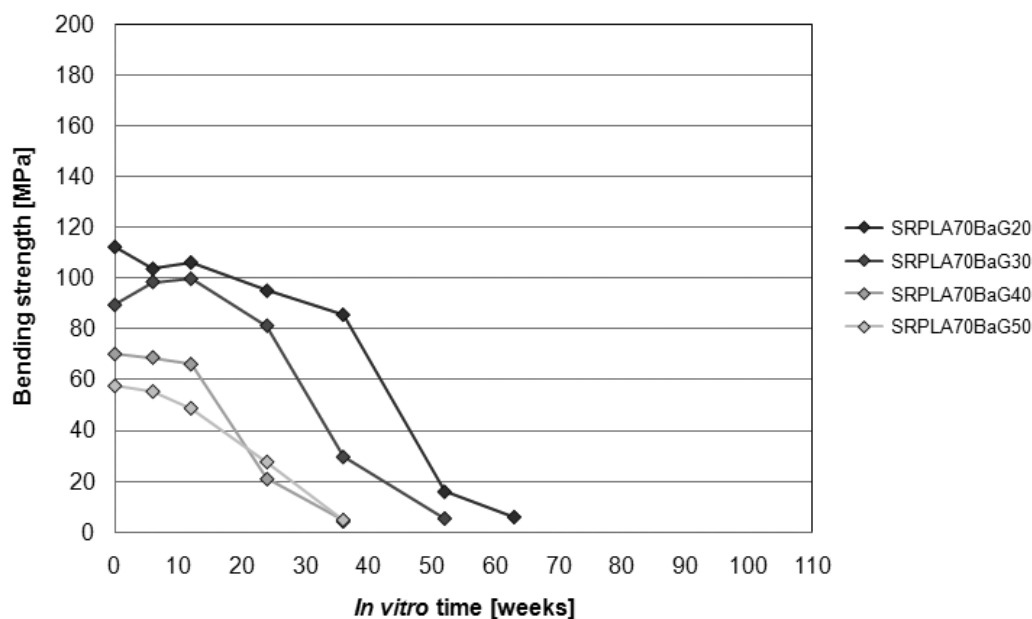

Figure 15.
Decrease of the bending strength of the self-reinforced γ-sterilized BaG containing poly-L/DL-lactide 70/30 samples during hydrolysis (PBS). Each point represents the mean of at least three independent measurements.

4.4.2. Visual characterization and dimensional changes *in vitro*

The visual characterization of the self-reinforced plain matrix polymers showed that they were initially transparent, but turned white and opaque during hydrolysis. The changes were observed after different times *in vitro*. Self-reinforced poly-L-lactide-co-glycolide 80/20 (SRPLGA) already started to become opaque after 10 weeks *in vitro*, poly-L/DL_lactide 70/30 (SRPLA70) after 12 weeks *in vitro* and poly-L/D-lactide 96/4 (SRPLA96) after 20 weeks *in vitro*. The composites containing filler material were white and opaque initially and throughout the whole hydrolysis.

Figure 16 represents the behavior of the plain self-reinforced matrix polymers during hydrolysis in PBS. The differences between the polymers are easily seen. For example, after 52 weeks' hydrolysis SRPLGA (Figure 16f) disintegrated, SRPLA70 (Figure 16b) was shrunk and swollen and SRPLA96 (Figure 16c) was still quite intact, only a slight opacity was noticed. The addition of the BaG changed this behavior, as seen in Figure 17. The most significant change was the better dimensional stability of the self-reinforced 20 wt-% of BaG containing poly-L/DL-lactide 70/30 (SRPLA70BaG20).
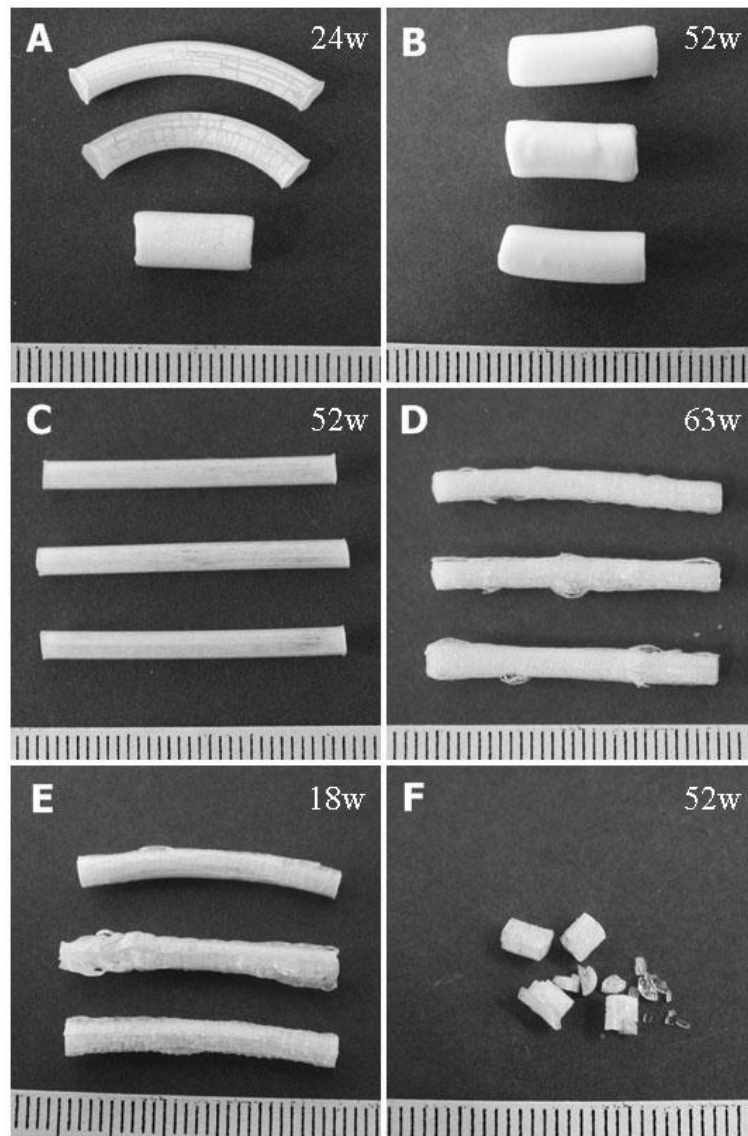
Figure 16.
Digital photographs of the self-reinforced γ-sterilized plain matrix polymers during hydrolysis (PBS). a) SRPLA70 after 24 weeks, b) SRPLA70 after 52 weeks, c) SRPLA96 after 52 weeks, d) SRPLA96 after 63 weeks, e) SRPLGA after 18 weeks and f) SRPLGA after 52 weeks.
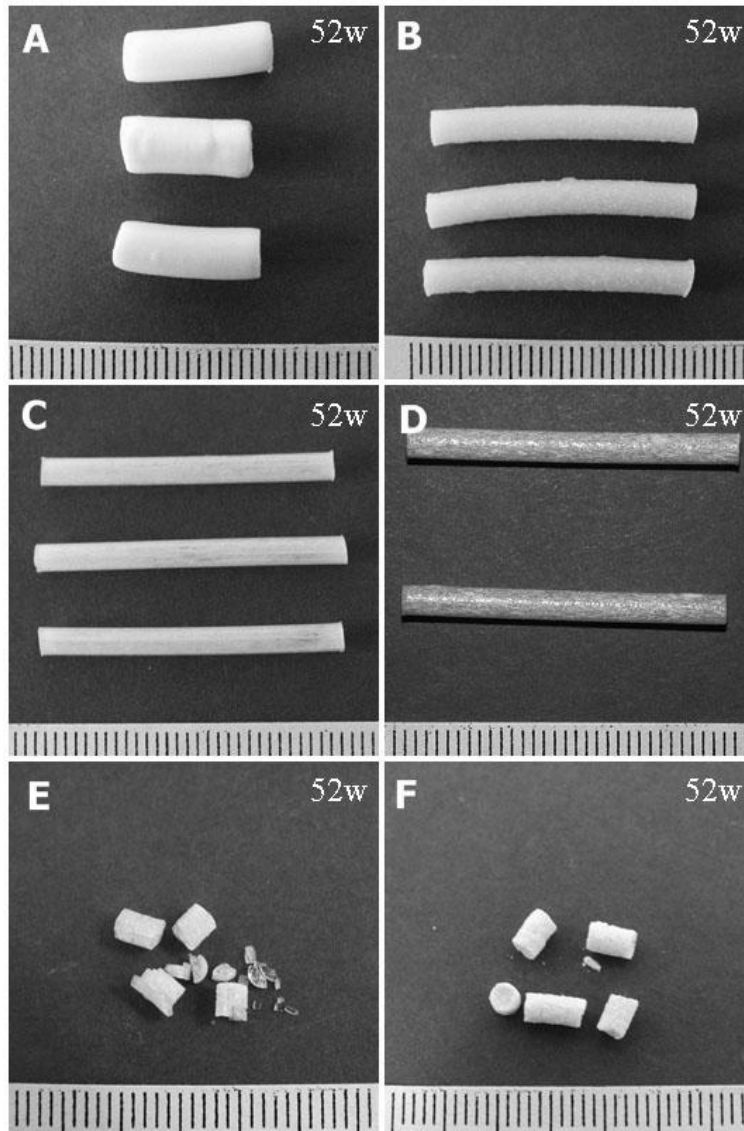
Figure 17.
Comparison of the self-reinforced plain matrix polymers and self-reinforced samples containing 20 wt-% of BaG after 52 weeks in vitro (PBS). a) SRPLA70, b) SRPLA70BaG20, c) SRPLA96, d) SRPLA96BaG20, e) SRPLGA and f) SRPLGABaG20.

β-TCP addition has been observed to have a similar effect on the dimensional stability of the samples to the addition of BaG. At the hydrolysis point at which the plain matrix polymer started to shrink and swell, the composites still maintained their size and shape. The effect of filler addition was the most significant in poly-L/DL-lactide 70/30 based samples. Figure 18 illustrates the changes measured in the dimensions of the SRPLA70 and SRPLA70TCP20 during the *in vitro* hydrolysis and Figure 19 the corresponding visual changes in SRPLA96 and SRPLA96TCP20.
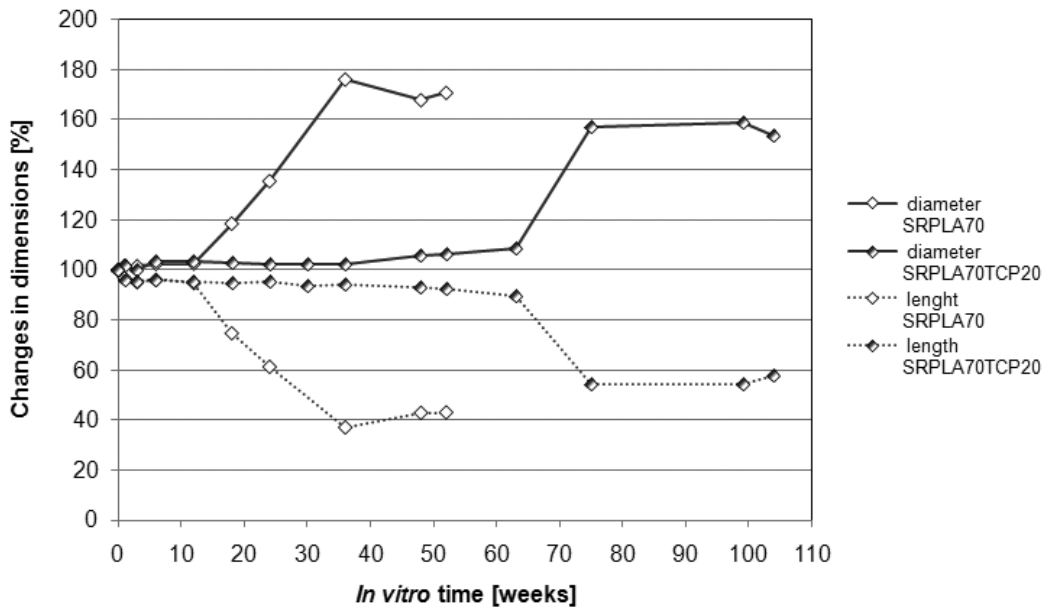
Figure 18.
Changes in dimensions (length and diameter) of SRPLA70 and SRPLA70TCP20 during hydrolysis (PBS).
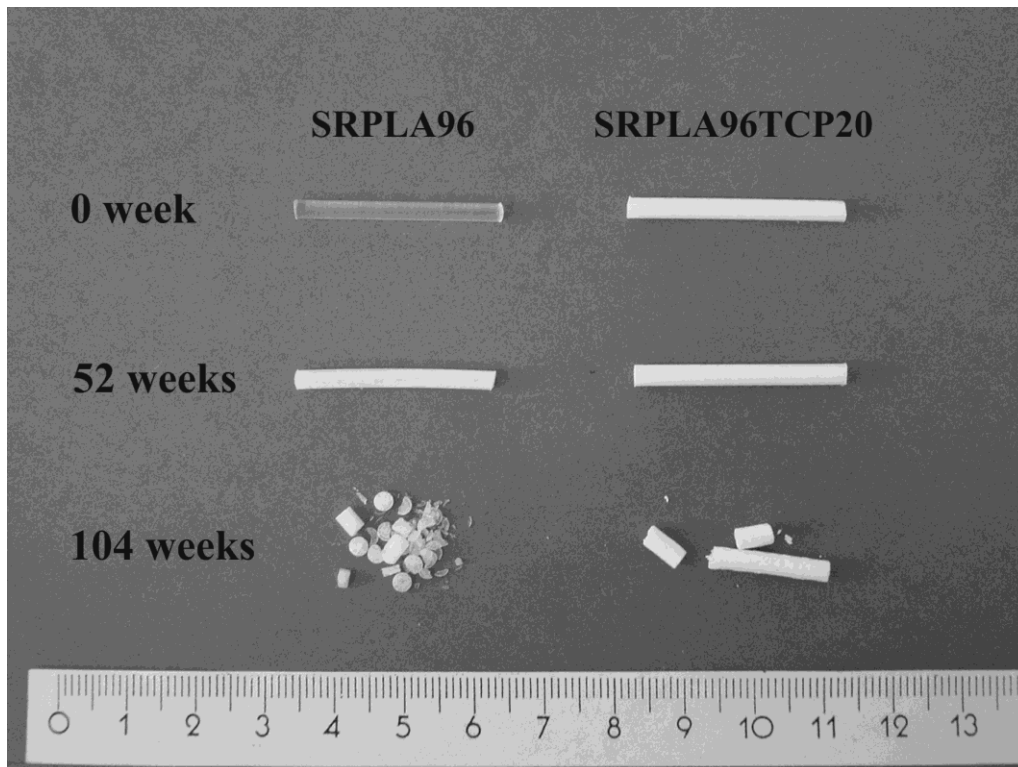
Figure 19.
Visual characterization of SRPLA96 and SRPLA96TCP20 during hydrolysis in PBS. (Publication III)

4.4.3. Bioactivity *in vitro*

The bioactivity of certain samples was examined in Publication II. The study was performed on the samples containing poly-L/DL-lactide 70/30 as a matrix material and BaG as a filler material. The aim was to ascertain the effect of the four different filler contents (20, 30, 40 and 50 wt-%) on the bioactivity of the samples.

The scanning electron microscopy (SEM) studies during the 12 days' hydrolysis in PBS confirmed the formation of the calcium phosphate precipitation, which was considered to be a sign of bioactivity, on the surface of the certain samples. The BaG content together with self-reinforcing was observed to affect precipitation formation. The open pores on the composite surface formed during the self-reinforcing are necessary for the BaG reactions. BaG needs to be in direct contact with the buffer solution to enable the rapid reactions. The reactions at the BaG surface, calcium phosphate precipitation formed, were already detected visually from SEM images after 72 hours immersion in PBS if the BaG was in direct contact with the buffer solution (Figure 20a). However, if the BaG was polymer-covered it did not prove a sign of bioactivity even after 12 days' immersion in PBS (Figure 20b).
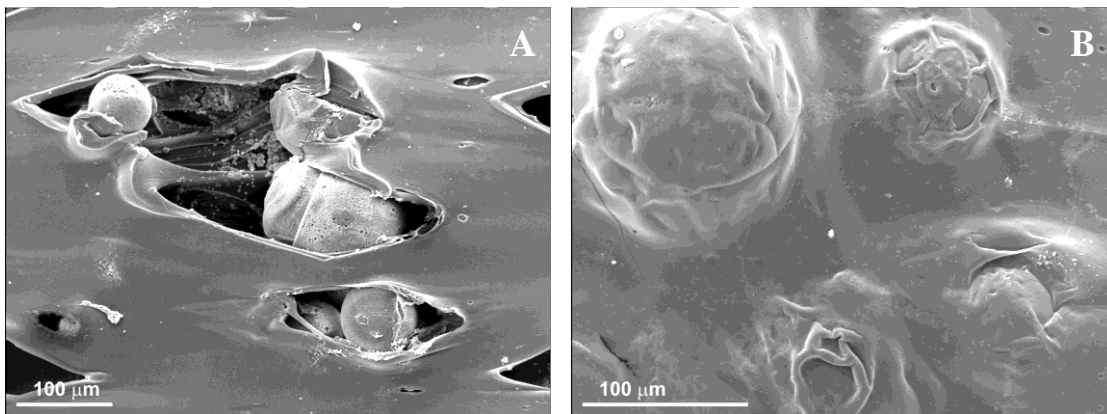
Figure 20.
a) Calcium phosphate precipitation formed on the surface of the BaG spheres at the self-reinforced sample containing 40 wt-% of BaG (SRPLA70BaG40) after 72 hours' immersion in PBS. b) The surface of the self-reinforced sample containing 50 wt-% of BaG (SRPLA70BaG50) after 12 days' immersion in PBS. The reactions of BaG were not seen due to the polymer skin covering the BaG spheres. (Publication II)

Energy dispersive x-ray (EDX) analysis was used to confirm the reactions of the BaG. The spectrum of the analysis taken from the surface of the reacted BaG spheres after 72 h immersion in PBS was compared to the analysis of non-reacted BaG surface (Figure 21). The results differed from each other, which mean that the ion exchange reactions of the BaG had started.

	Precipitation formed at 72 hours		BaG sphere at 0 hours
Element	Atomic-%		Atomic-%
C	17.75		
O	1.69		60.66
Na	0.13		2.66
Mg	0.68		2.51
Si	7.48		24.34
P	**25.19**		0.57
K	1.08		3.70
Ca	**45.99**		5.55
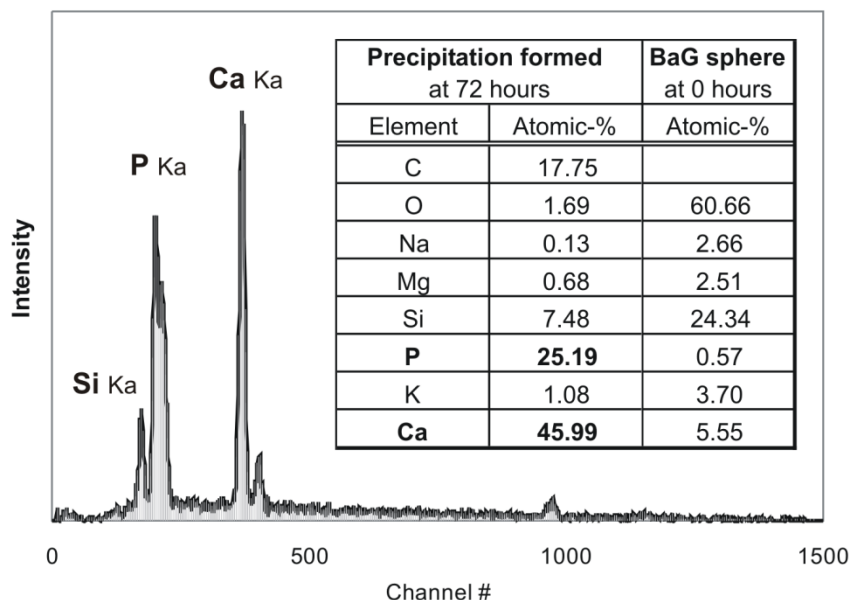
Figure 21.

Quantitative results of the selected elements of EDX analysis. The analysis was performed on the precipitation at the surface of BaG in SRPLA70BaG40 after 72 hours in vitro (Figure 20a). The analysis (atomic-%) of the non-reacted BaG spheres is presented as a comparison. (Publication II)

4.4.4.   Weight change and water absorption *in vitro*

All samples studied lost some weight during hydrolysis in PBS. At the same time they also absorbed some water. The remaining mass and water absorption of the γ-sterilized self-reinforced samples are presented in Table 11. It can be seen that the filler addition affected water absorption more than mass loss. The samples started to absorb water the earlier the more filler was added. Mass loss was also slightly faster with samples containing filler than to the plain matrix polymers. The samples containing filler absorbed water quite linearly throughout the hydrolysis, whereas the plain matrix polymers seemed to have two steps. At the beginning they did not absorb water at all and when uptake started it started very rapidly. The differences between the matrix polymers are also apparent. Poly-L-lactide-co-glycolide based samples started to absorb water and lost their weight first.

Table 11.

Remaining mass and water absorption results of the γ-sterilized self-reinforced samples. At the end of hydrolysis some samples had disintegrated and thus mass loss and water absorption could not be measured (marked as line (-) in the Table). All values are means of three independent measurements.

Sample abbreviation	Remining mass during the hydrolysis [%]							Time when remaining mass under approx. 95%
	0w	12w	18w	36w	52w	75w	104w	
SRPLA70	100	100	100	100	95	-	-	52 weeks
SRPLA70BaG20	100	99	99	99	96	69	37	52 weeks
SRPLA70BaG30	100	n.m.	99	98	95	69	45	48 weeks
SRPLA70BaG40	100	n.m.	98	94	88	59	33	30 weeks
SRPLA70BaG50	100	n.m.	98	96	87	66	51	30 weeks
SRPLA70TCP20	100	100	100	100	100	95	63	75 weeks
SRPLA96	100	100	100	100	100	82	62	63 weeks
SRPLA96BaG20	100	99	99	99	97	84	59	63 weeks
SRPLA96TCP20	100	100	100	100	100	96	79	72 weeks
SRPLA96TCP20(m)[a]	100	100	100	100	99	n.m.	n.m.	n.m.
SRPLGA	100	97	75	52	36	-	-	12 weeks
SRPLGABaG20	100	96	81	45	31	19	9	12 weeks

Sample abbreviation	Water absorption during the hydrolysis [%]						
	0w	12w	18w	36w	52w	75w	104w
SRPLA70	0	1	1	9	26	-	-
SRPLA70BaG20	0	5	7	10	41	54	157
SRPLA70BaG30	0	n.m.	12	35	46	67	-
SRPLA70BaG40	0	n.m.	25	57	62	n.m	252
SRPLA70BaG50	0	n.m.	28	51	76	111	162
SRPLA70TCP20	0	3	3	6	13	44	126
SRPLA96	0	1	1	1	4	21	54
SRPLA96BaG20	0	5	7	13	19	30	66
SRPLA96TCP20	0	4	5	8	11	24	42
SRPLA96TCP20(m)[a]	0	5	6	11	17	n.m.	n.m.
SRPLGA	0	4	26	70	-	-	-
SRPLGABaG20	0	17	35	100	198	-	-

n.m. not measured

4.4.5. Molecular weight *in vitro*

The molecular weight measurements were made on poly-L/DL-lactide 70/30 and poly-L/D-lactide 96/4 based samples. Poly-L-lactide-co-glycolide based samples could not be tested using GPC because the polymer did not dissolve in the chloroform. Table 12 presents the measured weight average molecular weight (M_w) during hydrolysis in PBS. When the raw materials of the matrix polymers were received from the manufacturers, their molecular weights were different to each other. However, after processing and γ-sterilization the initial molecular weight values were quite similar to each other

59.3 kDa (SRPLA70) and 59.1 kDa (SRPLA96). The filler addition decreased the initial molecular weight values further.

Sample abbreviation	raw material	Weight average molecular weight, M_w [kDa]						
		0w	12w	24w	36w	52w	75w	104w
SRPLA70	350 / 410	59.3	34.1	22.2	10.0	2.3	1.0	-
SRPLA70BaG20	350 / 410	53.6	41.7	31.4	21.0	11.2	-	-
SRPLA70BaG30	410	50.4	36.3	24.9	16.3	7.1	-	-
SRPLA70BaG40	410	39.9	23.7	16.3	9.6	5.0	-	-
SRPLA70BaG50	410	43.3	31.0	18.3	11.2	-	-	-
SRPLA70TCP20	410	55.7	36.2	25.6	27.6	10.9	10.1	-
SRPLA96	300	59.1	44.5	33.2	22.3	7.6	3.3	2.1
SRPLA96BaG20	300	46.8	31.5	31.5	22.2	11.0	4.7	-
SRPLA96TCP20	380	50.6	40.9	26.1	27.2	18.8	6.1	-
SRPLA96TCP20(m)[a]	380	49.0	31.9	n.m.	25.9	17.8	-	-
SRPLGA	n.m.	n.m	n.m	n.m.	n.m	n.m	n.m	n.m
SRPLGABaG20	n.m.	n.m	n.m	n.m.	n.m	n.m	n.m	n.m

n.m. not measured

During hydrolysis M_w started to decrease as soon as the samples were immersed in the buffer solution. Decrease was faster in plain matrix polymers than in samples containing filler and β-TCP addition seemed to slow the decrease more than BaG.

At the beginning of hydrolysis the molecular weight distributions (MWD) of all samples studied were monomodal. Poly-L/D-lactide 96/4 based samples mainly maintained their monomodality throughout the whole hydrolysis. Only small roughness and broadening was noticed at small M_w values (less than 5 kDa). However, the molecular weight distribution of the plain poly-L/DL-lactide 70/30 started to show a clear shoulder and transferred step by step to a bimodal curve. This occurred after 48 weeks *in vitro* and at the very low molecular weight values, less than 5 kDa. The filler containing poly-L/DL-lactide 70/30 based samples do not show such clear bimodality during the hydrolysis, but slight shoulders and broadening in the curves were observed.

The molecular weight plays an important role in the degradation of the studied samples. When the different properties are presented as a function of weight average molecular weight (M_w), their dependence on the molecular weight becomes apparent. Figure 22 illustrates the bending strength, mass loss and water absorption of the poly-L/D-lactide 96/4 based samples as a function of weight average molecular weight, M_w. Poly-L/DL-

lactide 70/30 based samples behaved very similarly. It was interesting to observe that the rapid mass loss of all samples occurred at very low molecular weight values (5 – 10 kDa) equally. The bending strength decreased slightly earlier (about 25 kDa) and also equally. The filler addition did not affect these much. However, the filler addition affected the water absorption, meaning that the samples containing filler started to absorb water slightly earlier. However, the rapid water uptake occurred at the very low molecular weight values (5 kDa) in all samples.
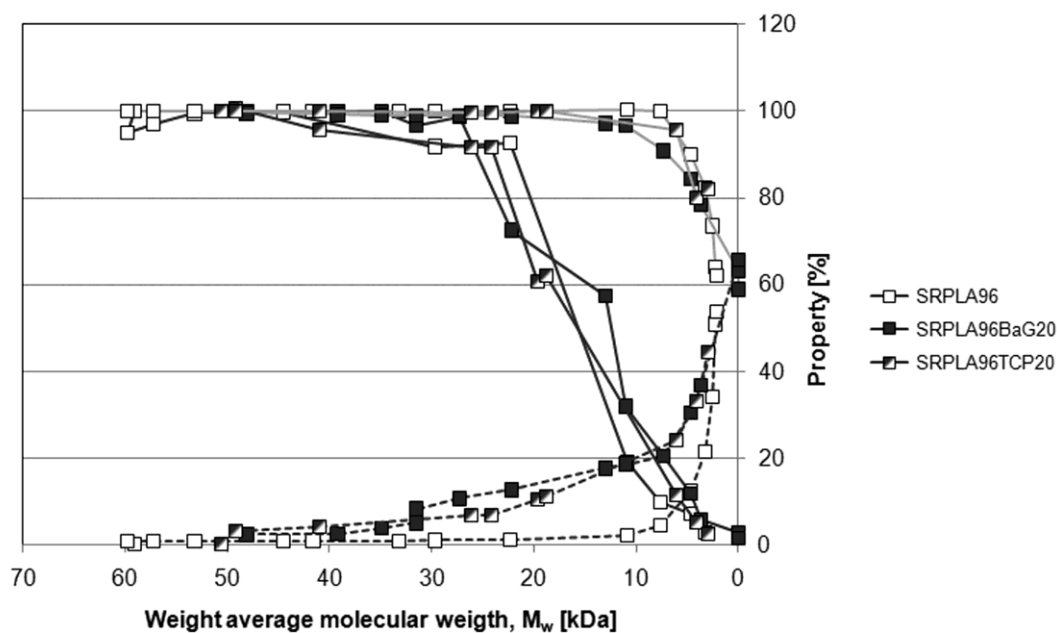
Figure 22.
Remaining bending strength, remaining mass and water absorption of the poly-L/D-lactide 96/4 based samples as a function of weight average molecular weight (M_w) during hydrolysis in PBS. M_w data are means of two repeat injections.

4.4.6. Thermal properties *in vitro*

Initially all samples studied were either amorphous or partially crystalline. Poly-L/DL-lactide 70/30 based samples were completely amorphous and glass transitions (T_g) were observed at 56 – 58 °C (heating B). Poly-L/D-lactide 96/4 and poly-L-lactide-co-glicolide based samples were partially crystalline. Their glass transitions were observed at 61 – 63 °C and 58 – 60 °C respectively. The addition of filler material had no remarkable influence on the glass transition temperature. During the hydrolysis the glass transition temperature transferred to the lower temperatures.

Because the poly-L/DL-lactide 70/30 based samples were initially amorphous, no melting temperatures were detected initially. However, during hydrolysis the

60

crystallinity of the samples increased and a melting peak was detected. A slight crystallization was also observed during the first heating (heating A). This crystallization occurred at lower temperatures than melting and thus after forming the crystals formed quickly melted when the heating was continued. This occurrence disappeared as the degradation proceeded.

The melting peak of the poly-L/DL-lactide 70/30 based samples was first seen at 123 – 127 °C and as hydrolysis proceeded, it transferred to lower temperatures. The time at which the melting peak appeared depended on the samples. For the plain matrix polymer the melting peak was first detected after 24 weeks *in vitro*. The BaG addition caused the melting peak to appear earlier than with the plain matrix polymer and the more BaG was added, the earlier the melting peak was detected. On the other hand, the addition of β-TCP caused the melting peak to occur somewhat later than with the plain matrix polymer. At the same time as the molecular weight distribution started to show some shoulders, very slight shoulders were also observed in the melting peaks of the poly-L/DL-lactide 70/30 based samples. However, in most cases the melting peak was still monomodal but became somewhat broader.

The poly-L/D-lactide 96/4 based samples were initially partially crystalline. The melting peak was initially detected at temperatures 154 – 157 °C (heating A). During the degradation process the melting temperature transferred to lower temperatures and the size and shape of the melting peak changed. The melting peak remained monomodal throughout the entire hydrolysis, but the bottom of the peak became broader. Crystallization was not detected during the first heating as it was with the poly-L/DL-lactide 70/30 based samples. However, during the second heating (heating B), crystallization and melting were observed after the glass transition temperature. The enthalpies of the crystallization and following melting were quite equal. At the beginning of the hydrolysis these were very small, but as the degradation proceeded the crystallization and melting peaks increased. The melting peak in heating B became bimodal at around 30 – 36 weeks *in vitro*. The addition of the filler material influenced the appearance of the bimodal peaks. If BaG was added, the bimodal peak appeared somewhat earlier and if β-TCP was added, the bimodal peak appeared somewhat later compared in the plain matrix material. Some examples of the DSC curves of the self-reinforced γ-sterilized plain matrix polymer poly-L/D-lactide 96/4 (SRPLA96) are presented in Figure 23.
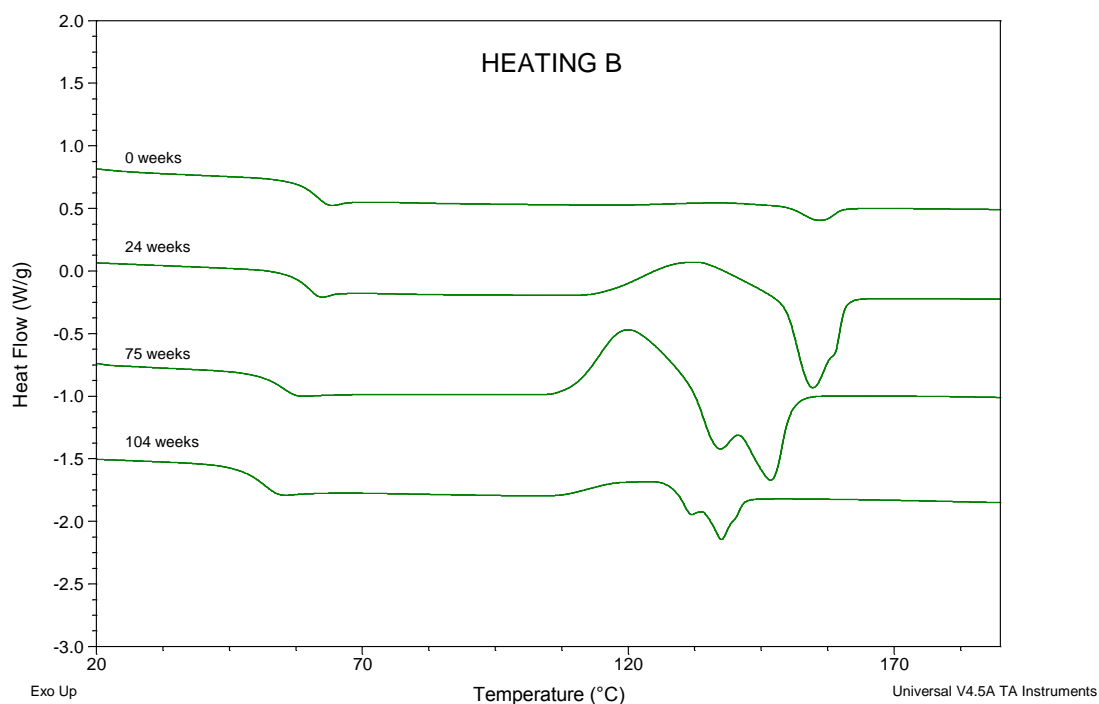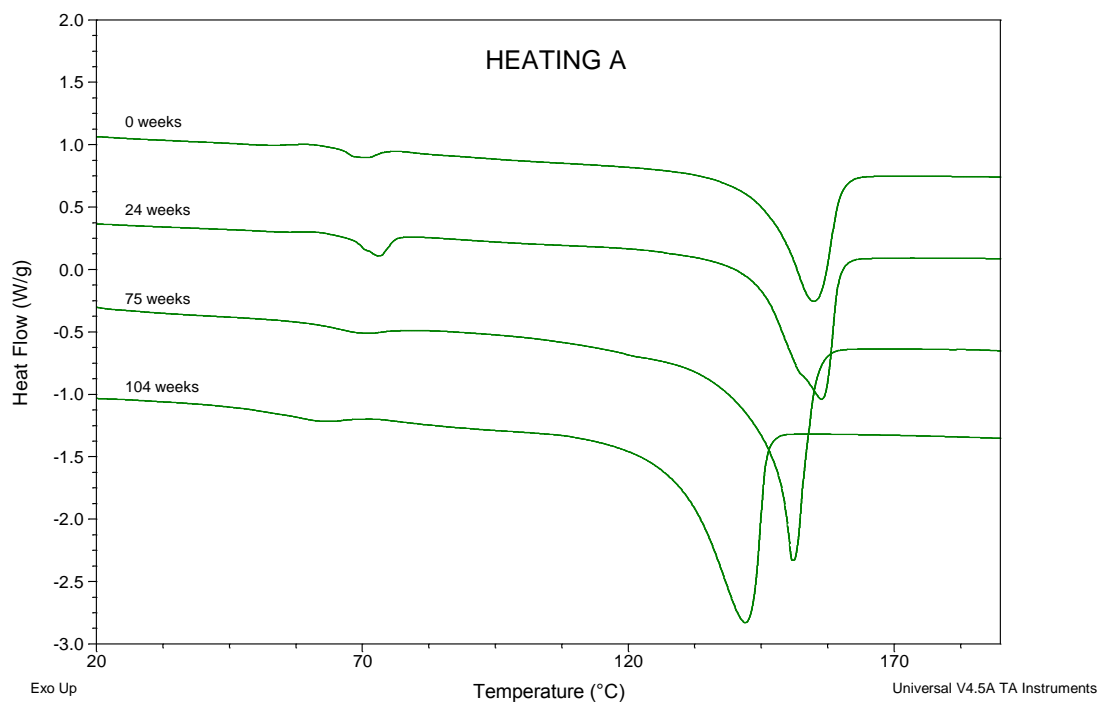
Figure 23.

DCS curves of the self-reinforced γ-sterilized plain matrix polymer poly-L/D-lactide 96/4 (SRPLA96) at different time points during hydrolysis in PBS. The melting peaks can be observed from the curves of the first heating (heating A). The melting temperature transferred to the lower temperatures and the melting enthalpy increased as the degradation proceeded. The glass transition temperatures can be detected from the curves of the second heating (heating B). Crystallization and bimodal melting peaks were also detected during eating B.

The poly-L-lactide-co-glycolide 80/20 based samples were also initially partially crystalline, but not to the same extent as the poly-L/D-lactide 96/4 based samples. At the beginning of hydrolysis the monomodal melting peak was detected around 160 – 164 °C (heating A). During the degradation process the melting temperature became lower and the size and shape of the melting peak changed. The behavior of the poly-L-lactide-co-glycolide 80/20 based samples differed from that of the others. The crystallization peak was already detected at the first heating before the melting peak at the very beginning of hydrolysis. The enthalpy of the crystallization peak was smaller than that of the melting peak and disappeared after 12 weeks *in vitro* while the melting peak continued to grow. The melting peak also became broader and turned to bimodal around 18 weeks *in vitro*. The bimodality of the melting peak remained until the end of the hydrolysis. The second heating (heating B) showed slight crystallization and melting around 6 – 36 weeks *in vitro*. The crystallization peak was monomodal, but the melting peak was bimodal with two clear peaks. The addition of BaG caused the bimodal melting peak to appear somewhat earlier than without the addition of BaG.

The overall melting enthalpy (ΔH) (melting enthalpy minus crystallization enthalpy) is directly proportional to the overall crystallinity of the samples and thus it was used to estimate the changes in the crystallinity of the samples during hydrolysis. During hydrolysis ΔH increased in all studied samples, meaning that the crystallinity of all samples increased. The ΔH values of the samples during the hydrolysis can be seen in Table 13.

Table 13.

Overall melting enthalpy (ΔH) and weight average molecular weight (M_w) of the samples during hydrolysis in PBS. The molecular weight of the all samples could not been measured at the end of hydrolysis and are thus marked as empty (-).

Sample abbreviation	0 weeks		12 weeks		24 weeks		36 weeks		87 weeks		104 weeks	
	ΔH [J/g]	M_w [kDa]	ΔH [J/g]	M_w [kDa]	ΔH [J/g]	M_w [kDa]	ΔH [J/g]	M_w [kDa]	ΔH [J/g]	M_w [kDa]	ΔH [J/g]	M_w [kDa]
SRPLA70	0	59.3	0	34.1	0.3	22.2	6.8	10.0	59.9	0.9	61.7	-
SRPLA70BaG20	0	53.6	0	41.8	0.7	31.4	3.8	21.0	47.4	-	52.4	-
SRPLA70BaG30	0	50.4	0	36.3	1.9	24.9	5.1	16.3	24.2	-	29.5	-
SRPLA70BaG40	0	39.9	0.7	23.7	5.3	16.3	9.3	6.4	31.5	-	33.8	-
SRPLA70BaG50	0	43.3	0	31.0	2.3	18.3	1.8	11.2	20.2	-	-	-
SRPLA70TCP20	0	55.7	0	36.2	0	25.6	1.3	27.6	6.7	5.2	18.5	-
SRPLA96	38.1	59.1	43.0	44.5	42.5	33.2	45.5	22.3	62.5	2.5	68.9	2.1
SRPLA96BaG20	30.6	46.8	32.5	31.5	37.5	31.5	37.5	22.2	53.4	3.7	50.2	-
SRPLA96TCP20	29.7	50.6	32.9	40.9	31.8	26.1	34.6	27.2	34.5	4.0	47.5	-
SRPLGA	17.5	n.m.	25.2	n.m.	48.2	n.m.	54.2	n.m.	55.6	n.m.	54.5	n.m.
SRPLGABaG20	10.2	n.m.	26.5	n.m.	38.0	n.m.	43.4	n.m.	56.0	n.m.	40.0	n.m.

n.m. not measured

The poly-L/DL-lactide 70/30 based samples had no initial crystallinity (0 weeks) due to the amorphous structure of the matrix polymer. Poly-L/D-lactide 96/4 and poly-L-lactide-co-glycolide 80/20 based samples did exhibited some initial crystallinity. The melting enthalpies were 30 – 38 J/g and 10 - 17 J/g respectively (Table 13). During hydrolysis the melting enthalpies and thus the crystallinity increased in all samples studied. The poly-L/DL-lactide 70/30 based samples also crystallized during the degradation process, so that the crystallinity of the plain matrix poly-L/DL-lactide 70/30 (SRPLA70) was almost as high as that of the plain matrix poly-L/D-lactide 96/4 (SRPLA96) at the end of hydrolysis. The addition of BaG affected the crystallization of the samples so that the final crystallinity of the samples containing BaG was lower than in the plain matrix polymer. The addition of β-TCP also seemed to prevent crystal formation, even more than BaG. During the *in vitro* period studied, the poly-L-lactide-co-glycolide 80/20 based samples reached the highest total crystallinity, melting enthalpy values approximately 75 J/g. This already occurred after 63 weeks *in vitro,* after which the crystallinity started to decrease.
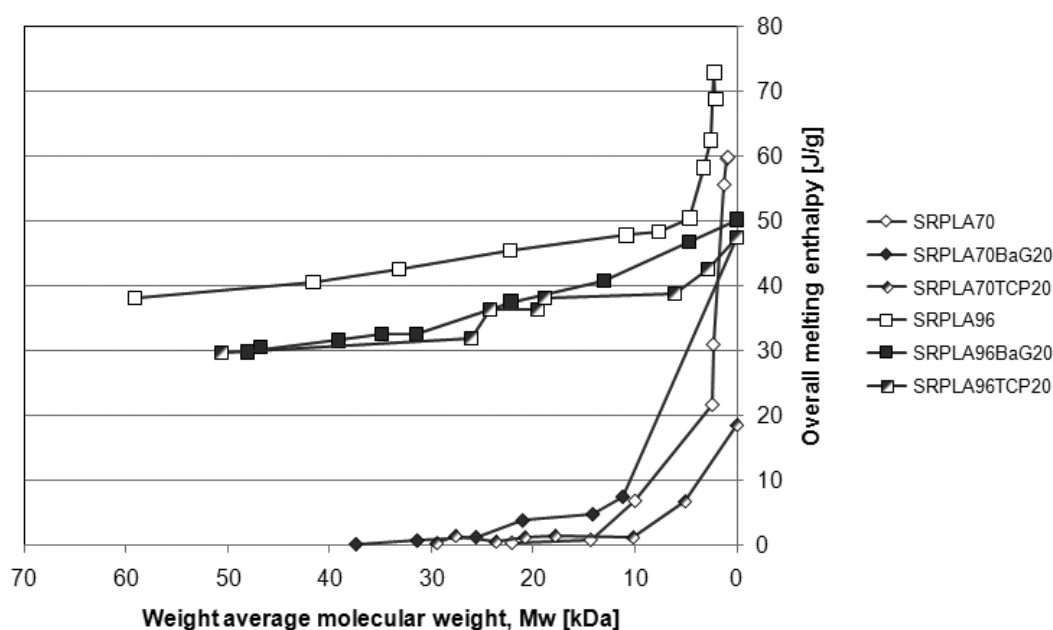
Figure 24.
Overall melting enthalpy (ΔH) of the poly-L/DL-lactide 70/30 and poly-L/D-lactide 96/4 based samples as a function of weight average molecular weight (M_w) during hydrolysis in PBS. Overall melting enthalpy was used to estimate the crystallinity of the samples because it is directly proportional to crystallinity. The data are means of two parallel scans and two repeat injections.

Many properties of the samples studied were observed to be dependent on the molecular weight of the samples as was already apparent in Figure 22. The crystallinity of the

samples was also heavily dependent on molecular weight. At first the increase in crystallinity during the degradation was quite steady, but when the molecular weight of the samples decreased sufficiently, the crystallization accelerated. This is obvious Figure 24, where the overall melting enthalpy is plotted as a function of the weight average molecular weight. The greatest crystallinities were observed at M_w values under 10 kDa.

5. DISCUSSION

The compounding of the osteoconductive filler material and bioabsorbable matrix material using twin-screw extrusion was found to be a sufficient processing method to achieve well dispersed samples with different filling contents of osteoconductive filler materials. The further processing of the samples using the self-reinforcing technique, in this thesis using solid state die-drawing, modified the properties of the samples. The original aim of the different self-reinforcing techniques is the improvement of the mechanical properties of the polymers. Non-reinforced extruded plain polylactide based products are commonly brittle (Törmälä 1992, Törmälä *et al.* 1998, Kellomäki *et al.* 2003) and this may lead to serious problems during and after implantation (McGuire *et al.* 1999). Self-reinforcing eliminates this problem and makes the initially brittle materials ductile. The improvement in the mechanical properties is based on the orientation of part of the micro-structure of the material. These stiff and strong oriented fibrous reinforcing elements are bound together with the matrix material, both having the same chemical composition. (Törmälä 1992). Due to self-reinforcing the mechanical properties of the bioabsorbable polymers have attained properties which are also sufficient for load bearing applications.

It was later discovered that self-reinforcing using die-drawing modified also the micro-structure of the filler containing samples (Törmälä *et al.* 2002). The filler particles initiated the formation of the pores both inside and on the surface of the samples during the self-reinforcing process (Niiranen and Törmälä 1999, Kellomäki *et al.* 2000, Niiranen *et al.* 2004). At the surface of the composite the initially polymer-covered particles were exposed and thus the filler particles came into direct contact with the surrounding fluids which was considered as a positive event. Because of it there was no need for further mechanical processing of the implant surface to expose the filler phase. However, the additional machining of the sample's surface seemed to expose even more filler particles and generate a rough surface. The porous and rough surface had been thought to be beneficial for the mechanical interlocking of the bone tissue to the implant surface (Kellomäki *et al.* 2000, Karageorgiou & Kaplan 2005). The pores inside the structure were found to be located close and around the filler particles and to be spindle-shaped. The pores were not seen to be interconnected and thus conventional porosity measurements, like mercury porosimeter, were not applicable.

Self-reinforcing reduces the diameter of the samples and thus the polymer chains need to be reorganized and therefore the filler particles are moved. This may cause problems if the filler content is high. In that case there are more filler particles and less matrix polymer in the cross-section area of the samples. The proportion of the matrix material will be too low to keep the structure cohesive and the structure failed. This may be the reason why the sample containing 50 wt-% of BaG could not achieve a draw ratio higher than 2.0.

Self-reinforcing is affected by many factors, such as drawing temperature, draw ratio and crystallinity of the used polymer. The properties of the die used, such as diameter, material, shape and coating, also have an effect. (Törmälä 1992, Törmälä *et al.* 1998, Kellomäki *et al.* 2003) The greatest strength is not necessarily achieved with the highest draw ratio since high fibrillation degree may cause delamination of the structure between the fibrils. Thus the combination of self-reinforcing parameters must be chosen carefully. In addition to the parameters, the characteristics of the materials used are also important. For example, the crystallinity of the matrix polymer influences the greatest strength which could be achieved in self-reinforcing. The more crystalline the polymer, the greater is the improvement in the initial strengths in the self-reinforcing (Kellomäki *et al.* 2003). Thus the different self-reinforced copolymers of polylactides have different initial mechanical properties. Self-reinforced poly-L/D-lactide 96/4 has mechanical properties lower than those of highly crystalline self-reinforced poly-L-lactide but higher than those of self-reinforced poly-L/DL-lactide 70/30, which is an amorphous polymer (Kellomäki *et al.* 2003). Crystallinity, of course, is not the only characteristic affecting the achieved properties. For example, the initial molecular weight also plays an important role (Vert *et al.* 1991).

In this thesis the micro-structure formed during manufacturing was studied mainly using scanning electron microscopy (SEM). SEM was a suitable method to assess the two-dimensional (2D) structural properties of the samples. The results obtained using SEM were only visual estimations, no quantitative results were obtained. From SEM images it could be observed that the filler particles were quite well dispersed throughout the whole samples. The formed porosity both inside and on the surface of the structure was also detected, but no numerical data was obtained. Thus micro-computed tomography (μ-CT) image analysis was performed for a more precise analysis of the micro-structure of certain samples. In this thesis μ-CT image analysis concentrated on the properties of the filler particles, especially their distribution inside the structure. More specific further studies are needed for a better understanding of the whole micro-structure, including porosity.

According to SEM images it has been assumed that the non-reinforced osteoconductive filler particles containing samples do not have many pores in their structure. Now the more accurate μ-CT image analysis of one of the non-reinforced samples, the sample which contained 20 wt-% of BaG in poly-L/DL-lactide 70/30 matrix, indicated that there was approximately as much as 15 vol-% porosity in the structure. This result was unexpected and interesting. The porosity was probably due to the compounding process of the raw materials. The surface of the BaG was known to be smooth and adhesion with the polymer very poor. Thus the filler material may elicit interfaces with empty spaces. Additionally there may be some air bubbles with no filler particle left inside the structure. To confirm this finding, and to compare it with other filler materials, it will be necessary to do more specific μ-CT image analyses of the several different non-reinforced samples.

The total porosity of the sample which contained poly-L/DL-lactide 70/30 and 20 wt-% of BaG seemed to increase during the self-reinforcing process, as could be supposed according to the SEM images and earlier studies (Niiranen and Törmälä 1999, Kellomäki *et al.* 2000, Niiranen *et al.* 2004). The filler particles initiated the formation of the pores during solid state die-drawing. The formation of the pores seemed to be dependent on the hardness, size, shape and structure, such as the porosity, of the filler materials. The hard, smooth and dense spherical BaG particles initiated more and larger pores than soft and porous (sintered) β-TCP particles. The hard particles were more resistant to the forces interacted during solid state die-drawing whereas the soft particles most often disintegrated under interacting forces. The small particles formed were no longer able to initiate large pores, even if a large amount of interfaces were formed. Thus the porosity of the sample containing poly-L/DL-lactide 70/30 and 20 wt-% of β-TCP was lower compared to the sample containing spherical BaG particles. The size, shape and number of the filler particles also influenced the porosity formed (Publication VI, Kellomäki *et al.* 2000, Niiranen *et al.* 2004).

The filler content achieved was determined using three different methods. All the results showed that the filler contents achieved were slightly lower than intended. This lowering of the content was most probably due to the extrusion process. Due to the electrically charged walls of the mixing bowl and the feeding hopper of the extruder, some of the filler particles were attached to them and thus the actual filler content was lower than the desired filler content. The filler content can be compensated using higher quantities of filler particles in mixing, as has been performed in poly-L-lactide-co-glycolide 80/20 based composites. It was also observed that the results obtained using μ-CT image analysis were systematically slightly lower than the others. This was thought to be due to the possibility that the μ-CT image analysis did not take into account all the filler particle volumes due to the partial volume effect (Dawant and Zijdenbos 2004). The very smallest particles (< 10 μm) were deliberately excluded from the analysis, which also influenced results achieved. The other reason may be fact that both the TGA and burning test are based on the heating and burning of the matrix polymer. With such methods, there is always a minor possibility that there is still polymer left in the residual and thus the values may appear slightly higher than they really are.

μ-CT image analysis was a suitable method to examine how the different components of the composite (filler material, matrix material and pores) were located inside the structure of the samples studied. This had not been possible to examine with any other methods and was thus important new piece of information. The volume distribution analyses were performed along both longitudinal axis and polar axes. Along the longitudinal axis the volume distributions actually remained unchanged. Along the polar axis the proportions of the different components remained almost unchanged throughout the entire radius. Only very close to the surface of the samples (about 100 μm) did the proportions of the filler particles and matrix material decrease sharply and at the same

time the amount of pores increased sharply. This behavior was observed in all three samples studied and may be due to the open pores and roughness on the surface. This property is considered favorable, because a porous and rough surface is thought to be beneficial for mechanical interlocking between the bone and implant.

When the volume distribution analyses of the non-reinforced and self-reinforced samples were compared some differences were observed. The self-reinforcing increased the porosity remarkably. It was also seen that the porosity was slightly greater along the longitudinal axis than along the polar axis. This was most probably due to the solid state die-drawing which occurred in the direction of the longitudinal axis. Thus the spindle-shaped pores were also oriented along this axis, as could also be seen in the SEM images. The self-reinforcing reduced the diameter of the samples. This caused the filler particles to reorganize. Probably they moved a short way along the longitudinal axis relative to the other particles since the polymer matrix stretched due to die-drawing. The consequence of it was that the average distances measured between the filler particles along the longitudinal axis were greater than along polar axis.

The manufacturing process affected not only to the porosity of the samples, but also the characteristics of the filler materials, especially their sizes, shapes and distributions. The particle size distributions analyzed after processing were wider than reported by manufacturers. This means that the filler particles were disintegrated during the processing. The disintegration was greatest in soft and porous samples containing β-TCP. This was to be expected because the soft particles did not withstand the forces affecting as well as the hard particles did. The shape of the filler particles was also found to affect the disintegration sensitivity. Sharply edged particles will split more easily than spherical particles (Publication IV). One remarkable factor affecting the disintegration was studied to be the extrusion process and especially the extruder type used. A single-screw extruder involves higher actual stresses during the compounding process than a twin-screw extruder. The stresses involved exceeded the yield point of the filler materials and caused the breakdown of the particles (Rauwendaal 2001). Thus the single-screw extruder was seen to cause more disintegration than twin-screw extruder (Publication IV).

After processing, none of the filler particles turned out to be perfect spheres according to μ-CT image analysis. The sphericity of the filler particles was studied by analyzing the shape indices. The spherical BaG particles had the lowest shape index and were therefore closest to the shape of a sphere. The β-TCP particles were broken down during manufacturing, as discussed above, and thus their shape had no significant analogy.

Some studies of the filler distribution and its effects on the properties of composites have been performed in different fields of composite science (Avérous *et al.* 1998, Wang *et al.* 2005, Wu *et al.* 2008). According to these studies it is very interesting and important to know the filler particle distribution inside the structure of the samples

studied. The most commonly used method to evaluate 2D filler distribution is microcopy, including SEM. SEM is an adequate method to estimate porosity and pore sizes, but quantitative analysis is very laborious. Thus some computerized image analysis is often combined with these methods to obtain more quantitative results of the distribution. (Avérous *et al.* 1998, Wu *et al.* 2008) 3D micro-structural analysis, such as μ-CT image analysis, would also be very useful for these purposes. μ-CT image analysis is a non-destructive 3D analysis method which can produce high resolution images. It is therefore a very promising method in the field of biomedical materials. The technique offers an excellent way to analyze the porosity characteristics of the material (Atwood *et al.* 2004, Tuan and Hutmacher 2005, Yeung *et al.* 2005, Jones *et al.* 2007, Renghini *et al.* 2009), anisotropy of the structure (Mathieu *et al.* 2006) and bone ingrowth in the scaffold (Jones *et al.* 2004, Jones *et al.* 2007, Guldberg *et al.* 2008).

In this thesis the main objective of μ-CT image analysis was to ascertain the 3D distribution of the filler particles. The particle distribution was determined in two directions: along the longitudinal axis and along the polar axis, as with the volume distribution above. The location of the filler particles in the cross sectional plane can be observed from the polar axis analysis. Non-reinforced and self-reinforced BaG containing poly-L/DL-lactide 70/30 samples had fairly constant distributions, only very close to the surface did the number of filler particles decrease dramatically, as already observed in the at the volume distribution analysis. A similar decrease was also detected in the β-TCP containing poly-L/DL-lactide 70/30 sample. Inside the structure, and especially near to the center of the sample, the β-TCP containing sample showed slightly more variation in filler particle distribution. This variation was probably due to the disintegration of the β-TCP particles during the manufacturing process and thus there were more small particles in the structure. When there were more particles the probability of variation was higher. Along the longitudinal axis the particle distributions were more uniform in all studied samples.

In Publication VI of this thesis the effect of the different extruders on filler particle distribution was also studied. It was seen that the samples manufactured using a twin-screw extruder had more homogenous distribution than those manufactured using a single-screw extruder. The result was obvious, because it is generally known that the twin-screw extruder is a better choice when the compounding is needed (Rauwendaal 2001).

Both matrix polymer and filler particles as well as the interface between these two play an important role in particulate filler composites. The matrix polymer is mainly responsible for the mechanical properties of the composites, because it is usually the main component of the composite. The addition of any osteoconductive filler material to the polymer matrix influenced both the properties and degradation behavior of the composites (Bonfield 1993, Li and Vert 1996, Guo *et al.* 1998, Ignatius *et al.* 2001, Kikuchi *et al.* 2002, Rich *et al.* 2002, Niiranen *et al.* 2004, Maquet *et al.* 2004, Zhou *et*

al. 2007, Cotton *et al.* 2008, Kobayashi and Sakamoto 2009, Zhou *et al.* 2009). The properties and degradation behavior could be varied by changing the matrix and filler materials and filler content. Also improvement of the interfacial bond strength influenced (Deb *et al.* 1996, Wang *et al.* 2000a). The selection of materials and contents depends on the application envisaged.

In this study the addition of osteoconductive filler material to the bioabsorbable matrix polymer affected the mechanical properties of both the non-reinforced and self-reinforced samples. The discontinuity of the structure increased when any filler material was added. The deterioration in the mechanical properties may be due to the weakness of the structure caused by these points of discontinuity. Moreover, there was no chemical bond between the osteoconductive filler material and the bioabsorbable matrix polymer, which explains the deterioration of the mechanical properties. If there was a chemical bond between the matrix polymer and filler particles, the mechanical properties could be better (Deb *et al.* 1996, Wang *et al.* 2000a, Stamboulis and Hench 2001, Wang 2003).

The non-reinforced, non-sterilized samples became weaker and more brittle when the filler material was added. The more filler material was added, the more the properties deteriorated. A similar effect has also been detected and reported for other non-reinforced composites (Bonfield 1993, Wang *et al.* 1998, Ignatius *et al.* 2001, Kikuchi *et al.* 2002, Kobayashi and Sakamoto 2006, Zhou *et al.* 2009) although opposite results have also been reported (Guo *et al.* 1998). The self-reinforcing improved the mechanical properties of the plain matrix polymers and made the samples ductile. The initially achieved mechanical properties of the γ-sterilized self-reinforced matrix polymers were very similar to those reported by other researchers (Pohjonen and Törmälä 1997, Törmälä *et al.* 1998, Saikku-Bäckström *et al.* 1999, Kellomäki *et al.* 2000, Veiranto *et al.* 2002, Kellomäki *et al.* 2003, Niiranen *et al.* 2004, Veiranto *et al.* 2004a, Veiranto *et al.* 2004b). The best properties were detected in self-reinforced plain poly-L/D-lactide 96/4 due to its highest initial crystallinity.

The self-reinforcing also improved the mechanical properties of the samples containing 20 wt-% of osteoconductive filler particles. The mechanical properties achieved were, however, inferior to the corresponding self-reinforced plain matrix polymers. This was presumably due to the increased porosity and thus the increased discontinuity of the structure. However, if the filler content was greater than 20 wt-%, the reinforcing effect was not detected although the brittleness was observed to diminish and the samples to become ductile. The lack of reinforcing effect was probably due to the greater number of large discontinuity points because of the greater number of filler particles.

During self-reinforcing the initial bending strength of the β-TCP containing samples was observed to improve more compared to BaG containing samples. The porosity formed during self-reinforcing was higher in BaG containing samples and thus the reinforcing effect was not so high. In addition to porosity formed, the surface of the

filler material was thought to have an influence. The surface of the BaG is known to be smooth and thus it has only very minimal mechanical interlocking with the matrix polymer. Sintered β-TCP has rough and slightly porous surface which is more favourable to mechanical interlocking. Thus it could be assumed that polymer matrix bonded more tightly to β-TCP than to BaG. However, although there is a slight mechanical interlocking the overall adhesion between the filler material and matrix polymer is quite non-existent.

In general, adhesion between the filler and matrix materials, and thus the mechanical properties, can also be improved by surface treatment, such as coupling (Hull and Clyne 1996). However, it may be necessary to question whether the coupling is suitable for this kind of self-reinforced osteoconductive bioabsorbable composites? There is a need to confirm if the coupling is still valid and functioning after die-drawing? It may be that the forces acting during the die-drawing are too high and the bonds formed can not withstand. Other thing is the behavior of the coupling agents during the biodegradation process. In bioabsorbable composites both filler and matrix materials are bioabsorbable and thus also the interface and coupling agent should be bioabsorbable.

The hydrolytic behavior of all γ-sterilized self-reinforced samples studied was studied *in vitro* in phosphate buffered saline (PBS) for up to 104 weeks (2 years). The majority of the samples could not be tested for so long because the structure of the samples became too brittle and broke down as degradation proceeded. The plain matrix polymers had higher initial mechanical properties than the corresponding samples containing filler material as described above. Poly-L/D-lactide 96/4 had the greatest bending strength and also retained it the longest, for up to about 36 weeks. Poly-L/DL-lactide 70/30 retained its bending strength for only about 12 weeks and poly-L-lactide-co-glycolide 80/20 for even less, about 6 weeks. The shear properties behaved very similarly. The addition of the filler material changed the strength behavior. The initial strength values were about 20 – 30 % lower than those of plain matrix polymers. However, the strength retentions during the *in vitro* tests were similar or even better. It was observed that the addition of β-TCP affected strength retention more than the addition of BaG. This could probably be due to the better mechanical interlocking between β-TCP and matrix polymer than between BaG and matrix polymer. The samples containing β-TCP retained their mechanical properties even longer than the plain matrix polymers and also longer than the samples containing BaG. The number of filler particles also affected the strength retention in addition to the initial mechanical strengths of the samples. The greater the filler content the faster the sample lost its mechanical properties. Similar longer strength retention during *in vitro* testing has also been reported also with other composites (Niiranen *et al.* 2004, Zhou *et al.* 2009) and opposite results with some non-porous composites (Ignatius *et al.* 2001).

The longer strength retention of the self-reinforced filler containing samples compared to the plain matrix polymers was thought to be due to their porous structure. The acidic

degradation products of the matrix materials were thought to be able to diffuse away from the internal structure through the pores and interfaces between the matrix polymer and filler particles. This may impede the formation of the acidic environment in the interior of the samples which further reduces the autocatalytic degradation of the matrix material. However, if there are many pores in the structure there is also a larger surface area in direct contact with the hydrolytic environment and this causes a more rapid degradation process. The samples containing more BaG were weaker and had also more pores and thus lost their mechanical properties faster.

When the matrix polymers started to degrade the pH of the buffer solution slightly decreased due to the release of the acidic degradation products of the poly-α-hydroxyacids (Vert *et al.* 1991, Li 1999, Li and Vert 1999, Middleton and Tipton 2000). With poly-L/D-lactide 70/30 and poly-L/DL-lactide 96/4 this happened around 52 weeks *in vitro* and with poly-L-lactide-co-glycolide 80/20 much earlier, around 12 weeks *in vitro*. The faster degradation of poly-L-lactide-co-glycolide 80/20 is due to the presence of the glycolic acid monomers which are more hydrophilic than lactic acid monomers (Li 1999, Middleton and Tipton 2000). The addition of the osteoconductive filler material, BaG or β-TCP, influenced the pH retention of all samples studied. The pH remained constant somewhat longer, which was thought to be due to the neutralizing reactions. It was assumed that the dissolution of the β-TCP particles and the bioactive reactions of BaG released phosphate ions into the surrounding buffer solution. Phosphate ions can bind hydrogen ions from the solution and thus act as an alkali. This phenomenon is thought to be the reason for the stabilizing of the pH of the buffer solution, the neutralizing of the acidic degradation product of the poly-α-hydroxyacids. No complete explanation of this phenomenon has been reported, but similar neutralizing and stabilizing effects have also been reported for other osteoconductive bioceramic / bioabsorbable polymer composites (Kikuchi *et al.* 2002, Maquet *et al.* 2003, Mellon *et al.* 2003, Kikuchi *et al.* 2004, Maquet *et al.* 2004, Niiranen *et al.* 2004, Li and Chang 2005, Zhou *et al.* 2009).

Initally all the plain matrix polymers were transparent. During hydrolysis they turned white and opaque. The samples containing osteoconductive filler material were already white and opaque initially and remained so throughout the whole hydrolysis. The visual characterization during the hydrolysis clearly showed that the samples containing filler maintained their size and shape longer than did the plain matrix polymers. However, there were significant differences between the different matrix polymers. During the first 52 weeks *in vitro* poly-L-lactide-co-glycolide 80/20 started to crack and finally crumble, poly-L/D-lactide 70/30 did not crack but swelled and shrunk and poly-L/DL-lactide 96/4 remained almost unchanged. The addition of osteoconductive filler material slowed these changes. The effect was the most significant in the poly-L/D-lactide 70/30 based samples. The added filler particles probably retarded the movement of the polymer chains and their relaxation during the hydrolysis.

It is known that when BaG is in direct contact with the surrounding fluids it has a rapid rate of surface reactions which leads to tissue bonding. These reactions result in the formation of a hydroxyl carbonate apatite (HCA) layer to which the tissue can bond. Thus the formation of the calcium phosphate precipitation on the surface of the glass was considered to be a sign of bioactivity (Hench and Andersson 1993, Hench and Wilson 1993, Cao and Hench 1996, Ben-Nissan and Ylänen 2006, Jones and Hench 2006). In this study the bioactivity of certain samples containing BaG was studied in PBS. The formation of the calcium phosphate precipitation was followed using SEM. It was seen that the BaG content together with the self-reinforcing influenced the formation of the calcium phosphate precipitation. The self-reinforcing formed pores on the surface of the samples, which allowed the BaG particles to be in direct contact with the surrounding buffer solution. This direct contact was observed to be essential for the rapid reactions of the BaG. No reactions of the polymer covered BaG were observed even after 12 days' immersion in PBS, whereas the reactions of the BaG which was in contact with the PBS were already observed after 72 hours' immersion. The reactions seen and calcium phosphate precipitation formed were localized to areas close to the BaG particles and thus if the sample contained more BaG it could be said to be more bioactive, assuming that the BaG particles were in direct contact with the buffer solution.

Niiranen and Törmälä (1999) observed that the calcium phosphate precipitation may spread over the polymer matrix surface in bioabsorbable plates covered with BaG spheres. A similar spreading of the precipitation was also detected in other composites (Marcolongo *et al.* 1997, Kellomäki *et al.* 2000, Paatola *et al.* 2001, Niiranen *et al.* 2004). Such spreading increases the calcified surface area and may thus improve the bonding of the tissue to the surface. In our studies only minor spreading was detected during the short *in vitro* period. This still does not exclude the possibility of subsequent spreading.

According to the bioactivity examination of the self-reinforced bioabsorbable osteoconductive composites, the samples proved to be bioactive if the BaG content was 20 – 40 wt-%. Open pores in the surface have been shown to be a requirement for the bioactivity of the rod-like samples. If the BaG content was much lower than 20 wt-% or higher than 40 wt-% not enough open pores were formed during self-reinforcing and thus the samples were not bioactive enough. Machining of the surface may be the solution in these cases.

The water absorptions of the various self-reinforced matrix polymers during the hydrolysis were different. In practice, γ-sterilized self-reinforced poly-L/D-lactide 96/4 and poly-L/DL-lactide 70/30 did not absorb any water before 52 weeks and 36 weeks respectively. Thereafter the water absorption accelerated rapidly, being about 54 % at the end of hydrolysis for self-reinforced poly-L/D-lactide 96/4. For self-reinforced poly-L/DL-lactide 70/30 the measurements of water absorption were unfeasible by to the end of hydrolysis due to the total disintegration of the samples. However, the studies by

Niiranen *et al.* (2004) showed that the water absorption of the self-reinforced poly-L/DL-lactide 70/30 also increased rapidly after 52 weeks *in vitro* being as much as 300 % after 87 weeks in PBS. Self-reinforced poly-L-lactide-co-glycolide 80/20 behaved significantly differently. The water absorption started much earlier and was already 70 % after 36 weeks *in vitro*. The earlier water absorption was due to glycolide copolymeration. Glycolic acid monomer is known to be more polar and thus more hydrophilic than lactic acid monomer (Li 1999, Middleton and Tipton 2000). This also contributed to on the faster degradation rate of the samples containing glycolic acid.

The addition of the osteoconductive filler material increased the water absorption of the samples in the early stage of hydrolysis in all samples studied. This was probably due to the porous structure. Moreover the interfaces between the matrix polymer and filler particles enabled the water to penetrate the structure. Thus the increase in filler content also increased the water absorption. The samples containing BaG seemed to absorb more water than samples containing β-TCP. This may be explained by the weaker mechanical interlocking between BaG particles and matrix polymer as well as by the higher porosity of the samples containing BaG. The hard and dense BaG was observed to induce more and larger pores than the soft and porous β-TCP. The water absorption was also observed to be slightly greater in the sample with a machined surface (SRPLA96TCP20(m)) than in the corresponding sample without machining. This supports the significance of porosity on the surface of the sample with regard to water absorption.

Besides the macroporosity formed during self-reinforcing, the microporosity also influenced the water absorption of the samples. Niiranen *et al.* (2004) reported that as the hydrolysis and degradation of the self-reinforced poly-L/DL-lactide 70/30 proceeded, micropores formed on the polymer matrix. This significant increased the water absorption after 48 weeks *in vitro*. There were probably no similar changes in the micro-structure of the self-reinforced poly-L/D-lactide 96/4, because the increase in water absorption was not so enormous. However, the rapid increase in water absorption after 52 weeks *in vitro* may be due to the so-called second stage of hydrolytic degradation. The hydrolytic degradation of the semicrystalline poly-α-hydroxyacids, such as poly-L/D-lactide 96/4, could be divided into two stages. In the first stage the water diffuses into the amorphous regions of the polymer, causing the breakdown of the long polymer chains. The crystalline regions still hold the structure together and the physical properties persist. In the second stage the crystalline regions fragments and the physical properties diminish. (Li 1999, Li and Vert 1999, Middleton and Tipton 2000)

The above assumption was supported by the mass loss of the self-reinforced poly-L/D-lactide 96/4, which was observed after 52 weeks *in vitro*. For the first 52 weeks the mass remained unchanged and then decreased linearly, being 60 % of the initial mass at the end of hydrolysis. The mass of the self-reinforced poly-L/DL-lactide 70/30 behaved very similarly. At the same time as the rapid water absorption was observed (after 48 weeks *in vitro*), the mass of the samples started to decrease. The difference between

the poly-L/D-lactide 96/4 and poly-L/DL-lactide 70/30 could be explained by the different quantities of amorphous and crystalline phases in the polymer. Poly-L/DL-lactide 70/30 is an amorphous polymer and thus has fewer crystalline regions holding the structure together than semicrystalline poly-L/D-lactide 96/4 (Li 1999, Vert *et al.* 1991). Self-reinforced poly-L-lactide-co-glycolide 80/20 maintained its mass only during the first 12 weeks *in vitro*. Thereafter the mass constantly decreased. This was again due to the hydrophilic glycolic acid monomers in the polymer.

The results showed that the addition of β-TCP to the self-reinforced samples reduced the overall degradation rate in terms of mass loss. The masses started to decrease a few weeks later than the masses of the plain matrix polymers. The addition of BaG also seemed to reduce the overall degradation rate, but not as much as did the addition of β-TCP. With BaG containing samples a slight mass loss was observed at the very beginning of the hydrolysis. This was attributed to the rapid dissolution of the BaG particles on the surface of the samples. After that fast dissolution the mass remained steady for up to 30 – 52 weeks *in vitro*, depending on the BaG content.

Processing and γ-sterilization affected the initial molecular weights of the samples. The polymer chains fragmented during processing and γ-sterilization as has also been reported in other studies (Niiranen *et al.* 2004, Paakinaho *et al.* 2009). Thus, although the molecular weights of the poly-L/D-lactide 96/4 and poly-L/DL-lactide 70/30 were initially different, after manufacturing they had a similar weight average molecular weight, approximately 60 kDa. The addition of filler material further decreased the molecular weight values.

Because the degradation of the poly-α-hydroxyacids occurred in the first stage through the cleavage of the ester bonds converting the long polymer chains into shorter ones, the weight average molecular weight of the samples started to decrease as soon as the sample game in contact with the buffer solution. The decrease seemed to be constant until a very low value of about 10 kDa was reached. Thereafter the decrease became slower. The plain matrix polymers were observed to lose molecular weight faster than the samples containing filler material and β-TCP again seemed to slow the decrease more than BaG.

Molecular weight plays an important role in the degradation of osteoconductive bioabsorbable composites. It was observed that the changes in the physical properties occurred at certain molecular weight values, generally very low ones. When the weight average molecular weight decreased to 20 – 30 kDa, the mechanical properties of the samples began to diminish. This happened in all samples regardless of the matrix polymer, filler material or filler content. Thus it can be stated that the molecular chains of the same length have approximately the same strength regardless of filler addition. As the weight average molecular weight continued decreasing until 10 – 20 kDa, the mass of the samples started to decrease. At that point the molecular chains probably became small enough to be soluble in the buffer solution, which reduced the mass of the

samples. Finally, when the weight average molecular weight reached values less than 10 kDa the water absorption increased enormously. Thus it can be stated that the properties of the samples were heavily dependent on the molecular weight rather than on the duration of hydrolysis.

Self-reinforced poly-L/DL-lactide 70/30 is an amorphous polymer and showed slight shoulders and bimodality in molecular weight distribution (MWD) during the *in vitro* degradation. The MWD gradually formed a bimodal curve after 48 weeks *in vitro*, indicating late-state degradation. A similar effect has previously been reported by Niiranen *et al.* (2004). At the same time, the weight average molecular weight of the sample decreased to very low values, under 5 kDa. The shoulders and bimodality of the MWD were assumed to be due to the crystallization of the degradation products rather than to heterogeneous degradation. Short polymer chains can recrystallize more easily than long ones. The addition of the filler material to the samples reduced the formation of the bimodal MWD. Only very small shoulders could be observed in the MWD curves. This probably resulted from a slower decrease in the weight average molecular weight of the samples containing filler than in the plain matrix material. The same molecular weight level, under 5 kDa, was not achieved during the hydrolysis period. Thus it was assumed that the filler particles inhibited the crystallization of the degradation products. The semicrystalline self-reinforced poly-L/D-lactide 96/4 and its filler containing composites maintained their monomodal MWD throughout the hydrolysis studied. At small weight average molecular weight values some roughness and broadening were detected.

A differential scanning calorimeter (DSC) was used to monitor the changes in the thermal properties of the samples studied during hydrolysis in PBS. The glass transition temperature (T_g) was detected from the second heating (heating B). At the beginning of the hydrolysis all the samples studied had glass transition temperatures around 56 – 62 °C. The lowest glass transition temperature was observed in the initially amorphous poly-L/DL-lactide 70/30 based samples, at 56 – 58 °C. Partially crystalline poly-L/D-lactide 96/4 and poly-L-lactide-co-glycolide 80/20 had slightly higher glass transition temperatures, 61 – 63 °C and 58 – 60 °C respectively. The addition of the osteoconductive filler materials did not seem to greatly affect the glass transition temperatures of the samples. Hydrolysis, however, affected the glass transition temperatures. During hydrolysis, the samples absorbed water, which plasticized the polymer and initiated the breakdown of the ester bond in the polymer chain. This caused a decrease in molecular weights (Li 1999). Due to these events the glass transition temperatures became lower as the degradation proceeded. Such observations have also been reported in other polylactide based samples (Niiranen *et al.* 2004, Li 1999).

At the beginning of the hydrolysis the DSC curves of the amorphous poly-L/DL-lactide 70/30 showed only the glass transition temperature. However, when the hydrolysis and degradation of the polymer proceeded the melting peak also appeared in the DSC curve of the first heating (heating A). The melting peak was first observed at 123 – 127 °C

and during the hydrolysis it transferred to the lower temperatures for the same reasons as did the glass transition temperature (Li 1999). The formation of the melting peak was thought to be a consequence of the crystallization of the polymer matrix during the degradation process *in vitro*. The molecular chains of a certain length could recrystallize at 37 °C. As the degradation continued, there were even more short molecular chains and degradation by-products which can recrystallize (Li 1999). This led to an increase in the overall melting enthalpy and thus in the crystallinity of the samples until the end of hydrolysis. The appearance of the melting peak was seen to be dependent on osteoconductive filler content. With the plain matrix polymer, poly-L/DL-lactide 70/30, the melting peak appeared around 24 weeks *in vitro*. The addition of BaG caused the melting peak to appear slightly earlier. The more BaG was added the earlier the melting peak appeared. This was probably due to the faster degradation of the samples with high BaG content. They reached a suitable molecular chain length sooner because they also degraded earlier. The addition of β-TCP, on the contrary, caused the melting peak to form slightly later than the plain matrix polymer. This was thought to be due to the delayed degradation rate when the β-TCP was added.

At the same time as the melting peak appeared in the DSC curve of the poly-L/DL-lactide 70/30 based samples, a slight crystallization peak during heating was also detected. The crystallization temperature was slightly lower than the melting temperature and thus the crystals formed during heating were melted quickly after formation. This crystallization was assumed to mean that the molecular chains of a certain length could crystallize at temperatures between the glass transition temperature and the melting temperature. Thus this was thought to be different than the crystallization during degradation *in vitro* at 37 °C. The crystallization during heating disappeared as the weight average molecular weight decreased to less than 10 kDa. At that time crystallization during hydrolytic degradation increased remarkably and thus there were no longer so many free molecular chains available to further crystallize during heating. Overall crystallization during degradation *in vitro* was greater in the plain matrix polymer than in the samples containing filler material. The addition of filler material was assumed to inhibit the recrystallization of the short polymer chains. The inhibition effect of the β-TCP was observed to be the greatest. This was thought to be due to the enormous number of small disintegrated β-TCP particles and thus the high discontinuity in the structure of the sample.

The shape of the melting peak in the DSC curves of the poly-L/DL-lactide 70/30 based samples were mostly monomodal throughout the whole hydrolysis. Only very slight shoulders and broadening were observed at the same time as the MWD started to show shoulders. These observations support the assumption that the bimodality in the MWD may have been due to morphological changes and the presence of the different crystalline fragments.

The behavior of the poly-L/D-lactide 96/4 differed from that of the poly-L/DL-lactide 70/30 according to the DSC analysis. The difference was due to the initial partial

crystallinity of the poly-L/D-lactide 96/4. Crystallinity is directly proportional to melting enthalpy and thus changes in crystallinity can be estimated by determining changes in melting enthalpies. Initially the melting peak of the poly-L/D-lactide 96/4 based samples was detected at 154 – 157 °C and the initial melting enthalpies were 30 – 38 J/g. The highest melting enthalpy was observed in the plain matrix polymer, which thus had the highest crystallinity. The addition of filler material seemed to decrease the melting enthalpy and thus crystallinity. The lower initial crystallinity may have been due to the crystallization inhibiting effect of the filler particles. During hydrolysis the melting peak of the heating A transferred to the lower temperatures. The shift was related to the degradation of the material and decrease in the molecular weight (Li 1999). The size and shape of the peak also changed. It remained monomodal but became higher and broader as the degradation proceeded. The melting enthalpy increased during the hydrolysis at 37 °C and thus the crystallinity of the samples increased. The increase in crystallinity during degradation was assumed to be due to the recrystallization of degradation products and short polymer chains (Li 1999). The plain matrix polymer, poly-L/D-lactide 96/4, was seen to degrade faster than its composites containing osteoconductive filler material, leading to shorter molecular chains and to faster crystallization. The sharp increase in melting enthalpy (crystallinity) was detected in plain matrix polymer at the very low molecular weight values, at values around 5 kDa. This led to the highest melting enthalpy, approximately 70 J/g. The absence of a similar sharp increase at the end of hydrolysis in the samples containing filler material was attributed to the filler particles, which inhibit the crystallization of the short polymer chain. The samples containing filler material achieved a melting enthalpy of approximately 47 – 50 J/g. Again the sample containing β-TCP had the lowest value.

During heating A no similar crystallization was detected in the poly-L/D-lactide 96/4 based samples to that in the poly-L/DL-lactide 70/30 based samples. However, the second heating, heating B, revealed a corresponding crystallization and melting after glass transition temperature. At the beginning of hydrolysis those peaks were quite small, but increased as hydrolysis proceeded. The enthalpies of the crystallization and melting were quite equal throughout the whole hydrolysis. This means that the crystals formed during the heating melted rapidly as the temperature arose. The thermal history of the samples was erased during the heating A and thus the molecular chains could recrystallize during the second heating in the most favourable way. Probably different crystalline fragments formed, because the melting peak became bimodal around 30 – 36 weeks *in vitro*. In that case the bimodal melting peak indicated the possible formation of different crystals which melted at different temperatures.

The initial crystallinity of the poly-L-lactide-co-glycolide 80/20 based samples was lower than that of the poly-L/D-lactide 96/4 based samples. Initial melting enthalpy was 17 J/g for plain polymer and 10 J/g for 20 wt-% of sample containing BaG. During hydrolysis the crystallinity increased and the melting enthalpy reached values of 75 J/g and 70 J/g respectively after 63 weeks *in vitro*. These were the highest enthalpies

achieved among the all samples studied. The molecular weights of the poly-L-lactide-co-glycolide 80/20 based samples could not be measured and thus nothing was known about the lengths of the polymer chains. However, the speculation was that the molecular weight might be quite low, because at that point of hydrolysis the samples were already totally broken down. Thus the crystallization of small chains was easier. When the degradation proceeded further the crystallinity began to decrease. This may have been due to the too small polymer chains, which were no longer capable of crystallization.

The thermal behavior of the poly-L-lactide-co-glycolide 80/20 based samples differed from that of the others. The crystallization peak was detected around 98 – 101 °C at the very beginning of the hydrolysis. This may indicate easier crystallization, probably due to the presence of glycolic acid units. The melting peak was detected around 160 – 164 °C, which was some degrees above the melting peak of the poly-L/D-lactide 96/4 based samples. As the hydrolysis continued, both the crystallization peak and the melting peak transferred to the lower temperatures due to the breakdown of the ester bonds and the resulting decrease in molecular weight (Li 1999). The enthalpy of the crystallization peak was smaller than that of the melting peak hence the sample already had a certain crystallinity before heating. After 12 weeks *in vitro* the crystallization peak disappeared whereas the melting peak continued to grow and became bimodal around after 18 weeks *in vitro*. The bimodality of the melting peak was most probably due to the different crystals formed from lactic acid and glycolic acid units. These different crystals melted at different temperatures. BaG addition affected the thermal behavior of the poly-L-lactide-co-glycolide 80/20 by inhibiting the recrystallization of the short polymer chains and thus the total crystallinity of the sample containing BaG reached lower values than plain polymer.

All the results in this thesis showed that the addition of osteoconductive filler material to the self-reinforced bioabsorbable polymer matrix modified the properties and the *in vitro* degradation behavior of the matrix polymer. The matrix polymer used, the filler material used, the shape, size and amount of filler material, the manufacturing method, interactions between the filler and matrix materials and also microstructural, macrostructural and environmental factors affect the degradation behavior of samples. Thus it is quite difficult to predict the effect of the added compound on the overall degradation. For example, the *in vivo* conditions (enzymes, implant movement) have been studied to further promote and modify the degradation behavior of the self-reinforced BaG containing samples. Samples degraded faster *in vivo* than *in vitro* (Niiranen *et al.* 2004, Pyhältö *et al.* 2005).

The degradation of the plain matrix polymers, poly-L/D-lactide 70/30, poly-L/DL-lactide 96/4 and poly-L-lactide-co-glycolide 80/20, *in vitro* was observed to follow the typical degradation behaviors for amorphous and semicrystalline poly-α-hydroxyacids (Li 1999, Li & Vert 1999, Middleton and Tipton 2000). The molecular weight started to decrease as soon as the samples were immersed in buffer solution. As the degradation

proceeded the mechanical properties also became weaker. At that point the water absorption, mass, dimensions and the pH of the buffer solution remained unchanged. When the degradation still proceeded further and the molecular weight achieved a sufficiently low level, the mass started to decrease, water absorption increased rapidly and the crystallinity showed a sharp increase. The addition of the osteoconductive filler material, either BaG or β-TCP, was seen to retard the overall *in vitro* degradation rate of the polylactide based matrix polymers. This was thought to be based on the neutralizing capability of the BaG and β-TCP. They acted as an alkali and neutralized the acidic degradation products of the poly-α-hydroxyacids and thus autocatalytic degradation was avoided. The presence of the osteoconductive filler material also created pores and interfaces assumed to facilitate the exchanges of the acidic degradation products between the external medium and the interior of the samples. However, the content of the osteoconductive filler material was also observed to influence degradation behavior. High filler content formed higher porosity, which made the samples weaker and thus they also degraded faster than samples with lower filler content.

β-TCP was seen to be more effective than BaG in slowing the degradation rate of the plain matrix polymer. Both BaG and β-TCP have earlier been reported to neutralize the degradation products of poly-α-hydroxyacids and thus retard the degradation rate of composites (Kikuchi *et al.* 2002, Maquet *et al.* 2003, Mellon *et al.* 2003, Kikuchi *et al.* 2004, Maquet *et al.* 2004, Niiranen *et al.* 2004, Li and Chang 2005, Zhou *et al.* 2009). Now the different retarding effect of the β-TCP could be attributed to the dimensions of the filler particles as well as to the mechanical interlocking in the interface between the filler particle and matrix polymer. The total proportion of the filler material was 20 wt-% in both types of filler materials. The particle size distribution of the filler materials was also similar at the beginning of sample manufacturing. However, μ-CT image analysis revealed that the size of β-TCP particles diminished remarkably during the manufacturing. Thus numerous small β-TCP particles were seen inside the sample. This caused more interfaces between the filler particles and matrix materials, through which the acidic degradation products can diffuse out of the internal structure. The surface area of the filler particles was also larger due to the smaller particles as well as the sintered structure of the β-TCP particles. Thus there were more interfaces for mechanical interlocking between the filler particles and matrix polymer. Also neutralizing effect was thought to be more effective.

As the results of the thesis already indicated the degradation behavior of the self-reinforced osteoconductive filler / bioabsorbable polymer composites is difficult to predict. There is not one single ideal composition for all applications. The optimal combination of matrix polymer, filler material and filler content will be largely dependent on the application envisaged. However, although further specific studies concerning, for example, the closer examinations of the crystallization kinetics, micro-structure, structural changes, osteoconductivity and *in vivo* degradation behavior are needed for a better understanding of the overall degradation behavior, the results

showed that self-reinforced osteoconductive filler / bioabsorbable polymer composites may have potential to produce an implant material, for example, for small bone fracture fixations.

6.   SUMMARY AND CONCLUSIONS

There is a variety of reasons for using composites in biomedical applications. Firstly, the mechanical properties of the implant can be tailored to match those of the tissue to be fixed. Secondly, the biological properties can also be tailored and a strong biological interface between the implant and tissue can be achieved. The third reason relates to biodegradable composites. Gradual degradation enables the gradual transfer of the load from the implant to the tissue. In view of all these considerations, the potential composite material for bone fixation could consist of osteoconductive filler material and bioabsorbable matrix material.

The purpose of this thesis was to examine self-reinforced osteoconductive bioabsorbable composites composed of either BaG or β-TCP as a filler material and different copolymers of polylactide and polyglycolide as a matrix material. Special attention was paid to the *in vitro* degradation behavior of different filler material / matrix material combinations.

All the results showed that the addition of osteoconductive filler materials, either BaG or β-TCP, to the self-reinforced polylactide based matrix modified the properties and the *in vitro* degradation of the matrix polymer. The addition of osteoconductive filler material was observed to impair the initial mechanical properties of the matrix material. However, it was also observed to retard the overall *in vitro* degradation rate of the bioabsorbable matrix polymer in terms of mechanical properties, dimensional stability, mass loss and molecular weight of the samples and the pH of the buffer solution. This was attributed to the neutralizing capability of BaG and β-TCP. They acted as an alkali and neutralized the acidic degradation products of the poly-α-hydroxyacids, thus autocatalytic degradation was avoided. The porous structure and interfaces formed during the self-reinforcing of the samples containing filler material affected the degradation behavior. The acidic degradation products of the matrix polymer are thought to be able to diffuse away from the internal structure through the pores and the interfaces between the matrix polymer and filler particles, which further reduces the autocatalytic degradation.

The properties of the samples during *in vitro* hydrolysis were seen to be heavily dependent on the molecular weight of the samples rather than on the duration of the hydrolysis. The molecular weight started to decrease as soon as the sample was immersed in buffer solution. As the hydrolysis proceeded and the weight average molecular weight reached certain values (20 – 30 kDa), the mechanical properties of the samples were impaired. The length of the molecular chains was no longer enough to maintain the mechanical properties. This occurred at different time points of the hydrolysis, but in the same molecular weight range. The mass of the samples started to decrease when the weight average molecular weight reached the range 10 – 20 kDa. At

that point the molecular chains probably became small enough to be soluble in the buffer solution, which reduced the mass of the samples. When the length of the polymer chains was extremely short (weight average molecular weight less than 10 kDa), the crystallinity of the samples increased sharply. However, the osteoconductive filler addition was observed to inhibit this final crystallization by increasing the discontinuity in the structure.

In conclusion can be said that an understanding of the effects of the added filler material on the properties and degradation behavior of the matrix polymer is important, especially for materials intended for use as implant materials. The material of the filler material added is not the only factor exerting influence. The matrix polymer used, the shape, size and amount of the filler material, manufacturing method, interactions between the filler and matrix materials as well as microstructural, macrostructural and environmental factors affect the degradation behavior of the composites. Thus as the results already indicated, the degradation behavior is usually specific to each filler material / matrix material combination and thus it is difficult to precisely predict beforehand. The optimal combination of matrix polymer, filler material and filler content will be largely dependent on the particular application. However, the results showed that self-reinforced osteoconductive bioabsorbable composites may have potential, for example, for small bone fracture fixations.

References

Aboudzadeh N, Imani M, Shokrgozar MA, Khavandi A, Javadpour J and Farokh M. 2010. Fabrication and characterization of poly(D,L-lactide-coglycolide) / hydroxyapatite nanocomposite scaffolds for bone tissue regeneration. Journal of Biomedical Materials Research, 94A. pp. 137-145.

Ara M, Watanabe M and Imai Y. 2002. Effect of blending calcium compounds on hydrolytic degradation of poly(DL-lactic acid-co-glycolic acid). Biomaterials, 23. pp. 2479-2483.

Arstila H. 2008. Crystallization characteristics of bioactive glasses. PhD Thesis, Åbo Akademi University, Finland.

Ashby MF. 2001. Composite materials, microstuctural design of. In: Buschow KHJ, Cahn RW, Flemings MC, Ilschner B, Kramer EJ and Mahajan S, editors. Encyclopedia of Materials: Science and Technology. Volume 2C. Elsevier Science Ltd. pp. 1357-1361.

Atwood RC, Jones JR, Lee PD and Hench LL. 2004. Analysis of pore interconnectivity in bioactive glass foams using X-ray microtomography. Scripta Materialia, 51. pp. 1029-1033.

Avérous L, Quantin J-C and Crespy A. 1998. Determination of the microtexture of reinforced thermoplastics by image analysis. Composite Science and Technology, 58. pp. 377-387.

Avérous L. 2008. Polylactide acid: Synthesis, properties and applications. In: Belgacem MN and Gandini A, editors. Monomers, Polymers and Composites for Renewable Resources. Elsevier. pp. 433-450.

Ben-Nissan B and Ylähen H. 2006. Bioactive glasses and glass ceramics. In: Akay M, Editor. Wiley Encyclopedia of biomedical Engineering, John Wiley & Sons, Inc. 13 p.

Blaker JJ, Gough JE, Maquet V, Notingher I and Boccaccini AR. 2003. In vitro evaluation of novel bioactive composites based on Bioglass®-filled polylactide foams for bone tissue engineering scaffolds. Journal of Biomedical Materials Research, 67A. pp. 1401-1411.

Bleach NC, Nazhat SN, Tanner KE, Kellomäki M and Törmälä P. 2002. Effect of filler content on mechanical and dynamic properties of particulate biphasic calcium phosphate – polylactide composites. Biomaterials, 23. pp. 1579-1585.

Bleach NC, Tanner KE, Kellomäki M and Törmälä P. 2001. Effect of filler type on the mechanical properties of self-reinforced polylactide – calcium phosphate composites. Journal on Materials Science. Materials in Medicine, 12. pp. 911-915.

Boccaccini AR, Roether JA, Hench LL, Maquet V and Jérôme R. 2002. A composite approach to tissue engineering. Ceramic Engineering and Science Proceedings, 23. pp. 805-816.

Boccaccini AR and Maquet V. 2003. Bioresorbable and bioactive polymer / Bioglass® composites with tailored pore structure for tissue engineering applications. Composite Science and Technology, 63. pp- 2417-2429.

Boccaccini AR, Samboulis AG, Rashid A and Roether JA. 2003. Composite surgical sutures with bioactive glass coating. Journal of Biomedical Material Research Part B: Applied Biomaterials, 67B. pp. 618-626.

Bonfield W. 1993. Design of bioactive ceramic-polymer composite. In: Hench LL and Wilson J, editors. An Introduction to Bioceramics, World Scientific Publishing, Singapore, 299-303.

Borden M. 2006. Biomaterials, Absorbable. In: Webster JG, editor. Encyclopedia of Medical Devices and Instrumentation, Second Edition. John Wiley & Sons, Inc. pp. 255-267.

Bretcanu O, Verné E, Borello L and Boccaccini AR. 2004. Bioactivity of degradable polymer sutures coated with bioactive glass. Journal of Materials Science. Materials in Medicine, 15. pp. 893-899.

Brink M, Pitkänen V, Tikkanen J, Paajanen M and Graeffe G. 1996. Spherical particles of a bioactive glass – manufacturing and reactions in vitro. In: Kokubo T, Nakamura T and Miyaji F, editors. Bioceramics Vol 9. Cambridge, England. Elsevier Science Ltd. pp. 127 – 130.

Brink M. 1997a. The influence of alkali and alkaline earths on the working range for bioactive glasses. Journal on Biomedical Materials Research, 36. pp. 109-117.

Brink M. 1997b. Bioactive glasses with a large working range. PhD Thesis, Åbo Akademi University, Finland.

BS2782. 1978. British Standard Methods of testing Plastics. Part 3. Mechanical properties. Method 340B. Determination of shear strength of sheet material. British Standards Institution. 3 p.

Callister WD. 2000. Materials science and engineering, an introduction. Sixth edition. John Wiley & Sons, Inc. 871 p.

Cam D, Hyon, S-H and Ikada Y. 1995. Degradationf of high molecular weight poly(L-lactide) in alkaline medium. Biomaterials, 16. pp. 833-843.

Cao W and Hench LL. 1996. Bioactive materials. Ceramic International, 22. pp. 493-507.

Chabot F, Vert M, Chapelle S and Granger P. 1983. Configurational structures of lactic acid stereocopolymers as determined by ^{13}C-{^{1}H} n.m.r. Polymer, 24. pp. 53-59.

Chuenjitkuntaworn B, Inrung W, Damrongsri D, Mekaapiruk K, Supaphol P and Pavasant P. 2010. Polycaprolactone/Hydroxyapatite composite scaffolds: Preparation, characterization, and in vitro and in vivo biological responses of human primary bone cells. Journal of Biomedical Materials Research, 94A. pp. 241-251.

Claes LE, Ignatius AA, Rehm KE and Scholz C. 1996. New bioresorbable pin for the reduction of small bony fragments: design, mechanical properties and in vitro degradation. Biomaterials, 17. pp. 1621-1626.

Cotton NJ, Egan MJ and Brunelle JE. 2008. Composites of poly(DL-lactide-co-glycolide) and calcium carbonate: In vitro evaluation for use in orthopedic applications. Journal of Biomedical Materials Research, 85A. pp. 195-205.

Daniel IM and Ishai O. 1994. Engineering mechanics of composite materials. Oxford University Press, Inc., New York. 395 p.

Dawant BM and Zijdenbos AP. 2004. Image segmentation. In: Sonka m and Fitzpatrick JM, editors. Handbook of Medical Imaging. Volume 2. Medical image processing and analysis. SPIE Press, Bellingham, Washingtion. pp. 73-127.

Deb S, Wang M, Tanner KE and Bonfield W. 1996. Hydroxyapatite-polyethylene composites: effect of grafting and surface treatment of hydroxyapatite. Journal of materials Science: Materials in medicine, 7. pp. 191-193.

De Santis R, Guarino V and Ambrosio L. 2009. Bone tissue engineering. In: Planell JA, editor. Bone repair biomaterials. Woodhead Publishing Limited, Cambridge, England. pp. 252-270.

Ehrenfried LM, Patel MH and Cameron RE. 2008. The effect of tri-calcium phosphate (TCP) addition on the degradation of polylactide-co-glycolide (PLGA). Journal of Materials Science. Materials in Medicine, 19. pp. 459-466.

Ellä V, Kellomäki M and Törmälä P. 2005. In vitro properties of PLLA screws and novel bioabsorbable implant with elastic nucleus to replace intervertebral disc. Journal of Materials Science. Materials in Medicine, 16. pp. 655-662.

Galois L, mainard D and Delagoutte JP. 2002. Beta-tricalcium phosphate ceramic as a bone substitute in orthopaedic surgery. International Orthopaedics, 26. pp. 109-115.

Gay S, Arosteguia S and Lemaitrea J. 2009. Preparation and characterization of dense nanohydroxyapatite/PLLA composites. Materials Science and Engineering C, 29. pp. 172-177.

Gomes M, Azevedo H, Malafaya P, Silva S, Oliveira J, Silva G, Sousa R, Mano J and Reis R. 2008. Natural polymers in tissue engineering applications. In: Van Blitterswijk C, editor. Tissue engineering. Academic Series in Biomedical Engineering, Elsevier. pp. 145-192.

Gough JE, Arumugam M, Blaker J and Boccaccini A. 2003. Bioglass® coated poly(DL-lactide) foams for tissue engineering scaffolds. Materialwissenschaft und Werkstofftechnik, 34. pp. 654-661.

Guldberg RE, Duvall CL, Peister A, Oest ME, Lin ASP, Palmer AW and Levenston ME. 2008. 3D imaging of tissue integration with porous biomaterials. Biomaterials, 29. pp. 3757-3761.

Guo X, Zheng Q and Du J. 1998. Biodegradation and mechanical properties of hydroxyapatite / poly-DL-lactide composites for fracture fixation. Journal of Wuhan University of Technology, 13. pp. 9 – 15.

Hench LL and Andersson Ö. 1993. Bioactive glasses. In: Hench LL and Wilson J, editors. An Introduction to Bioceramics, World Scientific Publishing, Singapore, pp. 41-61.

Hench LL and Wilson J. 1993. Introduction. In: Hench LL and Wilson J, editors. An Introduction to Bioceramics, World Scientific Publishing, Singapore, pp. 1-23.

Hench LL. 1996. Ceramics, glasses, and glass-ceramics. In: Ratner BD, Hoffmann AS, Schien FJ and Lemons JE, editors. Biomaterials Science: An Introduction to Materials In medicine. Academic Press, Inc. San Diego, California, USA. pp. 73-84.

Hench LL. 1998a. Bioceramics. Journal of American Ceramic Society, 81, pp. 1705-1728.

Hench LL. 1998b. Biomaterials: a forecast for the future. Biomaterials, 19. pp. 1419-1423.

Hench LL. 2001. A genetic theory of bioactive materials. Key Engineering Materials, 192-195. pp. 575-580.

Hench LL and Polak JM. 2005. Third-generation biomedical materials. Science, 295. pp. 1014-1017.

Hench LL. 2006. The story of Bioglass$^{®}$. Journal of Materials Science: Materials in Medicine, 17. Pp. 967-978.

Hill RG. 2005. Biomedical polymers. In: Hench LL and Jones JR, editors. Biomaterials, artificial organs and tissue engineering. Woodhead Publishing Limited, Cambridge, England. pp. 97-106.

Hine PJ, Ward IM, Olley RH and Bassett DC. 1993. The hot compaction of high modulus melt-spun polyethylene fibers. Journal of Materials Science, 28. pp. 316-324.

Huang J, Di Silvio L, Wang M, Tanner KE and Bonfield W. 1997a. In vitro mechanical and biological assessment of hydroxyapatite-reinforced polyethylene composite. Journal of Materials Science. Materials in Medicine, 8. p. 775-779.

Huang J, Di Silvio L, Wang M, Rehman I, Ohtsuki C and Bonfield W. 1997b. Evaluation of in vitro bioactivity and biocompatibility of Bioglass® -reinforced polyethylene composite. Journal of Materials Science. Materials in Medicine, 8. pp. 809-813.

Huang J and Best SM. 2007. Ceramic biomaterials. In: Boccaccini AR and Gough JE, editors. Tissue engineering using ceramics and polymers. Woodhead Publishing Limited, Cambridge, England. pp. 3-31.

Huang Z-M and Ramakrishna S. 2004. Composites in biomedical applications. In: Hin TS, editor. Engineering materials for biomedical applications, Biomaterials Engineering and Processing Series, Vol 1, World Scientific Publishing Ltd., Singapore. pp. 9-1 – 9-49.

Hull D. 1981. An introduction to composite materials, Cambridge University Press, Cambridge, England. 246 p.

Hull D and Clyne TW. 1996. An introduction to composite materials, second edition. Cambridge University Press, Cambridge, England. 326 p.

Huttunen M, Ashammakhi N, Törmälä P and Kellomäki M. 2006. Fibre reinforced bioresorbable composites for spinal surgery. Acta Biomaterialia, 2. pp. 575-587.

Hyon S-H, Jamshidi K and Ikadi Y. 1998. Effect of residual monomer on the degradation of DL-lactide polymer. Polymer International, 46. pp. 196-202.

Ignatius AA, Augat P and Claes LE. 2001. Degradation behavior of composite pins made of tricalcium phosphate and poly(L,DL-lactide). Journal of Biomaterials Science. Polymer Edition, 12. pp. 185-194.

Iooss P, Le Ray A-M, Grimandi G, Daculsi G and Merle C. 2001. A new injectable bone substitute combining poly(ε-caprolactone) microparticles with biphasic calcium phosphate granules. Biomaterials, 22. pp. 2785-2794.

ISO 1172. 1975. Textile glass reinforced plastics – Determination of loss on ignition. International Organization for Standardization. 3 p.

ISO 604. 1993. Plastics – Determination of compressive properties. International Organization for Standardization. 9 p.

ISO 62. 2008. Plastics – Determination of water absorption. 15 p.

Jaakkola T, Rich J, Tirri T, Närhi T, Jokinen M, Seppälä J and Yli-Urpo A. 2004. In vitro Ca-P precipitation on biodegradable thermoplastic composite of poly(ε-caprolactone-co-DL-lactide) and bioactive glass (S53P4). Biomaterials, 25. pp. 575-581.

Jones AC, Arns CH, Sheppard AP, Hutmacher DW, Milthorpe BK, Knacksted MA. 2007. Assessment of bone ingrowth into porous biomaterials using MICRO-CT. Biomaterials, 28. pp. 2491-2504.

Jones AC, Milthorpe B, Averdunk H, Limaye A, Senden TJ, Sakellariou A, Sheppard AP, Sok RM, Knackstedt MA, Brandwood A, Rohner D and Hutmacher DW. 2004. Analysis of 3D bone ingrowth into polymer scaffolds via micro-computed tomography imaging. Biomaterials, 25. pp. 4947-4954.

Jones JR and Hench LL. 2006. Biomaterials: Bioceramics. In: Webster JG, editor. Encyclopedia of Medical Devices and Instrumentation, Second Edition. John Wiley & Sons, Inc. pp. 283-296.

Jones JR. 2007. Bioactive ceramics and glasses. In: Boccaccini AR and Gough JE, editors. Tissue engineering using ceramics and polymers. Woodhead Publishing Limited, Cambridge, England. pp. 52-71.

Kalita SJ, Bhardwaj A and Bhatt HA. 2007. Nanocrystalline calcium phosphate ceramics in biomedical engineering. Materials Science and Engineering C, 27. pp. 441-449.

Karageorgiou V and Kaplan D. 2005. Porosity of 3D biomaterial scaffolds and osteogenesis. Biomaterials, 26. pp. 5474-5491.

Kasuga T, Ota Y, Nogami M and Abe Y. 2001. Preparation and mechanical properties of polylactic acid composites containing hydroxyapatite fibers. Biomaterials, 22. pp. 19-23.

Kellomäki M, Niiranen H, Puumanen K, Ashammakhi N, Waris T and Törmälä P. 2000. Bioabsorbable scaffolds for guided bone regeneration and generation. Biomaterials, 21. pp. 2495-2505.

Kellomäki M, Pohjonen T and Törmälä P. 2003. Self reinforced polylactides. Optimization of degradation and mechanical properties. In: Arshady R, editor. Biodegradable Polymers. The PBM Series Volume 2. Citus Books. pp. 211-235.

Kellomäki M, Törmälä P, Bonfield W and Tanner KE. 1997. Reinforced polylactide – hydroxyapatite composites. 13th European Conference on Biomaterials, European Society of Biomaterials, Göteborg, Sweden, 4-7 September 1997. No. 90.

Kellomäki M. 2000. Bioabsorbable and bioactive polymers and composites for tissue engineering applications. Dissertation, Tampere University of Technology, Tampere, Finland.

Kelly A and Mortensen A. 2001. Composite materials: Overview. In: Buschow KHJ, Cahn RW, Flemings MC, Ilschner B, Kramer EJ and Mahajan S, editors. Encyclopedia of Materials: Science and Technology. Volume 2C. Elsevier Science Ltd. pp. 1361-1371.

Kikuchi M, Koyama Y, Takakuda K, Miyairi H, Shirahama N and Tanaka J. 2002. In vitro change in mechanical strength of β-tricalcium phosphate / copolymized poly-L-lactide composites and their application for guided bone regeneration. Journal of Biomedical Materials Research, 62. pp. 265-272.

Kikuchi M, Koyama Y, Yamada T, Imamura Y, Okada T, Shirahama N, Akita K, Takakuda K and Tanaka J. 2004. Development of guided bone regeneration membrane composed of β-tricalcium phosphate and poly(L-lactide-co-glycolide-co-ε-caprolactone) composites. Biomaterials, 25. pp. 5979-5986.

Klein CPAT, Wolke JGC and de Groot K. 1993. Stability of calcium phosphate ceramics and plasma sprayed coating. In: Hench LL and Wilson J, editors. An Introduction to Bioceramics, World Scientific Publishing, Singapore, pp. 199-221.

Kobayashi S and Sakamoto K. 2006. Experimental and analytical characterization of b-tricalcium phosphate particle reinforced poly-L-lactide composites. JSME International Journal Series A: Solid Mechanics and Material Engineering, 49. pp. 314-320.

Kobayashi S and Sakamoto K. 2009. Effect of hydrolysis on mechanical properties of tricalcium phosphate / poly-L-lactide composites. Journal of Materials Science. Materials in Medicine, 20. pp. 379-386.

Koerten HK and van der Meulen J. 1999. Degradation of calcium phosphate ceramics. Journal of Biomedical Materials Reseach, 44. pp. 78-86.

Koerten HK, Van der Meulen J and Verhoeven MCH. 1992. Degradation of calcium phosphate ceramics: a comparative study on three types of calcium phosphate. In: Ducheyne P, Kokubo T and Van Blitterswijk CA, editors. Bone-bonding. Reed Healthcare Communications. pp. 85-94.

Kohn J and Langer R. 1996. Bioresorbable and bioerodible materials. In: Ratner BD, Hoffmann AS, Schien FJ and Lemons JE, editors. Biomaterials Science: An Introduction to Materials In medicine. Academic Press, Inc. San Diego, California, USA. pp. 64-74.

Kondo N, Ogose A, Tokunaga K, Ito T, Arai K, Kudo N, Inoue H, Irie H and Endo N. 2005. Bone formation and resorption of highly purified β-tricalcium phosphate in rat femoral condyle. Biomaterials, 26. pp. 5600-5608.

Ladizesky NH, Pirhonen EM, Appleyard DB, Ward IM and Bonfield W. 1998. Fibre reinforcement of ceramic / polymer composites for a major load-bearing bone substitute material. Composite Science and Technology, 58. pp. 419-434.

Ladizesky NH, Ward IM and Bonfield W. 1997a. Hydrostatic extrusion of polyethylene filled with hydroxyapatite. Polymers for Advanced Technologies, 8. pp. 496-504.

Ladizesky NH, Ward IM and Bonfield W. 1997b. Hydroxyapatite / high-performance polyethylene fiber composite for high-load-bearing bone replacement materials. Journal of Applied Polymer Science, 65. pp. 1865-1882.

Lakes RS. 2003. Composite biomaterials. In: Park JB and Bronzino JD, editrors. Biomaterials- Principles and applications. CRC Press LLC, Boca Raton, Florida. pp. 79-93.

Laurencin CT and Lu HH. 2000. Polymer-ceramic composites for bone-tissue engineering. In: Davies JE, editor. Bone Engineering. em squared incorporated, Toronto, Kanada. pp. 462-472.

LeGeros RZ. 2008. Calcium phosphate-based osteoinductive materials. Chemical Reviews, 108. pp. 4742-4753.

Li H and Chang J. 2005. pH-compensation effect of bioactive inorganic fillers on the degradation of PLGA. Composites Science and Technology, 65. pp 2226-2232.

Li H, Du R and Chang J. 2005. Fabrication, characterization, and in vitro degradation of composite scaffolds based on PHBV and bioactive glass. Journal of Biomaterials Applications, 20. pp. 137-155.

Li S. 1999. Hydrolytic degradation characteristics of aliphatic polyesters derived from lactic and glycolic acids. Journal of Biomedical Materials Research: Applied Biomaterials, 48. pp. 342-353.

Li S, Garreau H and Vert M. 1990a. Structure-property relationships in the case of the degradation of massive aliphatic poly-(α-hydroxy acids) in aqueous media, Part 1: Poly(DL-lactide acid). Journal of Materials Science: Materials in Medicine, 1. pp. 123-130.

Li S, Garreau H and Vert M. 1990b. Structure-property relationships in the case of the degradation of massive aliphatic poly-(α-hydroxy acids) in aqueous media, Part 2: Degradation of lactide-glycolide copolymers: PLA37.5GA25 and PLA75GA25. Journal of Materials Science: Materials in Medicine, 1. pp. 131-139.

Li S, Garreau H and Vert M. 1990c. Structure-property relationships in the case of the degradation of massive aliphatic poly-(α-hydroxy acids) in aqueous media, Part 3: Influence of the morphology of poly(L-lactic acid). Journal of Materials Science: Materials in Medicine, 1. pp. 198-206.

Li S and Vert M. 1996. Hydrolytic degradation of coral / poly(DL-lactic acid) bioresorbable material. Journal of Biomaterials Science. Polymer Edition, 7. pp. 817-827.

Li S and Vert M. 1999. Biodegradable polymers: Polyesters. In: Mathiowitz E, Editor. Encyclopedia of Controlled Drug Delivery, Volumes 1 & 2, John Wiley & Sons, Inc. pp. 71-93.

Lu HH, El-Amin SF, Scott KD and Laurencin CT. 2003. Three-dimensional, bioactive, biodegradable, polymer-bioactive glass composite scaffolds with improved mechanical properties support collagen synthesis and mineralization of human osteoblast-like cells in vitro. 2003. Journal of Biomedical Materials Research, 64A. pp. 465-474.

Mainil-Varlet P, Curtis R and Cogolewski S. 1997. Effect of in vivo and in vitro degradation on molecular and mechanical properties of various low-molecular-weight polylactides. Journal of Materials Research, 36. pp. 360-380.

Maquet V, Boccaccini AR, Pravata L, Notingher I and Jérôme R. 2003. Preparation, characterization, and in vitro degradation of bioresorbable and bioactive composites based on Bioglass®-filled polylactide foams. Journal of Biomedical Materials Research, 66A. pp. 335-346.

Maquet V, Boccaccini AR, Pravata L, Notingher I and Jérôme R. 2004. Porous poly(a-hydroxyacid) / Bioglass® composite scaffolds for bone tissue engineering. I: preparation and in vitro characterization. Biomaterials, 25. pp. 4185-4194.

Marcolongo M, Ducheyne P and LaCourse WC. 1997. Surface reaction layer formation in vitro on a bioactive glass fiber / polymeric composites. Journal of Biomedical Materials Research, 37. pp. 440-448.

Mathieu LM, Mueller TL, Bourban P-E, Pioletti DP, Müller R and Månson J-AE. 2006. Architecture and properties of anisotropic polymer composite scaffold for bone tissue engineering. Biomaterials, 27. pp. 905–916.

Maurus PB and Kaeding CC. 2004. Bioabsorbable implant material review. Operative Techniques in Sport Medicine, 12. pp 158-160.

McGuire DA, Barber FA, Elrod BF and Paulos LE. 1999. Bioabsorbable interference screws for graft fixation in anterior cruciate ligament reconstruction. Arthroscopy: The Journal of Arthroscopic and Related Surgery, 15. pp 463–473.

Mellon V, Best S, Cameron R and Bonfield W. 2003. Degradation of composite scaffolds of poly(D,L,lactic-co-glycolic acid) and tricalcium phosphate. 18th European Conference on Biomaterials, October 1-4, 2003. Stuttgart. Germany.

Merten HA, Wiltfang J, Grohmann U and Hoenig JF. 2001. Intraindividual comparative animal study of α- and β-tricalcium phosphate degradation in conjunction with simultaneous insertion of dental implants. The Journal of Craniofacial Surgery, 1. pp. 59-68.

Middleton JC and Tipton AJ. 2000. Synthetic biodegradable polymers as orthopedic devices. Biomaterials 21. pp. 2335-2346.

Nair LS and Laurencin CT. 2007. Biodegradable polymers as biomaterials. Progress in Polymer Science, 32. pp. 762-798.

Niiranen H and Törmälä P. 1999. Self-reinforced bioactive glass-bioabsorbable polymer composites. In: Neenan T, Marcolongo M and Valentini RF, editors. Biomedical materials – drug delivery, implant and tissue engineering, vol 550, 267-272.

Niiranen H, Pyhältö T, Rokkanen P, Kellomäki M and Törmälä P. 2004. In vitro and in vivo behavior of self-reinforced bioabsorbable polymer and self-reinforced bioabsorbable polyer / bioactive glass composites. Journal of Materials Research, 69A. pp. 699-708.

Niiranen H, Pyhältö T, Rokkanen P, Paatola T and Törmälä P. 2001. Bioactive glass 13-93 / P(L/DL)LA composites in vitro and in vivo. Key Engineering Materials, 192-195. pp. 721-724.

Ogose A, Kondo N, Umezu H, Hotta T, Kawashima H, Tokunaga K, Ito T, Kudo N, Hoshino M, Gu W and Endo N. 2006. Histological assessment in grafts of highly purified beta-tricalcium phosphate (OSferion®) in human bones. Biomaterials, 27. pp. 1542-1549.

Oonishi H and Oomamiuda K. 1998. Degradation / resorption in bioactive ceramics in orthopedics. In: Black J and Hasting G, editors. Handbook of Biomaterial Properties. Chapman & Hall, London. pp. 406-419.

Paakinaho K, Ellä V, Syrjälä S and Kellomäki M. 2009. Melt spinning or poly(L/D)lactide 96/4: Effect of molecular weight and melt processing on hydrolytic degradation. Polymer Degradation and Stability, 94. pp. 438-442.

Paatola T, Pirhonen E and Törmälä P. 2001. P. Coating of bioactive glass (13-93) fibers with bioabsorbable polymer. In Key Engineering Materials, 192 – 195. pp. 717-720.

Pohjonen T and Törmälä P. 1997. Self-reinforcing of amorphous bioabsorbable polymers. 13th European Conference on Biomaterials, 4-7 September 1997, Göteborg, Sweden. p. 88.

Pohjonen T, Helevirta P, Törmälä P, Koskikare K, Pätiälä P and Rokkanen P. 1997. Strength retention of self-reinforced poly-L-lactide screws. A comparison of compression moulded and machine cut screws. Journal of Materials Science. Materials in Medicine 8. pp. 311 – 320.

Pyhältö T, Lapinsuo M, Pätiälä H, Niiranen H, Törmälä P and Rokkanen P. 2005. Fixation of distal femoral osteotomies with self-reinforced poly(L/DL)lactide 70:30 and self-reinforced poly(L/DL)lactide / bioactive glass composite rods. An experimental study on rabbits. Journal of Biomaterials Science. Polymer Edition, 16. pp. 725-744.

Rauwendaal C. 2001. Polymer Extrusion. Revised 4th edition. Hanser Verlag. 777 p.

Reinhart TJ and Clements LL. 1987. Introduction to composites. In: Engineered Materials Handbook, Volume 1. Composites. ASM International. pp. 27-34.

Renghini C, Komlev V, Fiori F, Verné E, Baino F, Vitale-Brovarone C. 2009. Micro-CT studies on 3-D bioactive glass-ceramic scaffolds for bone regeneration. Acta Biomaterialia, 5. pp. 1328–1337.

Rey C, Combes C, Drouet C and Somrani S. 2008. Tricalcium phosphate-based ceramics. In: Kokobo T, editor. Bioceramic and their clinical applications. Woodhead Publishing Limited, Cambridge, England. pp. 326-366.

Rezwan K, Chen QZ, Blaker JJ and Boccaccini AR. 2006. Biodegradable and bioactive porous polymer / inorganic composite scaffolds for bone tissue engineering. Biomaterials, 27. pp. 3413-3431.

Rich J, Jaakkola T, Tirri T, Närhi T, Yli-Urpo A and Seppälä J. 2002. In vitro evaluation of poly-ε-caprolactone-co-DL-lactide) / bioactive glass composites. Biomaterials, 23. pp. 2143-2150.

Roether JA, Boccaccini AR, Hench LL, Maquet V, Gautier S and Jérôme R. 2002. Development and in vitro characterization of novel bioresorbable and bioactive composite materials based on polylactide foams and Bioglass® for tissue engineering applications. Biomaterials, 23. pp. 3871-3878.

Rokkanen PU, Böstman O, Hirvensalo E, Mäkelä EA, Partio EK, Pätiälä H, Vainionpää S, Vihtonen K and Törmälä P. 2000. Bioabsorbable fixation in orthopeadic surgery and traumatology. Biomaterials, 21. pp. 2607-2613.

Saikku-Bäckström A, Tulamo R-M, Pohjonen T, Törmälä P, Räihä JE and Rokkanen P. 1999. Material properties of absorbable self-reinforced fibrillated poly-96L/4D-lactide (SR-PLA96) rods; a study in vitro and in vivo. Journal on Materials Science, Materials in Medicine, 10. pp. 1-8.

SFS-EN 1097-7. 2008. Tests for mechanical and physical properties of aggregates. Part 7: Determination of the particle density of filler. Pyknometer method. 13 p.

SFS-EN ISO 178. 1997. Plastics – Determination of flexural properties. Finnish Standards Association SFS. 16 s.

Stamboulis A and Hench L. 2001. Bioabsorbable polymers: their potential as scaffolds for Bioglass® composites. Key Engineering Materials, 192-195. pp. 729-732.

Stamboulis A, Hench LL and Boccaccini AR. 2002a. Mechanical properties of the biodegradable polymer sutures coated with bioactive glass. Journal of Materials Science. Materials in Medicine, 13. pp. 843-848.

Stamboulis AG, Boccaccini AR and Hench LL. 2002b. Novel biodegradable polymer / bioactive glass composites for tissue engineering applications. Advanced Engineering Materials, 4. pp. 105-109.

Tanner KE. 2010. Hard tissue applications of biocomposites. In: Ambrosio L, editor. Biomedical composites. Woodhead Publishing Limited, Cambridge, England. pp. 44-58.

Törmälä P. 1992. Biodegradable self-reinforced composite materials; manufacturing, structure and mechanical properties. Clinical Materials, 10. pp. 29-34.

Törmälä P, Pohjonen T and Rokkanen P. 1998. Bioabsorbable polymers: materials technology and surgical applications. Proceedings of the Institution of Mechanical Engineers, Part H: Journal of Engineering in Medicine, vol. 212. pp. 101-111.

Törmälä P, Välimaa T, Niiranen H, Pohjonen T and Rokkanen P. 2002. Bioactive, bioabsorbable surgical composite material. Pat. US6406498.

Tuan HS and Hutmacher DW. 2005. Application of micro CT and computation modeling in bone tissue engineering. Computer-Aided Design, 37. pp. 1151-1161.

Van der Meer SAT, De Wijn JR and Wolke JGC. 1996. The influence of basic filler materials on the degradation of amorphous D- and L-lactide copolymer. Journal of Materials Science. Materials in Medicine, 7. pp. 359-361.

Van Dijkhuizen-Radersma R, Moroni L, van Apeldoorn A, Zhang Z and Grijpma D. 2008. Degradable polymers for tissue engineering. In: Van Blitterswijk C, editor. Tissue engineering. Academic Series in Biomedical Engineering, Elsevier. pp. 193-221.

Veiranto M, Suokas E, Ashammakhi N and Törmälä P. 2004b. Novel bioabsorbable antibiotic releasing bone fracture fixation implants. In: Hasirci N and Hasirci V, editors. Biomaterials: From molecules to engineered tissues. Advances in experimental medicine and biology: Volume 553. Kluwer Academic/Plenum Publishers. pp. 197-208.

Veiranto M, Tiainen J, Niemelä S, Suokas E, Ikäheimo I, Koskela M, Syrjälä H, Ashammakhi N and Törmälä P. 2004a. Novel ciprofloxacin releasing SR-PLGA miniscrews. 7th World Biomaterials Congress, 17 – 21 May 2004, Sydney, Australia. p. 173.

Veiranto M, Törmälä P and Suokas E. 2002. In vitro mechanical and drug release properties of bioabsorbable ciprofloxacin containing and neat self-reinforced P(L/DL)LA 70/30 fixation screws. Journal of Materials Science. Materials in Medicine, 13. pp. 1259-1263.

Verheyen CCPM, Klein CPAT, De Blieck-Hogervorst MA, Wolke JGC, Van Blitterswijk CA and De Groot K. 1993. Evaluation of hydroxyapatite / poly(L-lactide) composites: physic-chemical properties. Journal of Materials Science. Materials in Medicine, 1. pp. 58-65.

Vert M, Li S and Garreau H. 1991. More about the degradation of LA / GA –derived matrices in aqueous media. Journal of Controlled Release, 16. pp. 15-26.

Vert M, Li SM, Spenlehauer G and Guerin P. 1992. Bioresorbability and biocompatibility of aliphatic polyesters. Journal on Materials Science. Materials in Medicine, 3. pp. 432-446.

Vert M. 2005. Aliphatic polyesters: Great degradable polymers that cannot do everything. Biomacromolecules, 6. pp. 538-546.

Wang CC, Donnet JB, Wu SH and Wang TK. 2005. Study of microdispersion of filler in polymers by AFM image analysis. Microscopy and Microanalysis, 11, pp. 1672-1673.

Wang M, Hench L and Bonfield W. 1998. Bioglass® / high density polyethylene composite for soft tissue application: preparation and evaluation. Journal of Materials Research, 42. pp. 577-586.

Wang M, Deb S and Bonfield W. 2000a. Chemically coupled hydroxyapatite-polyethylene composites: processinga nad characterization. Materials Letters, 44. pp. 119-124.

Wang M, Ladizesky NH, Tanner KE, Ward IM and Bonfield W. 2000b. Hydrostatically extruded HAPEX^{TM}. Journal of Materials Science, 35. pp. 1023-1030.

Wang M, Yue CY and Chua B. 2001. Production and evaluation of hydroxyapatite reinforced polysulfone for tissue replacement. Journal of Materials Science. Materials in Medicine, 12. pp. 821-826.

Wang M. 2003. Developing bioactive composite materials for tissue replacement. Biomaterials, 24. pp. 2133-2151.

Williams DF. 1999. The Williams Dictionary of Biomaterials. Liverpool University Press, Liverpool, UK. 343 p.

Wiltfang J, Merten HA, Schlegel KA, Schultze-Mosgau S, Kloss FR, Rupprecht S and Kessler P. 2002. Degradation characteristics of α and β tri-calcium-phosphate (TCP) in minipigs. Journal of Biomedical Materials Research (Applied Biomaterials), 63. pp. 115-121.

Wu D, Gao D, Mayo SC, Gotama J and Way C. 2008. X-ray ultramicroscopy: A new method for observation and measurement of filler dispersion in thermoplastic composites. Composite Science and Technology, 68. pp. 178-185.

Yang Z, Best SM and Cameron RE. 2009. The influence of α-tricalcium phosphate nanoparticles and microparticles on the degradation of poly(D,L-lactide-co-glycolide). Advanced Materials, 21. pp. 3900-3904.

Yeung H-Y, Qin L, Lee K-M, Ming Z, Leung K-S and Cheng JC. 2005. Novel approach for quantification of porosity for biomaterial implants using microcomputed tomography. Journal of Biomedical Materials Research Part B. Applied Biomaterials, 75B. pp. 234-242.

Yuan H, de Bruijn JD, Li Y, Feng J, Yang Z, de Groot K and Zhang X. 2001. Bone formation induced by calcium phosphate ceramics in soft tissue of dogs: a comparative study between porous α-TCP and β-TCP. Journal of materials Science: Materials in Medicine, 12. pp. 7-13.

Zhang D. 2008. In vitro characterization of bioactive glass. PhD Thesis, Åbo Akademi University, Finland.

Zhang M and James SP. 2006. Biomaterials, Polymers. In: Webster JG, editor. Encyclopedia of Medical Devices and Instrumentation, Second Edition. John Wiley & Sons, Inc. pp. 329-342.

Zhou Z, Ruan J, Zou J, Zhou Z and Shen X. 2007. Bioactivity of bioresorbable composite based on bioactive glass and poly-L-lactide. Transaction of Nonferrous Metals Society of China, 17. pp. 394-399.

Zhou Z, Yi Q, Liu X, Liu L and Liu Q. 2009. In vitro degradation behaviors of poly-L-lactide / bioactive glass composite materials in phosphate-buffered solution. Polymer Bulletin, 63. pp. 575-586.